



**Feature-based Support Generation in Fused  
Deposition Modeling (FDM) Machine**

by

**Khairul Fauzi bin Karim**

**(0640610108)**

A thesis submitted in fulfilment of the requirements for the degree of  
Doctor of Philosophy

**School of Mechatronic  
UNIVERSITI MALAYSIA PERLIS**

2017

UNIVERSITI MALAYSIA PERLIS

**DECLARATION OF THESIS**

Author's full name : Khairul Fauzi bin Karim  
Date of birth : 6 February 1974  
Title : Feature-based Support Generation in Fused Deposition  
Modeling (FDM) Machine  
Academic Session : Dec. 2006 – Dec. 2016

I hereby declare that the thesis becomes the property of Universiti Malaysia Perlis (UniMAP) and to be placed at the library of UniMAP. This thesis is classified as :

- CONFIDENTIAL** (Contains confidential information under the Official Secret Act 1972)\*
- RESTRICTED** (Contains restricted information as specified by the organization where research was done)\*
- OPEN ACCESS** I agree that my thesis is to be made immediately available as hard copy or on-line open access (full text)

I, the author, give permission to the UniMAP to reproduce this thesis in whole or in part for the purpose of research or academic exchange only (except during a period of \_\_\_\_ years, if so requested above).

Certified by:

\_\_\_\_\_  
**SIGNATURE**

740206-09-5089  
**(NEW IC NO. / PASSPORT NO.)**

Date : \_\_\_\_\_

\_\_\_\_\_  
**SIGNATURE OF SUPERVISOR**

Prof. Dr Hazry bin Desa  
**NAME OF SUPERVISOR**

Date : \_\_\_\_\_

**NOTES: \* If the thesis is CONFIDENTIAL or RESTRICTED, please attach with the letter from the organization with period and reasons for confidentiality or restriction.**

## ACKNOWLEDGEMENT

Firstly, I would like to express my sincere gratitude to my research supervisor, Associate Professor Dr Hazry Desa of the School of Mechatronic, University Malaysia Perlis (UniMAP) and co-supervisor, Associate Professor Dr Abdul Halim Zulkifli of the Department of Mechanical Engineering, University Teknologi Mara (UiTM) Pulau Pinang for their invaluable knowledge, direction, guidance, advice and encouragement throughout the course of accomplishing my research project. The insight and wisdom gained are undoubtedly immense.

I also would like to thank to technical officers and supporting staff at Universiti Malaysia Perlis (UniMAP), Universiti Sains Malaysia (USM) and Universiti Teknologi Mara (UiTM) for their great support and assistance while completing my experimental work.

Special thanks to my beloved parent Haji Karim Salleh and Hajjah Ramlah Hamid for their endless love. I also would like to dedicate special thanks to my wife, Fatmawati Yacob and my great children, Nur Hidayah, Nur Syafiqah, Muhammad Nur Mu'izzuddin, Muhammad Nur Naquiddin, Muhammad Nur Wafiuddin and Nur Fatin Zahirah for their understanding, constant love and patience during the hard time of my work. To my late parent in-law, Haji Yacob Warnor and Hajjah Ngaibah Sapuan, thanks for sharing the happiness along my research journey and may Allah bless both of them.

Last but not the least, I also would like to convey my gratitude to my colleague and everyone who have contributed to the completion of this thesis.

Khairul Fauzi Karim

June 2017

## TABLE OF CONTENTS

	<b>PAGE</b>
<b>THESIS DECLARATION</b>	i
<b>ACKNOWLEDGEMENT</b>	ii
<b>TABLE OF CONTENTS</b>	iii
<b>LIST OF APPENDICES</b>	vii
<b>LIST OF TABLES</b>	viii
<b>LIST OF FIGURES</b>	ix
<b>LIST OF SYMBOLS</b>	xii
<b>LIST OF ABBREVIATIONS</b>	xiv
<b>ABSTRAK</b>	xvi
<b>ABSTRACT</b>	xvii
<b>CHAPTER 1: INTRODUCTION</b>	1
1.1 Overview	1
1.2 Definition of Feature	3
1.3 Statement of the Problems	4
1.4 Research Objectives	5
1.5 Scope of Research Work	6
1.6 Organization of the Thesis	6
<b>CHAPTER 2: LITERATURE REVIEW</b>	8
2.1 Introduction	8
2.2 Layered Manufacturing - Fused Deposition Modeling Machine	9
2.3 Features in Layered Manufacturing	10
2.3.1 Feature-based in Layered Manufacturing	10
2.4 Features Extraction and Identification in Layered Manufacturing	12
2.5 Process Planning	13
2.6 Layered Manufacturing Process Planning in FDM	14

2.7	Orientation of Part Deposition and Support Structure	15
2.8	Artificial Neural Network	17
2.8.1	Artificial Intelligent in Layered Manufacturing	18
2.9	Surface Quality and Mechanical Properties of End Product	21
2.10	Process Parameters	24
2.11	Fused Deposition Modeling 3000 (FDM 3000)	25
2.11.1	Drive Blocks	26
2.11.2	The Heating Chamber/Envelope	27
2.11.3	Tips	27
2.12	Current Technology Adopted the FDM Method	28
2.13	Summary	28
 <b>CHAPTER 3: METHODOLOGY</b>		 30
3.1	Introduction	30
3.2	Part 1 - Feature-Based Support Generation System	31
3.2.1	Methodology	31
3.2.1.1	Permitted Overhang Area and Offset Generation	31
3.2.1.2	Area of New Lower Layer	36
3.2.1.3	Layer Adjacency and Area Difference for Feature Verification	38
3.3	Case Study	38
3.3.1	Case Study 1: Non-Supported Features (NSF)	38
3.3.2	Case Study 2: Self-Supported Features (SSF) Require Non-Support Material	39
3.3.3	Case Study 3: External-Supported Features (ESF) using Support Material	40
3.3.4	Case Study 4: Non-Adjacency External-Supported Features (ESF) using Support Material	41
3.4	Part 2 - Optimum Part Deposition Orientation Determination using Artificial Neural Network	42
3.4.1	Methodology	42
3.4.2	Phase 1: 2D Polygon Generation	44

3.4.3	Phase 2: Features Identification	46
3.4.3.1	External-Supported Features (ESF)	46
3.4.3.2	Base-Support Structure (BSF)	48
3.4.4	Phase 3: Optimum Part Deposition Orientation (OPDO)	51
	Determination using MLP Network	
3.4.4.1	Structure 1	52
3.4.4.2	Structure 2	53
3.4.4.3	Structure 3	54
3.4.4.4	Structure 4	55
3.4.4.5	Structure 5	56
3.5	Part 3 – Surface Improvement	60
3.5.1	Methodology	60
3.5.1.1	Step 1: Detection of ESF	61
3.5.1.2	Step 2: Development of ESS	61
3.6	Summary	65
<b>CHAPTER 4: RESULTS AND DISCUSSION</b>		<b>66</b>
4.1	Introduction	66
4.2	Optimum Part Deposition Orientation	66
4.2.1	Extraction of ESF in Determining Volume and Number of Support Group	66
4.2.1.1	Analysis of Orientation of Part Deposition in Direction 1	67
4.2.1.2	Analysis of Orientation of Part Deposition in Direction 2	70
4.2.2	Results for Orientation of Part Deposition in All Pre-defined Directions	73
4.3	Artificial Neural Network	74
4.3.1	Training and Testing Data	75
4.3.2	Summary	80
4.4	Computation Analysis using Multilayer Perceptron Network	82
4.4.1	Model 1: New Model	82

4.4.2	Models 2 and 3: Existing Models	84
4.5	General Discussion	87
4.5.1	Advantages and Limitations	89
4.6	Summary	90
4.7	Results and Discussion – Surface Improvement	90
4.7.1	Introduction	96
4.7.2	Discussion	97
4.7.3	Summary	98
<b>CHAPTER 5: CONCLUSION AND RECOMMENDATION FOR FUTURE WORK</b>		99
5.1	Conclusion	99
5.2	Recommendation for Future Work	100
5.3	Contribution to the Knowledge	100
<b>REFERENCES</b>		102

## LIST OF APPENDICES

APPENDIX A	Data for training and testing processes to determine optimum hidden node (Structure 1).	113
APPENDIX B	Data for training and testing processes to determine optimum hidden node (Structure 2).	115
APPENDIX C	Data for training and testing processes to determine optimum hidden node (Structure 3).	117
APPENDIX D	Data for training and testing processes to determine optimum hidden node (Structure 4).	119
APPENDIX E	Data for training and testing processes to determine optimum hidden node (Structure 5).	121
APPENDIX F	Construction of part model used to evaluate various of features using Feature-based Support Generation using Solid Works software.	123
APPENDIX G	Development and simulation of part model using Insight software.	124
APPENDIX H	List of Publications.	125



## LIST OF TABLES

NO.		PAGE
2.1	Development of LM and related technologies (Pulak M Pandey, 2012).	9
2.2	Heating parameters in FDM 3000.	27
3.1	Part model in six directions with regard to the $\pm x$ , $\pm y$ and $\pm z$ axes.	45
3.2	Structures of MLP 1 and 2 networks.	52
3.3	One MLP 2 network outputs has number “1”.	58
3.4	More than one MLP 2 network outputs have number “1”.	59
4.1	Support volume and amount of support structure in pre-defined directions.	74
4.2	Training and testing accuracies for MLP structures.	81
4.3	Input and output of MLP network (Structure 5) for Part Model 1.	83
4.4	Input and output of MLP network (Structure 5) for Part Model 2.	86
4.5	Input and output of MLP network (Structure 5) for Part Model 3.	87

## LIST OF FIGURES

NO.		PAGE
2.1	Process flow of the Feature-based Process Planning (Y. Yang <i>et al.</i> , 2003).	13
2.2	Permitted Overhang Area of part model (Kulkarni <i>et al.</i> , 2000).	16
2.3	Evolution of staking successor layer for several angles.	16
2.4	FDM 3000 machine ("http://www.stratasys.com/").	25
2.5	Extrusion Head of FDM ("http://www.stratasys.com/").	26
2.6	Zortrax M200 Professional Desktop 3D Printer ("https://zortrax.com/").	28
3.1	The general process flow of current work	30
3.2	Process of uniform slicing; (a) ESF and SSF and (b) POA. $\alpha$ is the support angle, $t$ is the uniform layer thickness and ESS is the External Support Structure.	33
3.3	Offsetting a slice. $V_i$ is the origin of the temporary coordinate system at the arbitrary vertices of the loop. $L_i$ and $L_{i+1}$ are the vectors produced by $V_{i-1}V_i$ and $V_iV_{i+1}$ , respectively.	34
3.4	Generation of a new area of lower layer due to offsetting operation. $A_{ex}$ denotes the area for external contour, $POA_{ex}$ denotes the area of POA for external contour ring and $POA_{in}$ denotes the area of POA for internal contour ring.	37
3.5	Case Study 1: Non-Supported Features.	39
3.6	Case Study 2: Self-Supported Features require non-support material.	40
3.7	Case Study 3: ESF using support material.	40
3.8	Case Study 4: Non-adjacency ESF using support material.	41
3.9	Flowchart for Feature-based Support Generation Data Extraction and analysis system.	43
3.10	Sample of part model in pre-defined directions of x, y and z axes.	45
3.11	ESS and BSS developed in FDM process.	46
3.12	Algorithm flowchart for ESF extraction.	50
3.13	Six inputs nodes and six outputs nodes of MLP 1 network (Structure 1).	53

3.14	Seven inputs nodes and six outputs nodes of MLP 1 network (Structure 2).	53
3.15	Parallel MLP structure (Structure 3).	55
3.16	12 input nodes and 6 output nodes of MLP 2 (Structure 4).	56
3.17	Combination of MLP 1 and MLP 2 networks (Structure 5).	57
3.18	Flowchart for Feature-based Support Generation Data Extraction and formation of new support volume.	60
3.19	Model used to evaluate various of features using Feature-based Support Generation.	63
3.20	Development of ESS for part model.	64
4.1	Illustrative example of Part Model 1 in Direction 1.	69
4.2	Illustrative example of Part Model 1 in Direction 2.	71
4.3	Process of support generation.	72
4.4	Dimensions of Part Model 1.	73
4.5	Accuracy of MLP 1 network for training and testing processes of Structure 1.	76
4.6	Accuracy of MLP 1 network for training and testing processes of Structure 2.	77
4.7	Comparison of testing accuracy between Structures 1 and 2 (for minimum and maximum input values).	78
4.8	Accuracy of MLP 1 network for training and testing processes of Structure 3.	78
4.9	Accuracy of MLP 2 network training and testing processes of Structure 4.	79
4.10	Accuracy of combination of MLP 1 and MLP 2 networks for training and testing processes (Structure 5).	80
4.11	Part Model 1 orientated in Direction 5.	83
4.12	Part Model 1 orientated in Direction 6.	84
4.13	Part models for validation using Feature-based Support Generation.	85
4.14	Comparison on the concept of feature-based extraction used in support generation; (a) without consideration of the OPDO (Y. Yang <i>et al.</i> , 2003) and (b) with consideration of the OPDO.	88

4.15	Actual part models produced by FDM machine; (a) Before improvement and (b) After improvement using Feature-based Support Generation.	91
4.16	Actual part models produced by FDM machine; (a) to (c) Contact surface area and (d) to (f) Non-contact surface area.	92
4.17	Actual part model produced by Zortrax 3D Printer machine; (a) Before improvement and (b) After improvement using Feature-based Support Generation.	94
4.18	Actual part model produced by Zortrax 3D Printer machine; (a) to (c) Contact surface area and (d) to (f) Non-contact surface area.	95
4.19	Construction of ESF.	96
4.20	Construction of ESS of part model. The part model and ESS interface; (a) contact surface (before improvement) and (b) Non-contact surface (after improvement) using Feature-based Support Generation.	97

©This item is protected by original copyright

## LIST OF SYMBOLS

$L_i$	Vector formed by $V_{i-1}V_i$
$L_{i+1}$	Vector formed by $V_iV_{i+1}$
$\vec{l}_i$	Unit vector of $L_i$
$\vec{l}_{i+1}$	Unit vector of $L_{i+1}$
$V_{i-1}$	Vertex of $V_{i-1}$
$V_i$	Vertex of $V_i$
$V_{i+1}$	Vertex of $V_{i+1}$
$V'_i$	New position vertex of $V_i$ due to offset by the layer thickness, $t$
$L'_i$	Equidistant line of $L_i$ due to offset by the layer thickness, $t$
$L'_{i+1}$	Equidistant line of $L_{i+1}$ due to offset by the layer thickness, $t$
$\alpha$	Self-Support angle
$t$	Layer thickness
$(x_i, y_i)$	Vector formed by coordinate $V_{i-1}V_i$ from the origin
$(x_{i+1}, y_{i+1})$	Vector formed by coordinate $V_iV_{i+1}$ from the origin
$POA_{ex}$	Area of POA for exterior contour ring
$POA_{in}$	Area of POA for internal contour ring
$A_{ex}$	Area of the external contour ring
$N$	Total amount of layers for part model
$n$	Number of internal contour ring
$\cap$	Intersection operation
$\cup$	Union operation
$P$	Layer $P$
$Q$	Layer $Q$
$P'$	Projection of layer $P$ to layer $Q$ in z direction
$Q'$	Offsetting of Layer $Q$
$CSRA_k$	Cross-Sectional slice Region Area of lower layer
$CSRA_{k+1}$	Cross-Sectional slice Region Area of upper layer
$CSRA'_k$	Cross-Sectional slice Region Area of offset lower layer
$k+1$	Level of upper layer
$k$	Level of lower layer

$RA$	Resultant Area between <i>CSRA</i> of upper layer and <i>CSRA</i> of lower layer
$RA'$	Resultant Area of upper and offset lower layers
$m$	Amount of Base-Support layer
$RA_1$	Resultant Area at level 1
$RA_2$	Resultant Area at level 2
$V_{pq}$	Input for MLP 1 network (total volume)
$O_{rq}$	Output and input for MLP 1 and MLP 2 networks, respectively
$S_{pq}$	Input for MLP 2 network (number of support structures)
$p$	Model used in the optimization
$q$	Pre-defined part deposition orientation direction
$r$	Stage of network

©This item is protected by original copyright

## LIST OF ABBREVIATIONS

ABS	Acrylonitrile Butadiene Styrene
AI	Artificial Intelligent
AM	Additive Manufacturing
ANN	Artificial Neural Network
BSS	Base-Support Structure
CAD	Computer Aided Design
CAM	Computer Aided Manufacturing
CNC	Computer Numerical Control
CSRA	Cross-Sectional slice Region Area
ESF	External-Supported Feature
ESS	External-Supported Structure
ESV	External-Supported Volume
FDM	Fused Deposited Modeling
FIL	Feature Interaction Loop
FIS	Feature Interaction Surface
FV	Flat Volume
GA	Genetic Algorithm
GP	Genetic Programming
LM	Layered Manufacturing
MLP	Multilayer Perceptron
NC	Numerical Control
NSR	Non-Supported Features
ODM	Orthogonal Deposition Manufacturing
OPDO	Optimum Part Deposition Orientation
POA	Permitted Overhang Area
RP	Rapid Prototyping
SLA	Stereolithography Apparatus
SSF	Self-Supported Feature
SSV	Self-Supported Volume
STL	Stereolithography
SVR	Support Vector Regression

WSS	Water Soluble Support
2D	Two Dimensioning
3D	Three Dimensioning

©This item is protected by original copyright



## **Pembentukan Sokongan Asas Sifat dalam Mesin Pemodelan Pengendapan Melakur**

### **ABSTRAK**

Pembentukan Sokongan Asas Sifat merupakan teknik yang dicadangkan di dalam mesin Pemodelan Pengendapan Melakur. Teknik ini mampu memberi maklumat tentang isipadu dan bilangan struktur sokongan di mana ia berkait rapat dengan penghalaan pengendapan model. Terdapat dua jenis asas sokongan dalam pembentukan model produk Pemodelan Pengendapan Melakur, iaitu Asas Sokongan Sendiri dan Asas Sokongan Luaran. Asas Sokongan Sendiri tidak memerlukan bahan sokongan manakala Asas Sokongan Luaran melibatkan penggunaan bahan sokongan tambahan dalam pembentukannya. Pada masa kini, pelbagai teknik telah dicadangkan untuk mengenal pasti sifat adalah terhad kepada proses pembuatan yang spesifik. Daripada aspek yang lain, proses perancangan LM adalah tidak automatic sepenuhnya dan menjuruskan ke arah penurunan kualiti produk dan meningkatkan keupayaan untuk membuat kesilapan. Tambahan pula, banyak kesilapan yang terjadi adalah di sebabkan penglibatan manusia dalam proses yang kritikal ini. Isu lain ialah format fail STL yang digunakan untuk memindahkan data CAD kepada proses perancangan pembuatan berlapis menghasilkan kehilangan maklumat rekabentuk dan fungsi sifat. Penentuan Penghalaan Pengendapan Model yang optimum adalah didapati sukar dan mengambil masa yang panjang untuk dibina yang mana ianya dipengaruhi oleh kelajuan dan pertukaran hujung muncung ketika pemendapan bahan. Objektif utama tugas ini adalah untuk mengintegrasikan antara Rekabentuk Terbantu Komputer dan Pembuatan Terbantu Komputer dengan menggunakan teknik asas sifat. Ini dapat membantu dalam mengautomatiskan perancangan proses Pemodelan Pengendapan Melakur sebelum pembuatan model dengan pengurangan ralat manusia. Dalam tugas ini, jumlah minimum isipadu dan bilangan struktur sokongan dipilih bagi menentukan penghalaan pengendapan model yang optimum. Tugas yang dijalankan juga tertumpu kepada penambahbaikan kawasan permukaan tidak bersentuh di antara struktur sokongan dan model. Ketepatan rangkaian ditentukan melalui lima struktur MLP (Struktur 1 hingga 5). Ketepatan untuk semua struktur MLP pada spesifik nod adalah dianalisis. Hasil gabungan struktur MLP 1 dan MLP 2 adalah dengan jumlah isipadu dan bilangan struktur sokongan yang minimum akan dipilih sebagai Penghalaan Pengendapan Model yang optimum. Proses mengoptimumkan parameter ini dilakukan dengan menggunakan rangkaian neural buatan. Proses mengoptimumkan jumlah isipadu dan bilangan struktur sokongan dilakukan dengan menggunakan rangkaian neural buatan. Parameter ini juga perlu dipertimbangkan disebabkan kos fabrikasi dan masa pembinaan. Model yang telah melalui proses penambahbaikan seterusnya dihasilkan dengan menggunakan mesin FDM-3000. Keputusan Penghalaan Pengendapan Model yang optimum dibandingkan dengan model yang telah digunakan di dalam kerja-kerja yang terdahulu. Hasil kajian ini menunjukkan bahawa penghalaan yang sama telah dikenalpasti. Keputusan eksperimen juga menunjukkan bahawa persentuhan antara struktur sokongan dan model telah ditambahbaik sebanyak 38%. Permukaan tidak bersentuh pada kawasan yang tidak diperlukan dari kedudukan yang paling atas hingga kedudukan yang paling bawah oleh struktur sokongan telah dihasilkan. Teknik ini juga boleh digunakan dalam percetakan teknologi 3D terkini.

# Feature-based Support Generation in Fused Deposition Modeling Machine (FDM)

## ABSTRACT

Feature-based Support Generation is a technique that has been proposed in Fused Deposition Modeling (FDM) machine. This technique can provide information of volume and amount of support structure which are closely related to orientations of part deposition. There are two types of support features in FDM part model development, which are Self-Supported Features (SSF) and External-Supported Features (ESF). The SSF requires no support material while ESF involves the use of additional support material in their fabrication. Currently, various techniques have been suggested to identify features are limited to a specific manufacturing process. In other aspect, the LM process planning is not fully automatic and lead to part quality degradation and increases the possibility of making errors. Furthermore, many errors are occurred due to the involvement of human in this crucial process. Other issue is that the Stereolithography (STL) file format representation is used to transfer the CAD data to the LM process planning resulting to the loss of design and functional feature information. Determining the OPDO was found to be difficult and consumed longer build times that influenced by the speed and the change of nozzle's tip during material deposition. The main objective of this work is to integrate between Computer Aided Design (CAD) and Computer Aided Manufacturing (CAM) using a feature-based technique. This will help in automation of FDM process planning prior to the manufacturing of part model with less human error. In this work, the minimum volume and amount of support structure are selected in order to determine the optimum part deposition orientation. This work also focuses on the improvement of the non-contact surface area between the support structure and part model. The accuracy of the network is determined through five MLP structures (Structures 1 to 5). The accuracies for all MLP structures at specific hidden nodes are analysed. The output of combination of MLP 1 and MLP 2 structures with a minimum total volume of support structure and a minimum number of support structure will be chosen as an OPDO. The optimization of total volume of support structure and number of support structure is performed using an Artificial Neural Network (ANN). These parameters are also to be considered due to their fabrication cost and build time. The improved part model is then manufactured by using a FDM-3000 machine. The results of OPDO are compared with the models that have been used in previous works. The findings show that the same orientation is identified. The experimental results also show that the contact between the support structure and part model is improved by 38%. The non-contact surface at unnecessary area from the top to the bottom of developed support structure was produced. This similar technique can also be used to produce the part using a current technology of 3D printing.

# CHAPTER 1

## INTRODUCTION

### 1.1 Overview

Traditionally, design and manufacturing activities in industry are performed at separate sections. The design engineer designs the part prior to the development of operation sequences by manufacturing engineer. However in some cases, the modification of design must be made by manufacturing engineer for some reasons such as manufacturability and cost of the product. The modified design will affect the original functions of the product. The changes in design delay the marketing, hence, reduce its market competitiveness. In conventional manufacturing, the integration of design and manufacturing of a product is therefore needed in order to reduce the design lead time (McMahon *et al.*, 1993; Zulkifli, 1999).

The scenario of prototype development in industry has changed. The development requires to introduce the product faster to the market at lower cost with less design modification. This requirement demands on how to shorten the product design time, the development cycle and reduce development cost. The product must also be able to form with any geometric complexity in various applications in order to increase the competitiveness (Daniel *et al.*, 2014; Shuaib *et al.*, 2015; Xueling *et al.*, 2012; Zhenwen *et al.*, 2015).

Layered Manufacturing (LM) is found to have new possibilities to fulfil the changes in this scenario (Dai *et al.*, 2014; Daniel *et al.*, 2014; Ivanova *et al.*, 2013;

Novakova-Marcincinova *et al.*, 2012; Yang *et al.*, 2014). The first LM process was developed by Charles Hull in 1986. The LM is a volume additive manufacturing process in which 2D layer-by-layer deposition of material is stacked gradually from lower to upper to develop 3D physical model directly from Computer Aided Design (CAD). This technology is able to build any complex shapes which are nearly impossible to carry out by using conventional machines. In LM, most of CAD data are converted into Stereolithography (STL) file format before transferring them to the machine. A major advantage of this technology is that the designer has the ability to actually print out any ideas and creativities without limit.

The steps involve in LM start with the development of CAD model. Current activities in LM require human involvement in order to integrate between CAD and CAM systems especially to determine the orientation of part deposition in process planning. The errors and the repeating LM cycles due to human involvement lead to the development of automatic system for all steps in process planning.

In this research, the feature is introduced in order to automate the selection of orientation of part deposition in Fused Deposition Modeling (FDM) machine. The FDM is an extrusion-based LM process which requires support generation to prop up hollow geometrics and overhanging features of a part during manufacturing process. The features that have been identified in FDM process planning is as the key elements in the integration of orientation of part deposition and support generation (Kulkarni *et al.*, 2000).

This work will focus on manufacturing feature in FDM. The feature is considered to represent the way how to manufacture it. It can be extracted by decomposing the successor layer into volumetric units belong to non-support or support feature (overhanging area). The non-support feature is defined as successor layer areas or volumes which have full support from the immediate previous stacked layers, while the

support feature is known as successor layer areas or volumes covered partially or may not be covered at all by the immediate previous stacked layers. The External-Support Structures (ESSs) are employed to improve the manufacturability of layers which do not have a layer adjacency or with only partial adjacency in the build direction (Yang *et al.*, 2003).

In FDM, the support features contain Self-Supported Feature (SSF) and External-Supported Feature (ESF). This work focuses on extracting ESF which is able to determine the volume and number of ESS. These features will be studied in details for the optimization of part deposit orientation in FDM.

The ESS traditionally has contact with the part model that tend to degrade the quality of surface finish (Ahn *et al.*, 2005, 2007; Alexander *et al.*, 1998; Majhi *et al.*, 1999; Pandey, 2003). This problem can be resolved by implementing the concept of features during fabricating the support structure.

## **1.2 Definition of Feature**

In manufacturing process, features are used to integrate between CAD and CAM systems. In general, feature can be divided into three categories and they are: 1) Functional feature, which is related to their function, design and performance; 2) Design feature, which is expressed in geometric terms, primitive design functions (such as block, cylinder and slot) and their combination and 3) Manufacturing feature, is that the volumetric unit to be removed or added in conventional machining and LM, respectively, during manufacturing processes (Salomons *et al.*, 1993). Through features, the integration between CAD and Computer Aided Manufacturing (CAM) systems can be used to resolve this problem.

The Artificial Neural Network (ANN) is used to optimize the orientation of part deposition based on the total volume and number of support structure as a main input parameters.

### 1.3 Statement of the Problems

The issues related to this work are identified and stated in this section.

- i. Feature-based technique is highly significant for integrating CAD and CAM systems. Various techniques have been suggested in this system to identify features but they are limited to specific manufacturing process (e.g. volume removal for Computer Numerical Control (CNC) machining. (Kerbrat *et al.*, 2010).
- ii. In manufacturing process, the LM process planning is not fully automatic and lead to part quality degradation (e.g. dimensional accuracy and surface finish) (Pandey *et al.*, 2007) and increases the possibility of making errors. In this process planning, most of the steps such as creation of geometric model using a solid modeler, determination of suitable deposition orientation, slicing, generation of material deposition paths, part deposition and then post processing operations are done automatically except the orientation of part deposition. The specific manufacturing standard makes feature-based techniques difficult for the manufacturing system to adopt an existing feature extraction system.
- iii. There is no generic interface to accommodate the use of features in the LM process. Furthermore, the Stereolithography (STL) file format (as a de facto standard) representation is used to transfer the CAD data to the LM process planning resulting to the loss of design and functional feature information.

- iv. In feature extraction, it is difficult to reconstruct geometric and manufacturing features from a volume enclosed by spatial triangles without any topological relationship (Yang *et al.*, 2003).
- v. Other issue is also related to the process planning in selecting the Optimum Part Deposition Orientation (OPDO). Furthermore, many errors are occurred due to the involvement of human in this crucial process. Determining the OPDO was found to be difficult and consumed longer build times that influenced by the speed and the change of nozzle's tip during material deposition for both part model and support (Thrimurthulu *et al.*, 2004).

In FDM, there is only one build direction (vertical direction). Hence, the adjacency is considered in a single building direction. This study is work on the system that can extract the features with respect to the FDM. The ANN is proposed in this system in order to automate the process planning for selecting the OPDO.

#### **1.4 Research Objectives**

The objectives of the research are listed below.

- i. To employ a Feature-based Support Generation data extraction technique to automate the process planning in FDM.
- ii. To select the OPDO through features in which the information of support structure can be determined. The automation of this work can be achieved by the integration between CAD and CAM.
- iii. To improve the contact areas between part model and support structures using extracted features. The reduction of unnecessary support volume assures to

enhance the surface quality of final part model by reducing unnecessary support volume.

## **1.5 Scope of Research Work**

The scope of this work involve the use of Artificial Intelligence (AI) to determine the optimum part deposition orientation. Six pre-defined orientations of the part are identified. Two main parameters, the total volume of support structure and the number of support structure which have a significant effect on final product are chosen. The optimization approach using ANN is used for this purpose. The work is also looking at the improvement of the parts' surface using feature-based technique. Overall, the activities in process planning of FDM machine will be automated.

## **1.6 Organization of the Thesis**

The thesis is presented in six chapters as follows:

Chapter 1 introduces the background of Layered Manufacturing (LM) technology. The problem statement and objectives of the research are stated. It also gives the overviews of the topics to be included in the thesis.

Chapter 2 reviews the work in the field of feature-based method and process planning in LM. The emphasis on the systems that utilize the Artificial Intelligent (AI) approach for selecting the OPDO are presented.

Chapter 3 describes the methodology and system organization of the Feature-based Support Generation system developed in this work. This methodology is applied when dealing with the support features for generating the support structure.



Chapter 4 presents the implementation of the Feature-based Support Generation concept to identify the OPDO. The ANN results obtained are experimentally tested and discussed. Some results are then compared and verified with the previous work. This chapter also discusses the concept of Feature-based Support Generation to improve the contact areas between part model and support structures. The improvement of the surface contact for selected part models are reported and discussed.

Chapter 5 states the overall conclusions of the research and suggestion for future work in the related field of study. The contributions to knowledge and research limitations are finally drawn.

©This item is protected by original copyright

## CHAPTER 2

### LITERATURE REVIEW

#### 2.1 Introduction

Selection of orientation of part deposition is an imperative element as it influences amount of developing time and cost, structure to support the overhang area, precision of dimensions and surface irregularity. An appropriate orientation of part deposition can enhance precision of part and quality of surface and minimize the manufacturing time and required structures to support the part (Pandey *et al.*, 2007; Thrimurthulu *et al.*, 2004).

The reviews on the feature-based in LM, the orientation of part deposition determination and the use of Artificial Intelligent (AI) which are related to the research work are discussed in the following sections.

Nowadays, LM, which is currently known as Additive Manufacturing (AM) has changed from a process for Rapid Prototyping (RP) to an appropriate manufacturing process for producing commercial and customized healthcare products (Huang *et al.*, 2013).

The analysis of the work using an Artificial Neural Network (ANN) provides algorithms, pre-trained models, and able to create, train, visualize, and simulate both training and testing data set (“<https://www.mathworks.com/products/neural-network.html>”). The ANN using MATLAB is an advanced interactive software designed for scientific and engineering computation. This software is very flexible and used for solving problem in many area (Martinez and Martinez, 2007).

The development and revolution in LM and related technologies are summarized in Table 2.1.

Table 2.1: Development of LM and related technologies (Pandey, 2012).

<b>Year</b>	<b>Technology</b>
1770	Mechanization
1946	First computer
1952	First Numerical Control (NC) machine tool
1960	First commercial laser
1961	First Commercial Robot
1963	First interactive graphics system (early version of CAD)
1988	First commercial LM system

## 2.2 Layered Manufacturing - Fused Deposition Modeling Machine

Layered manufacturing (LM) is the technology that fabricates an object from one layer to another from a CAD model. A part consisting desired geometry is produced by adding required layers of materials which also known as additive manufacturing process. Much work on LM processes such as Stereolithography Apparatus (SLA), and FDM have been discovered since these technologies were introduced.

The development of LM technology changed rapidly in order to cater high demands in various applications. This technology has been applied in automotive, biomedical micro devices, jigs and fixtures, machine components and other industries (Daniel *et al.*, 2014; Li *et al.*, 2014; McCullough *et al.*, 2013; Zhang *et al.*, 2014).

However, earlier authors (Byun *et al.*, 2006a, 2006b; Durgun *et al.*, 2014; Massod *et al.*, 2000, 2003; Phatak *et al.*, 2012; Thrimurthulu *et al.*, 2004) attempted to determine the Optimum Part Deposition Orientation (OPDO) for FDM process.

An FDM machine is a Numerical Controlled machine consisting of two miniature extruder head nozzles (Bellehumeur *et al.*, 2004; Tyberg *et al.*, 1999). The prototypes are fabricated by semi-molten Acrylonitrile Butadiene Styrene (ABS) plastic filament through a heated nozzle onto a working table. The extrudate in a predetermined pattern will bond with adjacent previous deposited plastic after it cools and solidifies (Bellehumeur *et al.*, 2004; Tyberg *et al.*, 1999). This process occurs at both part model and support structure.

### **2.3 Features in Layered Manufacturing**

Salomans *et al.* (1993) reported that the feature can be divided into three types and defined as follows: 1) Functional features, which are explained based on their usage as compared to their size and location; 2) Design features, which are described in geometric terms like the primitive geometric (slot, pocket, rib and hole) and 3) Manufacturing feature, which is possible to be defined as the volumetric unit to be discarded or added during manufacturing processes.

#### **2.3.1 Feature-based in Layered Manufacturing**

Features technology has been explored for the last few decades since before LM technology was introduced in the market. However, Kerbrat *et al.* (2010) reported that the features usually rely on a specific field. The specific manufacturing standard makes

features which are developed for conventional manufacturing system i.e. Computer Numerical Control (CNC) machining solely fit to its domain. The same features-based technique is not applicable in LM and is still under development.

Much work have been conducted in LM using Feature-based Process Planning (Mani *et al.*, 1999; Qian *et al.*, 2001; Yang *et al.*, 2003). Mani *et al.* (1999) proposed a region based slicing technique in LM. They employed a distinct layer thickness for various regions on the surface of the parts which corresponds to its surface finish. This technique is performed manually and restricted to the choice of different layer thickness. Futhermore, Yang *et al.* (2003) stated that the work conducted by Mani *et al.* (1999) was difficult to be automated.

Qian and Dutta (2001) explored the use of features in LM. They recommended an algorithm for the recognition of feature and decomposition of volume based on ACIS geometric 3D modelling kernel. The established algorithm dealt with the interactive feature in LM. Their work indicated that the interactive feature displayed the staircase interaction which decreased the surface finish quality. They also proposed Feature Interaction Loop (FIL) and Feature Interaction Surface (FIS) to specify the feature interaction for LM regardless of the interaction category. They found that the FIL was formed when the adjacent features interacted. The adjacent features are conditions where features share the same topological entities, such as edge(s) or face(s), in the part volume. The authors stated that the feature interactions due to surface features can also be identified and characterized by the feature interaction surface. The feature used in their work is the feature defined in the manufacturing domain without the consideration of LM process.

Yang *et al.* (2003) described LM features in two-direction LM or Orthogonal Deposition Manufacturing (ODM) system by employing volumetric approaches. The

automatic feature extraction in their work had taken into consideration both layer and path adjacency from STL model. These approaches divided the orthogonal LM features into three distinct volumetric elements which are Self-Supported Volume (SSV), External-Supported Volume (ESV) and Flat Volume (FV). Each characteristic is defined based on the different method during manufacturing. The SSV feature is the characteristic which does not need the ESS in its fabrication and ESV features and vice versa. The FV feature is identified from each SSV feature for the purpose of improving the staircase error in the process of fabrication. The efficiency of fabricated layers and the minimal additional external support were achieved and significantly improved the surface quality via the analysis of feature and decomposition of volume.

#### **2.4 Features Extraction and Identification in Layered Manufacturing**

LM manufacturing process has unique characteristics. The fabrication of 3D part model from 2D layers using additive layer-by-layer create features. These features must be extracted for each successor layer for its manufacturability. Both non-support feature and self-supported feature can be manufactured without ESS. However, the ESF which requires ESS is identified in order to increase its manufacturability (Yang *et al.*, 2003).

The process flow chart for the Feature-based Process Planning explored by Yang *et al.* (2003) is illustrated in Fig. 2.1

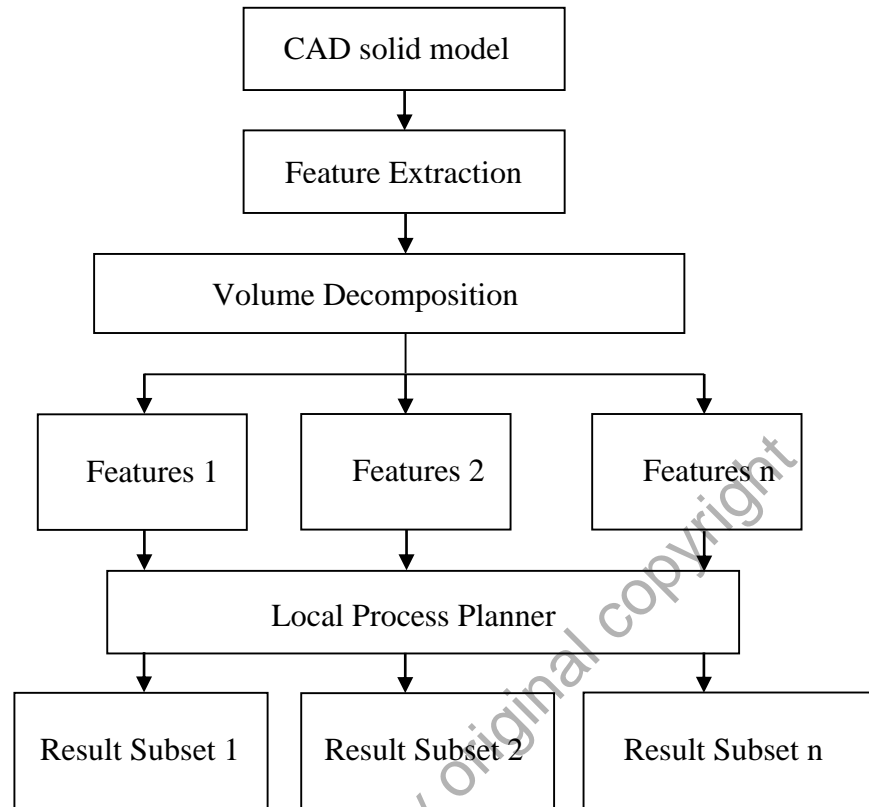


Figure 2.1: Process flow of the Feature-based Process Planning (Yang *et al.*, 2003).

## 2.5 Process Planning

Manufacturing of part model from the raw materials to the desired prototype requires a proper process planning (Zhang *et al.*, 1994). In LM, process planning activities include orientation of part deposition determination, slicing, support structure generation, and path planning (Kulkarni *et al.*, 2000).

Conventionally, the orientation of part deposition is manually determined while other activities are automatically generated. The orientation of part deposition affects the results of the other process planning activities. At this stage, the result of the following activities can be used as a guide to determine the orientation of part deposition (Kulkarni *et al.*, 2000). In current LM process planning, the determination of orientation of part

deposition is possibly a source of errors (Pandey *et al.*, 2007; Thrimurthulu *et al.*, 2004). In addition, the repeating process planning increases unnecessary cost. The best solution to this problem is to integrate between CAD and CAM for process planning in selecting the best orientation of part deposition (Pandey *et al.*, 2007; Thrimurthulu *et al.*, 2004).

## **2.6 Layered Manufacturing Process Planning in FDM**

Process planning in FDM is a crucial activity which is responsible for the transformation of product design specification into an effective fabrication process. The process planning activities consist of orientation of part deposition determination, the development of structures to support the part, slicing and path planning. This process planning occur recursively before the final part model is produced. In this planning, the result of the previous activity will be used as input to the next activity. Meanwhile, the output of this activity will then be used to alter the process of the previous activity (Kulkarni *et al.*, 2000). Among these activities of process planning, orientation of part deposition is not automatically operated and hence, increases the likelihood of errors (Kulkarni *et al.*, 2000). The orientation of part deposition has a significant effect on many key characteristics that determines the quality and cost of the final part model (Alexander *et al.*, 1998). In this case, Pandey *et al.* (2007) and Thrimurthulu *et al.* (2004) found that the effective solution for this difficulty is to automate the selection of orientation of part deposition.



## 2.7 Orientation of Part Deposition and Support Structure

Many attempts (Cheng *et al.*, 1995; Frank *et al.*, 1995; Lan *et al.*, 1997; McClurkin *et al.*, 1998; Xu *et al.*, 1997) have been made to find a suitable orientation of part deposition using different criteria like part accuracy, surface quality, build time, volume of support structure and cost (Pandey *et al.*, 2007). This is in agreement with Kulkarni *et al.* (2000) who suggested that other factors that are affected by the orientation of part deposition include shrinkage, curling, distortion, roundness, flatness of part model, resin flow, material cost and trapped volume.

The orientation of part deposition determination and support structure generation are interrelated (Kulkarni *et al.*, 2000; West *et al.*, 2001). Kulkarni *et al.* (2000) reported that the processes used ESS in LM, the optimum part orientation were affected by total volume of support structure and total area of contact with support structure.

The total volume of support structure can relate to the build time and total cost of the material used in the fabrication process (Hur *et al.*, 1998). Meanwhile, the total area of contact with support structure is related to the time required for post-processing stage (removing and cleaning of ESS).

The support is considered as an important element in FDM (Dutta *et al.*, 2001; Huang *et al.*, 2009; Jin *et al.*, 2015; Kulkarni *et al.*, 2000; Marsan *et al.*, 1998; Xiaomao *et al.*, 2009). It is used to determine the manufacturability of part of overhang geometry structures. Kulkarni *et al.* (2000) noted that the orientation of part deposition was typically chosen to be the least overhang area to be supported.

In general, the overhang area of part can be classified into SSF and ESF (Huang *et al.*, 2009; Yang *et al.*, 2003). For self-supported feature, the support structure is not required during the fabrication process but it is necessary for the ESF. Kulkarni *et al.*

(2000) stated that the ESF are the area where the surface normal,  $N$  is pointing downwards, i.e. the vertical component of the surface normal is negative as shown in Fig. 2.2.

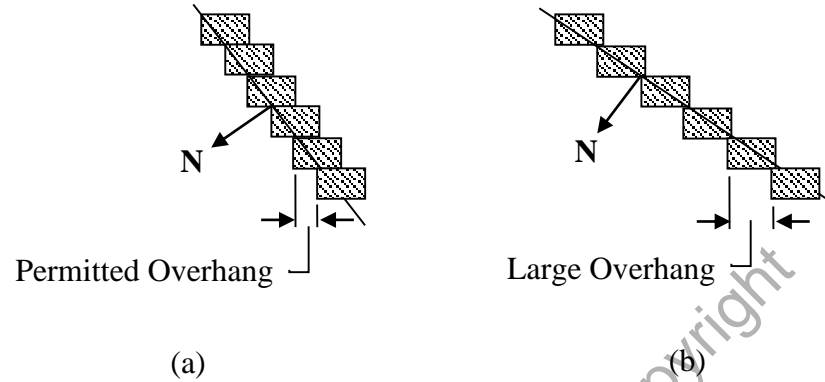


Figure 2.2: Permitted Overhang Area of part model (Kulkarni *et al.*, 2000).

The self-supported feature can be manufactured without supports if the maximum angle of permitted overhang is  $45^\circ$  (Chalasanani *et al.*, 1995; Montero *et al.*, 2001). The evolution of staking successor layer for several angles  $\alpha=15^\circ$ ,  $\alpha=30^\circ$ ,  $\alpha=45^\circ$  and  $\alpha >45^\circ$  as shown in Fig. 2.3. The angle  $\alpha=45^\circ$  can be applied at both part (Montero *et al.*, 2001) and support structure (Huang *et al.*, 2009).

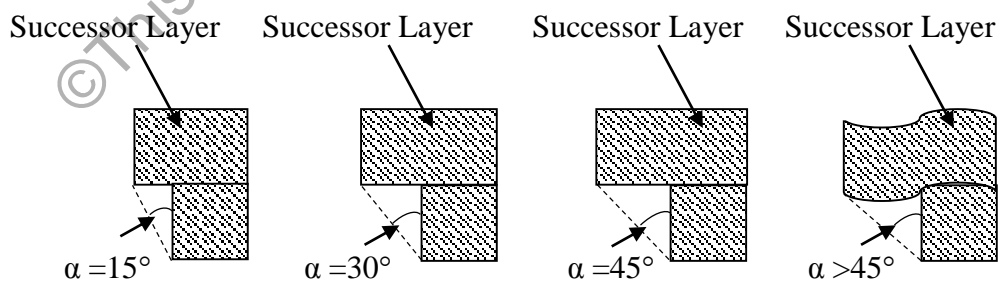


Figure 2.3: Evolution of staking successor layer for several angles.

Huang *et al.* (2009) noted that the supports can be designed with straight and slant wall structures. They proved that the ESSs can be manufactured successfully with slant wall structure in which the slope is not smaller than self-support angle. The functions of ESS are listed below (Onuh *et al.*, 1998):

- i. To act as a mounting device for holding the part in position as it is built.
- ii. To act as a constraint for reducing part distortion.
- iii. To support overhanging cross section.
- iv. To support unattached islands.

However, the ESS also affect the quality of final product which includes poor surface finish (as it touches the part model) and fabrication efficiency (e.g. high build time) (Ahn *et al.*, 2005; Majhi *et al.*, 1999). In this case, the marks left by support structure degrade the surface quality of most LM parts. Additional post-machining such as grinding and coating which consume higher processing time is then required. In the worst case, this process needs high skilled operators to prevent detrimental damage to the original part geometry. Much work have been conducted to improve the drawbacks on part model (Ahn *et al.*, 2005) in which ESS is compromised.

## **2.8 Artificial Neural Network**

Artificial Neural Network (ANN) is a system that is considered to have the capability of learning, adapting to changes and imitating human thought processes. Learning in a neural network can be categorized into two. First, supervised mode, provided with training data, which is a deterministic set of input and corresponding output vectors, to establish a mapping between them. Second, unsupervised mode, which has no

external teaching using training data, and the network learns by self-organizing and classifying input information using internal rules (Kasabov, 1996).

The Multi-Layer Perceptron (MLP) network is categorized as supervised learning ANN. The elements for MLP network are an input layer, an output layer, and a number of hidden layers. The methodology of ANNs consists of two processes which are network training and testing (Kankal *et al.*, 2011). The MLP network training was chosen because it can provide a systematic and proper learning using training data. It is also capable to generalize feature recognition issues using testing data (Haykin and Network, 2004). The reviews indicated that the Levenberg-Marquardt algorithm was used to train the moderate-sized feed forward neural networks due to the fastest back propagation (Mirzadeh and Najafizadeh, 2008; Zhang *et al.*, 2012). Witten *et al.* (2016) stated that to hold out one-third of the data for testing and use the remaining two-thirds for training.

### **2.8.1 Artificial Intelligent in Layered Manufacturing**

Generally, human interference in LM can be replaced by using AI technology. This technology has a capability to automatize the manual planning processes which are usually carried out by human into an automatic system (Huang *et al.*, 2016).

In FDM, the optimization of input (e.g. temperature, velocity) and output variables (e.g. orientation of part deposition, support structure, build time, surface roughness) using various AI methods such as ANN, fuzzy logic, adaptive-network-based fuzzy inference system, Genetic Programming (GP) and Support Vector Regression (SVR) (Nezhad *et al.*, 2009; Peng *et al.*, 2014; Vijayaraghavan *et al.*, 2015). The advantage of these methods is that the relationship between input-output variables and mechanical behaviours of

FDM parts can be estimated (Boschetto *et al.*, 2013; Ludmila *et al.*, 2013a; Villalpando *et al.*, 2014).

Xu *et al.* (1999) employed Genetic Algorithm (GA) by considering the build time, accuracy and part stability for the optimum part orientation in the SLA systems. They also introduced the variable thickness slicing technique which has a significant effect on the total build time of the part model. Masood *et al.* (2003) used a Generic Algorithm (GA) to find the optimum part deposition orientation using the Volumetric Error (VE) for tessellated CAD models in FDM system. In their work, uniform slicing of tessellated CAD model and VE was computed by considering the build edges of slices as rectangular.

Lirabi and Amirabi (2013) employed GA to find the optimum values for the proposed model based on heat and process constraints. In FDM, GA is usually employed to optimize the manufacturing process parameters such nozzle temperature and nozzle speed in producing parts and products.

In order to determine suitable values for variables, fuzzy logic is employed in LM. Sahu *et al.* (2013) used a combination of fuzzy logic and Taguchi method in order to present the experimental data for improving the dimensional accuracy of FDM using. The results shows that the length and width decreases but thickness shows positive deviation from desired value of the built part. These two methods of AI are suitable to find the parameter optimization. However, current work in this thesis is for feature recognition in which ANN is widely employed for feature recognition as it offers some advantages (Sunil and Pande, 2009).

Reviews from the literature show that the study in LM has been extended to the scope of investigating and analysing feature recognition using ANN. For example, Cheng *et al.* (1995) presented a multi-objective approach for determining suitable orientation of

part deposition for Stereolithography parts. They concluded that dimensional accuracy and build time are conflicting requirements. The primary objective was to obtain a desired part accuracy and the secondary objective was to minimize the build time. Both of these objectives can be achieved by calculating for different types of surfaces and by reducing the number of slices. Other work shows that ANN is a reliable method to predict model of surface quality for any developed shapes (Boschetto *et al.*, 2013).

Nowadays, modern manufacturing practises an intelligent system to control the process activities and to produce high quality products (Ipek *et al.*, 2013; Ngai *et al.*, 2014).

Much work related to the system were performed by previous authors (Aylor *et al.*, 1992; Barschdorff *et al.*, 1991; Huang *et al.*, 1993; Huang *et al.*, 1994; Márkus *et al.*, 1987; Nguyen *et al.*, 1991). Huang *et al.* (1994) found that the application of ANN in manufacturing has a potential to increase the quality of product. They also stated that the ANN is capable to reduce the reaction time of a manufacturing system and improve its reliability and intelligent. Márkus *et al.* (1987) claimed that ANN had a high potential for automated manufacturing through his analysis. Barschdorff *et al.* (1991) stated that the advantages of ANN are that the desirable in intelligent manufacturing practices. The other reason of choosing ANN is due to the desirable output that can be achieved with a considerable degree of accuracy using a number of network architectures (Huang *et al.*, 1993). For example, Nguyen *et al.* (1991) found that the ANN approach in solving kinematic problem for robot can be an effective method to learn the manipulator. Aylor *et al.* (1992) developed the ANN in robot manufacturing that has a capability to consider the unknown number of faults, errors and limitations of poorly constructed system (robot) by providing a high accuracy of solution.

## 2.9 Surface Quality and Mechanical Properties of End Product

In current manufacturing technology, the net-to-shape product is emphasized to eliminate the unnecessary activities, additional time, material waste and total cost. LM technology offers the manufacturing process of the part without considering the complexity of the geometric. In some cases, the LM has limitations which include poor surface finish due to staircase effect (Ahn *et al.*, 2008; Ahn *et al.*, 2009; Galantucci *et al.*, 2009; Jin *et al.*, 2015; Pandey *et al.*, 2003b).

Much work has been conducted by previous researchers (Ahn *et al.*, 2009; Ahn *et al.*, 2012; Hope *et al.*, 1997; Ma *et al.*, 1999; Pandey *et al.*, 2003a) to improve the part surface finish and mechanical properties of part model.

The experiments were conducted by Ahn and his workers (2012) to quantify the surface roughness of the parts processed by Laminated Object Manufacturing (LOM). The result shows that this approach could be practicable and valuable for predicting the surface roughness of parts fabricated by LM technology.

Ahn *et al.* (2009) proposed the method to predict the surface roughness of LM processed parts. The work released that the surface roughness values could be calculated at surface angles that were difficult or impossible to measure.

Ma and He (1999) presented an adaptive slicing and selective hatching strategy for layered manufacturing. This technique is able to produce an accurate and smooth part surface. Their finding showed that the developed algorithms operate directly upon a Non-Uniform Rational Basis Spline (NURBS) based CAD surface model for avoiding possible problems in connection to the STL interface. In addition, their work also provides an optional solution to the problem with mixed tolerances for the slicing of an LM model.

Hope *et al.* (1997) introduced an adaptive slicing procedure for improving the geometric accuracy of layered manufacturing techniques uses layers with sloping boundary surfaces that closely match the shape of the required surface. This method reduces the stair case effect which is characteristic of layered components with square edges.

Recent work in LM extents to improve profile shape, dimensional accuracy and surface quality of parts. Process parameters resulting poor surface finish, accuracy and quality of FDM part models are also reviewed. For example, many authors stated that the surface roughness, dimensional accuracy and shape quality of models depend on layer thickness and orientation of part deposition (Boschetto *et al.*, 2012; Latiff *et al.*, 2014; Rahmati *et al.*, 2015; Song *et al.*, 2014). The lower the layer thickness which incorporated with the OPDO produces better surface finish and high accuracy part models (Campbell *et al.*, 2002; Nezhad *et al.*, 2009).

However, the orientation of part deposition also affect build time (Luo *et al.*, 2015; Villalpando *et al.*, 2014), cost (Raut *et al.*, 2014; Zhang *et al.*, 2015) and the complexity of support structure (Huang *et al.*, 2015; Kumar *et al.*, 2012; Leary *et al.*, 2013; Leary *et al.*, 2014). Determining the OPDO which results in a good surface finish may take a longer build time.

The support structures required in FDM manufacturing process has its own drawbacks. These support structures further hinder the fabrication efficiency and part surface quality of the marks left (Ahn *et al.*, 2005; Majhi *et al.*, 1999). In some cases, it is unable to produce the part model at lower cost and shorter time with a good surface finish due to variation in shape and orientation of part deposition. This support the review by Kulkarni *et al.* (2000) who stated that the selection of orientation of part deposition resulted in a reduction of considered factors such as build time and cost.



The experimental results by Li *et al.* (2010) showed that the optimization model increase the efficiency of the LM process thus reduce the cost. Other works in related fields (Ghorpade *et al.*, 2007; Moroni *et al.*, 2015) found that the optimize part orientation as a key factor in reducing build time. In certain applications, other considerations (i.e. surface finish, strength and amount of trapped material) are taken into account. Studies by other workers (Fatimatuzahraa *et al.*, 2011; Huang *et al.*, 2014; Jin *et al.*, 2015) focused on raster angle (range between 30° and 45°) which have significant effects on the mechanical properties and surface quality.

The reviews of this work cover two types of layers, flat and curve. Chakraborty *et al.* (2008) found that the part fabricated by curved layers result in better strength. This finding is consistent with the work by Savalani *et al.* (2015) in which high strength was produced through bending test.

Previous work (Kim *et al.*, 2008; Masood *et al.*, 2010; Rayegani *et al.*, 2014; Sood *et al.*, 2009, 2010) studied on the effects of process parameters likes orientation of part deposition, build materials, build speed and build volumes on surface quality and mechanical properties of FDM part model. These parameters are important to determine the desired tensile strength, compressive strength, dimensional accuracy, surface finish, part build time and process cost (Boschetto *et al.*, 2015; Ivan *et al.*, 2015; Leacock *et al.*, 2015; Panda *et al.*, 2015).

Work by Mishra *et al.* (2014) attempted to maximise the tensile strength of the FDM processed parts by controlling the process parameters. Their results show that the change in raster deposition angle gives maximum tensile strength of part. This finding is consistent with the work conducted by previous researches (Ludmila *et al.*, 2013c; Rayegani *et al.*, 2014).

## 2.10 Process Parameters

The study on effects of FDM process parameters on quality and precision of part model were carried out by Huang *et al.* (2014). The factors that contributed to a better quality products include the extrusion temperature, envelope temperature, extrusion velocity, filling velocity are identified as important parameters to produce a better quality products (Chang *et al.*, 2011; Li *et al.*, 2011; Peng *et al.*, 2010; Ramanath *et al.*, 2008). Peng *et al.* (2010) stated that the parts accuracy, however, can also be influenced by errors in numerical system influenced and material shrinkage.

ABS is a common thermoplastic used in FDM due to its unique properties such as low cost, good process ability, strength and rigidity (Jami *et al.*, 2013; Masood *et al.*, 2010). According to Jami *et al.* (2013) this plastic can retain its original shape at slightly elevated temperatures. Due to current demand by industry, other materials deposition in FDM process are introduced including polyamide, polycarbonate, polyethylene and polypropylene (Ludmila *et al.*, 2013b).

The mechanical properties of thermoplastic materials in FDM was improved in order to fulfil medical application (Drummer *et al.*, 2012), engineering applications (Lee *et al.*, 2005) and industrial requirements (Garg *et al.*, 2015; Masood *et al.*, 2010). The coating of ABS with metal and the combination of polyethylene with wood flour are some examples of new composite materials used in FDM. Both materials were tensile tested and provide a higher strength compared with common thermoplastic materials (Hui *et al.*, 2011; Kannan *et al.*, 2013). Ceramic material can be used as another option in FDM because of its excellent strength property. The innovation of new materials make the FDM becomes a viable competitive manufacturing process (Bandyopadhyay *et al.*, 2006; Bellini *et al.*, 2005).

Previous researchers used a few models of FDM machines in their work since it was introduced in 1986. The work focused improving process parameters such as temperature and velocity for better quality product (Ahn *et al.*, 2002; Bellini *et al.*, 2003; Pandey *et al.*, 2003b). For examples, two 3D printing machines, FDM 3000 and Zortrax (adoptions of FDM technology) are discussed.

### 2.11 Fused Deposition Modeling 3000 (FDM 3000)

The FDM 3000 machine used in this work is shown in Fig. 2.4. This machine uses the Insight software manufactured by Stratasys to manipulate and prepare the incoming STL data. Both part model and support material used in this machine is acrylonitrile butadiene styrene (ABS) provided in wire filament form. The Water Soluble Support (WSS) type of ABS is used for support structures that can be easily removed from the part model.



Figure 2.4: FDM 3000 machine ("<http://www.stratasys.com/>").

The removable extrusion head of FDM 3000 machine is illustrated in Fig. 2.5. The main features of this head are ABS filament stock, drive wheels, liquefier and tips.

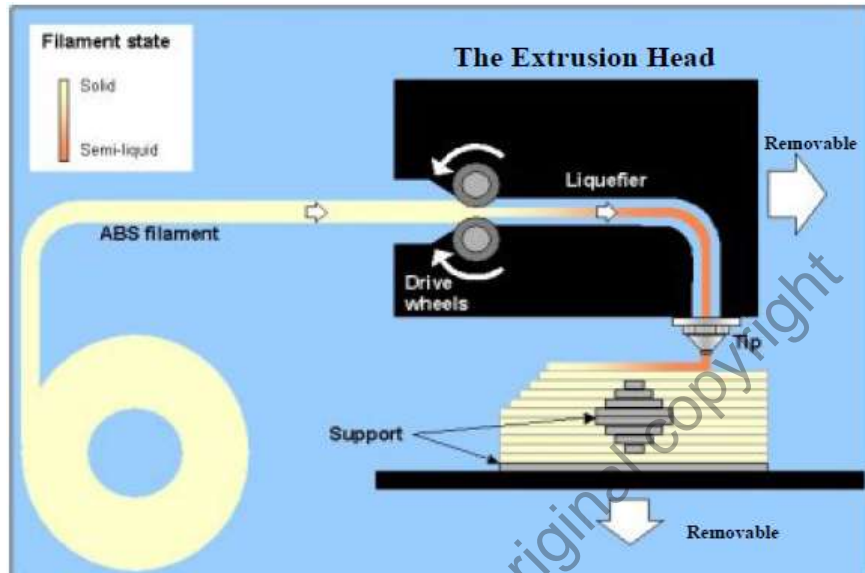


Figure 2.5: Extrusion Head of FDM ("http://www.stratasys.com/,").

### 2.11.1 Drive Blocks

The drive blocks refer to the raw-material feeding mechanisms and they are mounted on the back of the head. The drive blocks are controlled by computer and are able to load precision unload the filament. They are composed of two parallel wheels fixed to a small electric motor by gears. The wheels have a plastic or rubbers tread and turn opposite to each other with small gap. When the wheels are operating and the end of the filament is located between them, they continue to pull the material, according to the rotation direction. While loading, the filament is pushed in a horizontal direction on the platform by a tip. This process starts with the development of base support structure on machine platform before any part model and ESS are developed.

### 2.11.2 The Heating Chamber/Envelope

The chamber for heating in FDM 3000 machine is a 90° curved elbow covered in a heating element. It has two main functions; 1) to alter the direction of the filament flow so that the material is extruded in a vertically downward position and 2) to function as a melting area for the material. The heating element is closed-loop controlled, and has feedback thermopiles to ensure the consistent temperature throughout. The filament coming from the chamber exit is in a semi molten state for easy extrusion. The heating parameters used in FDM 3000 machine are listed in Table 2.2.

Table 2.2: Heating parameters in FDM 3000.

<b>Parameters</b>	<b>Min. Value ( °C)</b>	<b>Med. Value ( °C)</b>	<b>Max. Value ( °C)</b>
Model Temperature	265	268	270
Support Model Temperature	210	218	233
Chamber Temperature	60	65	70

### 2.11.3 Tips

Two tips for part model and support structure are utilized to decrease the diameter of the extruded filament for better detailed modeling. The extruding surface of the tip is flat and heated to maintain the shearing surface of material.

The common problems such as nozzle clogging, uncertain substance invasion, substrate deformation and collapse lead to unexpected total cost including time consuming and money (Kim *et al.*, 2015). The research work by Kim *et al.* (2015) looked

at material deposition process with different in pressure and supplied current to feed motor are able to eradicate these problems.

## 2.12 Current Technology Adopted the FDM Method

Zortrax was founded by Tomasiak and Olchanowski in 2011. This machine (Fig. 2.6) makes 3D physical models by depositing melted materials such as Z-ABS resins. Unlike FDM, the Zortrax uses a single tip to produce the model and the support structures in their manufacturing process. The incoming STL data obtained from this machine are manipulated and prepared using Zortrax Z-Suite software ("<https://zortrax.com/>,").



Figure 2.6: Zortrax M200 Professional Desktop 3D Printer ("<https://zortrax.com/>,").

## 2.13 Summary

Feature-based technique is able to integrate the CAD and CAM systems for process planning in both machining and LM manufacturing processes. However, from

the reviews, the specific features used for machining is not applicable to be used in LM, vice versa. The reason is because of these processes contain different characteristics in which the volumetric unit has to be discarded (machining) or added (LM) during the manufacturing of the part model. In addition, the volumetric unit in FDM is also used to develop the support for the part model.

In FDM process planning, the support generation and orientation of part deposition are interrelated. The information of support generation can be used to automate the choice of orientation of part deposition in process planning.

The contact area between support and part model degrades the surface quality. The minimal contact area between these two entities is in interest to improve the surface quality of part model produced using FDM technology.

Thus, this work will propose a method for optimization of orientation of part deposition using ANN. The support volume and amount of support structure are the main parameters used as inputs for the ANN. The process planning for this work can be automated and lead to low manufacturing time, increase quality of product and less human errors. Besides that, the contact surface between the part and support structure is also improved thus, improve the quality of final part surface.

## CHAPTER 3

### METHODOLOGY

#### 3.1 Introduction

This chapter describes the methodology of this research work which can be divided into three parts. Part 1 is Feature-Based Support Generation System, Part 2 is Optimum Part Deposition Orientation (OPDO) Determination using Artificial Neural Network and Part 3 is Surface Improvement.

The general process flow of this work is displayed in Fig. 3.1.

Process flow	Machine/Equipment/Software
<b>1. Feature-Based Support Generation System</b> a) Convert CAD drawing to .STL file. b) Redraw the 2D slices and offset operations for lower layer.	Solid Works CAD Visual Basic
<b>2. OPDO Determination using ANN</b> a) Data extraction (ESF). i) Determine volume of support structure. ii) Determine number of support structure. b) Accuracy of ANN (Structures 1 – 5). c) Feature recognition. d) Fabrication of product.	Visual Basic MATLAB – ANN MATLAB – ANN FDM machine
<b>3. Surface Improvement</b> a) Recognize feature (ESF). b) Fabrication of product. c) Determine surface roughness between part model and ESS.	Visual Basic FDM machine Mitutoyo Tester

Figure 3.1: The general process flow of current work.



## 3.2 Part 1 - Feature-Based Support Generation System

This section explains describes the methodology used in the current research. The work commences with the generation of 2D polygon. The offsetting operations for internal and external of the lower layer by considering Permitted Overhang Area (POA) are introduced. Next, the features based on the adjacency of upper and lower layers are identified. The volumes of ESS and Base-Support Structure (BSS) will be then measured.

### 3.2.1 Methodology

In developing part model, the 2D slices were produce through a slicing technique. The slices are planar polygon which are composed of internal and external contour rings (Guo *et al.*, 2007). In this work, the recognition of the support feature depends on distinct area of these pair of slices (i.e. upper layer and lower layer). The utilization of POA to offset the internal and external of the lower layer was introduced.

#### 3.2.1.1 Permitted Overhang Area and Offset Generation

POA is based on angle in which the support feature has an ability to support by themselves and is known as self-support angle (Kulkarni *et al.*, 2000). At this angle, the overhang area of successor layer (either part model or support structure) can be produced with no support. In this experiment, the highest self-support angle is  $\alpha = 45^\circ$  (Chalasan *et al.*, 1995; Montero *et al.*, 2001). Therefore, the largest span of the POA is similar to the height of the layer thickness. The uniform slicing process and the support feature formation is shown in Fig. 3.2. This figure shows the POA, the developed at Self-Support

angle,  $\alpha$ , and the layer thickness,  $t$ . These parameters were used to identify the features prior to the construction of part model and ESS.

In this work, the concept of feature-based was introduced. Two support features of SSF (Layer 2 overhang area) and ESF (Layer 3 overhang area) are shown in Fig. 3.2(a). The SSF is the feature that is identified when the overhang area is within the range of POA while the ESF is the feature when the overhang area exceeded POA. The ESS is needed for the purpose of obtaining the adjacency in developing direction for ESF as shown in Fig. 3.2(b).

©This item is protected by original copyright

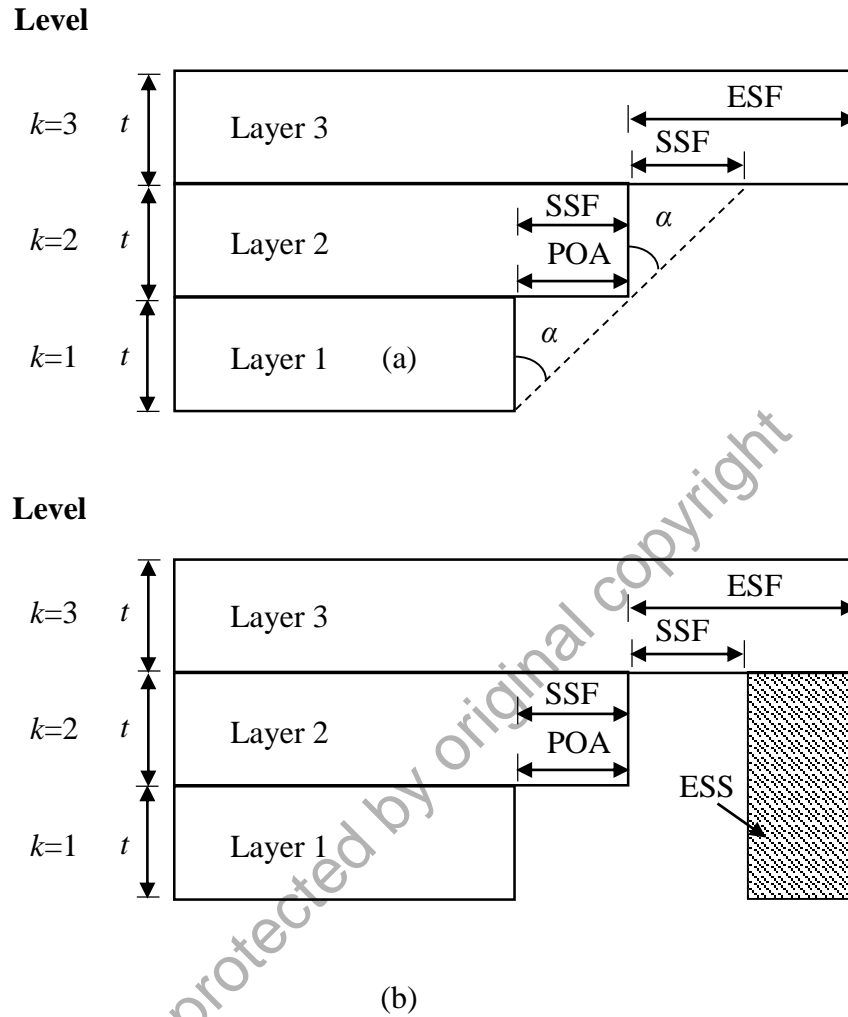
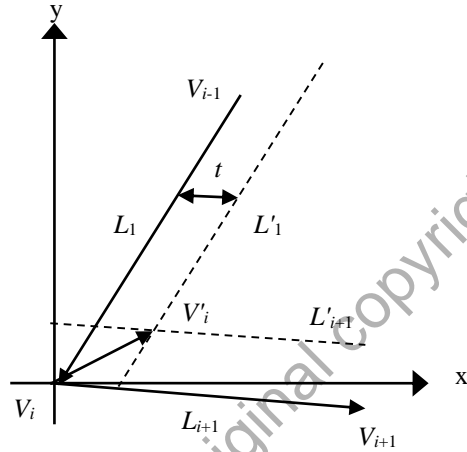


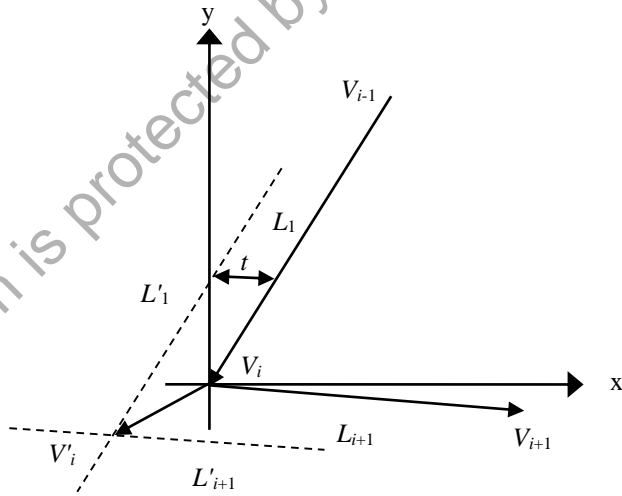
Figure 3.2: Process of uniform slicing: (a) ESF and SSF and (b) POA.  $\alpha$  is the support angle,  $t$  is the uniform layer thickness and ESS is the External Support Structure..

The maximum POA ( $\alpha = 45^\circ$ ) is a basis for the new lower layer generation. Therefore, the external and internal rings of lower layer contour were offset by a continuous distance,  $t$ . The external contour ring(s) were offset towards the outside and the internal ring(s) were offset towards the inside as shown in Figs. 3.3(a) and (b), respectively. Then, the new unit vectors for external and internal are given by  $\vec{l}_i$  and  $\vec{l}_{i+1}$  and shown in the figures. These unit vectors for external and internal are given by the corresponding towards the outside and towards the inside offset of the original location

of the vertices enclosure which are identified by  $V_{i-1}$ ,  $V_i$  and  $V_{i+1}$ . The offset distance for both towards the outside and towards the inside are referred as  $t$ .  $L'_i$  and  $L'_{i+1}$  are the equidistant lines of  $L_i$  and  $L_{i+1}$ , respectively due to  $t$  value as shown in Fig. 3.3.



(a) Offsetting of an external ring (dashed lines).



(b) Offsetting of an internal ring (dashed lines).

Figure 3.3: Offsetting a slice.  $V_i$  is the origin of the temporary coordinate system at the arbitrary vertices of the loop.  $L_i$  and  $L_{i+1}$  are the vectors produced by  $V_{i-1}V_i$  and  $V_iV_{i+1}$ , respectively.

If  $\vec{l}_i$  and  $\vec{l}_{i+1}$  are unit vectors of  $L_i$  and  $L_{i+1}$  respectively, hence the formula can be expressed as (Yang *et al.*, 2002):

$$\begin{aligned}\vec{l}_i &= x_i \vec{i} + y_i \vec{j} \\ \vec{l}_{i+1} &= x_{i+1} \vec{i} + y_{i+1} \vec{j}\end{aligned}\quad (3.1)$$

As for new offsetting of lower layer's internal rings:

$$\begin{aligned}-y_i x + x_i y &= t \\ -y_{i+1} x + x_{i+1} y &= t\end{aligned}\quad (3.2)$$

As for new offsetting of lower layer's external rings:

$$\begin{aligned}-y_i x + x_i y &= -t \\ -y_{i+1} x + x_{i+1} y &= -t\end{aligned}\quad (3.3)$$

where, vectors  $(x_i, y_i)$  and  $(x_{i+1}, y_{i+1})$  are the vectors formed by coordinates  $V_{i-1}V_i$  and  $V_iV_{i+1}$  from the origin, respectively.

As  $L'_i$  and  $L'_{i+1}$  are not parallel, then  $x_i y_{i+1} - x_{i+1} y_i \neq 0$ . Thus, by solving Equations (3.2) and (3.3), towards the inside and towards the outside coordinates can be described as following:

$$(x, y)_{\text{towards the inside}} = \left( \frac{(x_{i+1} - x_i)t}{\begin{vmatrix} x_i & y_i \\ y_i & y_{i+1} \end{vmatrix}}, \frac{(y_{i+1} - y_i)t}{\begin{vmatrix} x_i & y_i \\ y_i & y_{i+1} \end{vmatrix}} \right)\quad (3.4)$$

and;

$$(x, y)_{\text{towards the outside}} = \left( -\frac{(x_{i+1} - x_i)t}{\begin{vmatrix} x_i & y_i \\ y_i & y_{i+1} \end{vmatrix}}, -\frac{(y_{i+1} - y_i)t}{\begin{vmatrix} x_i & y_i \\ y_i & y_{i+1} \end{vmatrix}} \right)\quad (3.5)$$

### 3.2.1.2 Area of New Lower Layer

The area of new lower layer because of offsetting generation can be measured as follows:

$$\text{Area of New Lower Layer} = POA_{ex} \cup A_{ex} \cup_i^n POA_{in} \quad (3.6)$$

where,  $POA_{ex}$  is the area of POA for external contour ring,  $A_{ex}$  is the area of the external contour ring,  $n$  is the number of internal contour ring and  $POA_{in}$  is the area of POA for internal contour ring.

The area for new lower layer cause of offsetting generation was performed again for each pair of layers in the order that started from the Upper\_most layer to the Lower\_most layer and will be discussed in following section. The area of new lower layer generation is illustrated in Fig. 3.4.

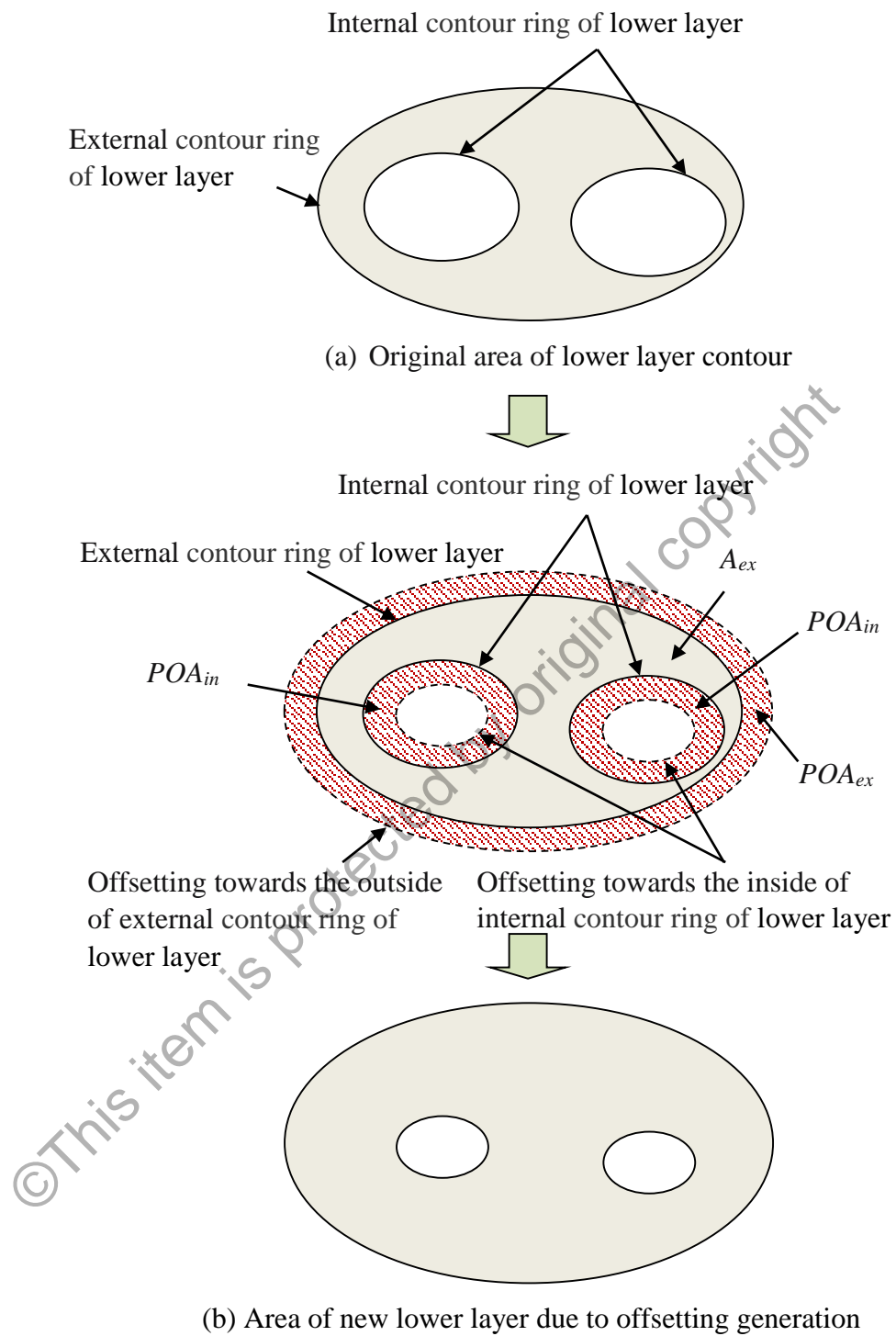


Figure 3.4: Generation of a lower layer new area as a result of offsetting operation.  $A_{ex}$  denotes the area for external contour,  $POA_{ex}$  denotes the area of POA for external contour ring and  $POA_{in}$  denotes the area of POA for internal contour ring.

### 3.2.1.3 Layer Adjacency and Area Difference for Feature Verification

The techniques of layer adjacency and difference of area between upper and lower layers were proposed to obtain the same result of feature verification in a simple way. In this work, the methods are divided into four case studies. For each case, the *Cross-Sectional slice Region Area (CSRA)* of subsequence layers for sample manufacturability are depicted in Figs. 3.5 to 3.8. The Layer  $P$  was manufactured after Layer  $Q$  was produced. The Layer  $Q'$  is offsetting of Layer  $Q$ . The Layer  $P'$  is the projection of Layer  $P$  to Layer  $Q$  in  $z$  direction.

## 3.3 Case Study

### 3.3.1 Case Study 1: Non-Supported Features (NSF)

If  $(P' \cap Q) \in Q$ , then Layer  $P$  has adjacency in  $z$  direction. If  $(P' \cap Q)' \cap P' = \emptyset$ , then Non-Supported Feature (NSF) was recognized among these two layers. Therefore, the Layer  $Q$  is the full adjacent of Layer  $P$ . By employing the method of area difference between the upper and lower layers, similar outcome was achieved if  $P' - Q' \leq 0$  (Fig. 3.5).



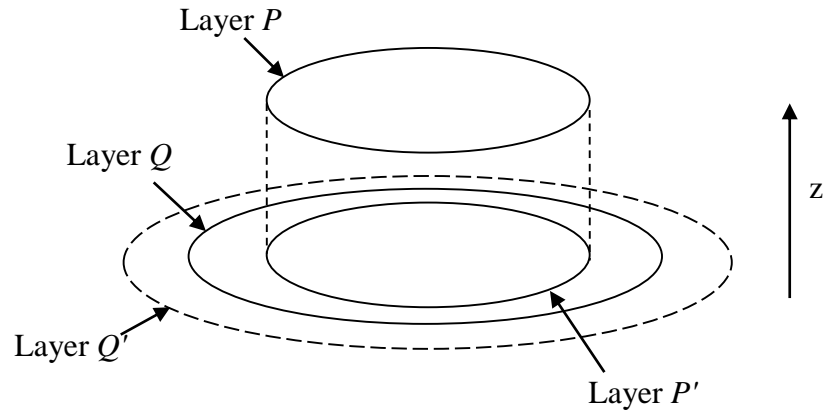


Figure 3.5: Case Study 1: Non-Supported Features.

### 3.3.2 Case Study 2: Self-Supported Features (SSF) Require Non-Support

#### Material

For this case, the same situation to Case Study 1 was taken (If  $(P' \cap Q) \in Q$ , then Layer  $P$  has adjacency in  $z$  direction). However, if  $(P' \cap Q)' \cap P' = \emptyset$ , then the support feature was identified among the layers as shown in Fig. 3.6. If  $((P' \cap Q)' \cap P') \cap (Q')' = \emptyset$ , subsequently the support feature that was identified does not need the support volume since all of its area were covered in the POA. In other words, the Layer  $P$  has partial adjacency in the vertical direction from its former Layer  $Q$  and can be manufactured with no support. By employing the area difference between the upper and lower layers method, similar outcome of feature verification was obtained if  $P' - Q' \leq 0$ .

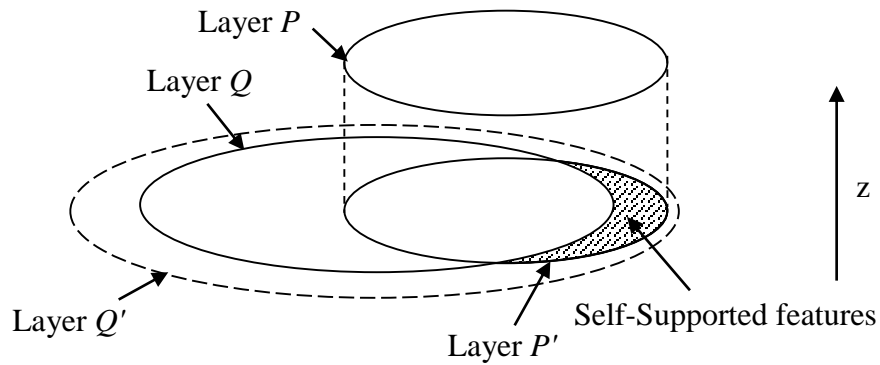


Figure 3.6: Case Study 2: Self-Supported Features require non-support material.

### 3.3.3 Case Study 3: External-Supported Features (ESF) using Support Material

This case study is similar to Case Study 2. However, if  $((P' \cap Q)' \cap P') \cap (Q')' = \emptyset$ , next the Layer  $P$  had a partial adjacency in the vertical direction from its former Layer  $Q$ . It required an ESS under Layer  $P$  support feature to obtain the adjacency in creating  $z$  direction, and is thus easily manufactured. By using the method of difference in area between upper and lower layers, the similar outcome of feature verification was achieved if  $P' - Q' > 0$  (Fig. 3.7).

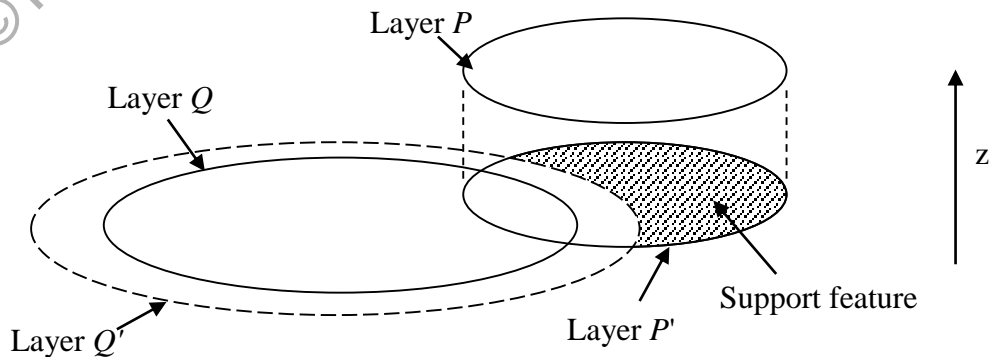
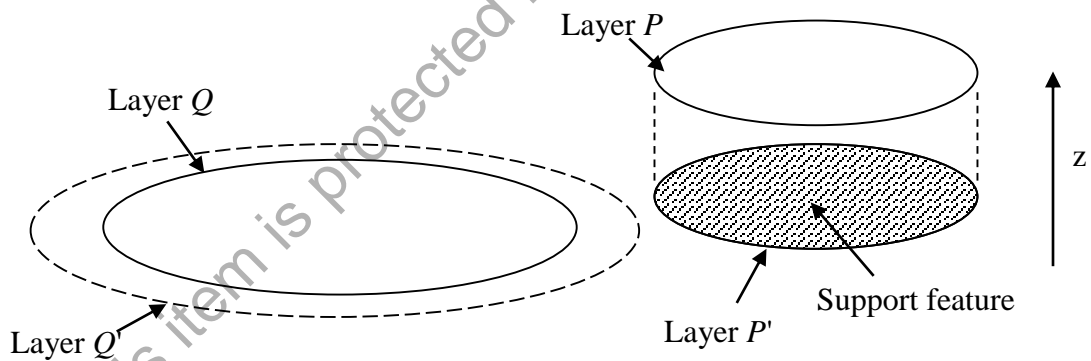


Figure 3.7: Case Study 3: ESF using support material.

### 3.3.4 Case Study 4: Non-Adjacency External-Supported Features (ESF) using Support Material

In this case, Layer  $P$  does not have the adjacency in  $z$  direction (i.e. If  $P' \cap Q = \emptyset$ , next the support feature was recognised as presented in Fig. 3.8. Layer  $P$  was unable to discover an adjacency in the direction that was vertical from its former Layer  $Q$ , hence, all area contain in Layer  $P$  was recognized as support features. The ESS was needed to support the entirety of Layer  $P$  for the purpose of increasing the adjacency in creating  $z$  direction, and can be easily manufactured. By utilizing the method of area difference between upper and lower layers, similar result of feature verification was gained if  $P' - Q' > 0$  (Fig. 3.8)



© Figure 3.8: Case Study 4: Non-adjacency ESF using support material.

## **3.4 Part 2 - Optimum Part Deposition Orientation Determination using Artificial Neural Network**

### **3.4.1 Methodology**

This section describes the system implementation in selecting the Optimum Part Deposition Orientation (OPDO). The integration of these techniques have three phases: Phase 1 - 2D Polygon Generation; Phase 2 - Feature Identification and; Phase 3 - Optimum Part Deposition Orientation Determination using Multilayer Perceptron (MLP) Network.

In this study, 100 models were used for the accuracy analysis. 600 data set were generated in which, for each model, 6 data set represent different orientations of pre-defined directions. These data set were then partitioned into two types, training and testing. The training data set was used to train the network in order to fit the model. Meanwhile, the testing data set was used to evaluate its performance and generalization ability. Out of 600 data set, 400 set were used for training and 200 set were used for testing. In general, the process flow of the system is illustrated in Fig. 3.9.

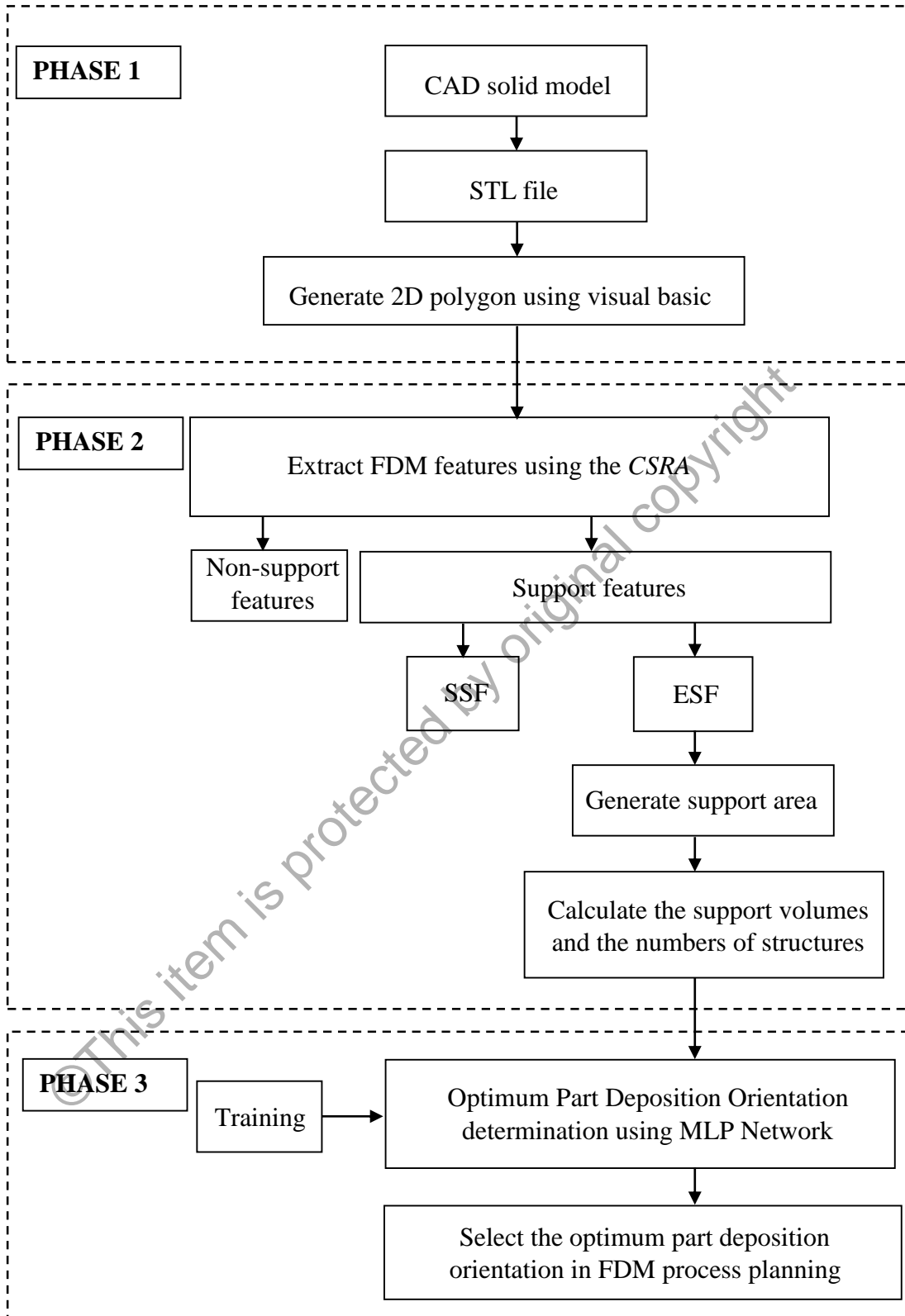


Figure 3.9: Flowchart for Feature-based Support Generation Data Extraction and analysis system.

### 3.4.2 Phase 1: 2D Polygon Generation

Phase 1 starts with the steps that follow: 1). The part model employed in this work (Fig. 3.10) was evaluated in six pre-defined directions (Table 3.1). The part model original orientation was originated as appeared in CAD; 2) The uniform slicing technique was applied on the part model (in STL file) from the lower to the upper and; 3) At one time, each pair of two layers were used and the part's *CSRA* was subtracted. This operation was performed again for every pair of layers, in the order starting from the Upper most layer to the Lower most layer. These steps involved the use of Visual Basic (VB) software. The VB is a computational programming language providing features such as graphical user interfaces, object-oriented features, structured programming and much more. (Deitel *et al.*, 2002).

For a 2D, *CSRA* plane surface area created by a uniform slicing method across the part at layer  $k$ -th can be written as follows:

$$CSRA_{Upper\_layer} = CSRA_{k+1} \quad (3.7)$$

$$CSRA_{Lower\_layer} = CSRA_k \quad (3.8)$$

where,  $k \in \{1, 2, \dots, (N-1)\}$ . The *CSRA* is the *Cross-Sectional Slice Region Area*,  $k$  is the layer of part model and  $N$  is the amount number of layers for part model.

*Resultant Area (RA)* between the  $k+1$  (Upper layer) and  $k$ -th (Lower layer) layers is described as a subtraction of Equations (3.7) and (3.8). Then, the *RA* can be expressed as below:

$$RA = CSRA_{k+1} - CSRA_k \quad (3.9)$$

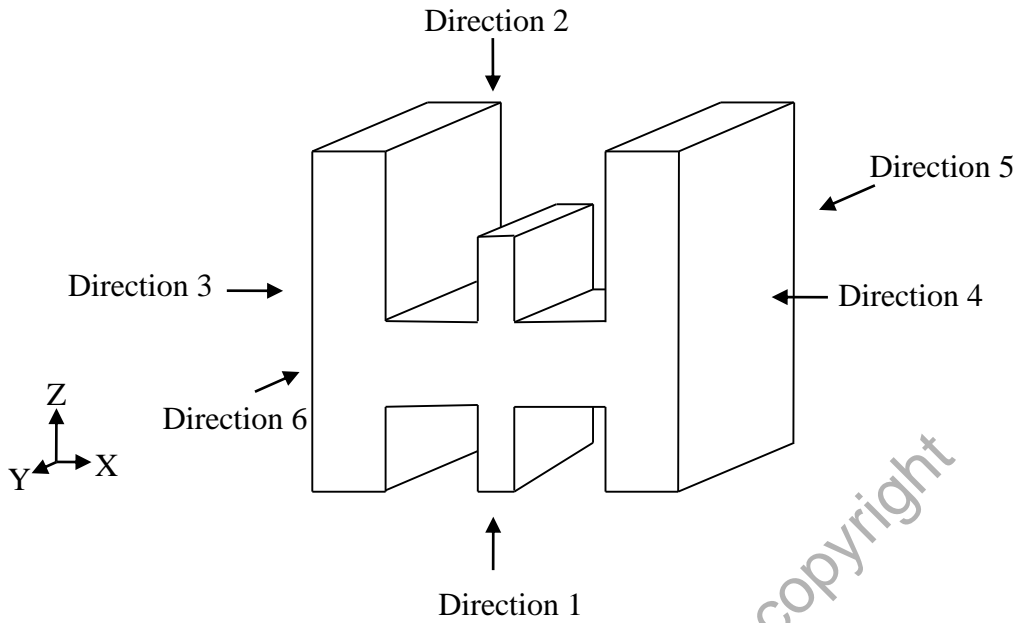


Figure 3.10: Sample of part model in pre-defined directions of x, y and z axes.

Table 3.1: Part model in six directions with regard to the  $\pm x$ ,  $\pm y$  and  $\pm z$  axes.

Orientation	Plane parallel to FDM machine working table	Direction of deposition	Uniform slicing direction
Direction 1	XY plane	Z	Parallel to XY plane
Direction 2	XY plane	-Z	Parallel to XY plane
Direction 3	YZ plane	X	Parallel to YZ plane
Direction 4	YZ plane	-X	Parallel to YZ plane
Direction 5	XZ plane	Y	Parallel to XZ plane
Direction 6	XZ plane	-Y	Parallel to XZ plane

### 3.4.3 Phase 2: Features Identification

In this phase, the support structure is categorized into ESS and BSS as presented in Fig. 3.11. The elaborations of these structures in relation to the working features are exposed in next section.

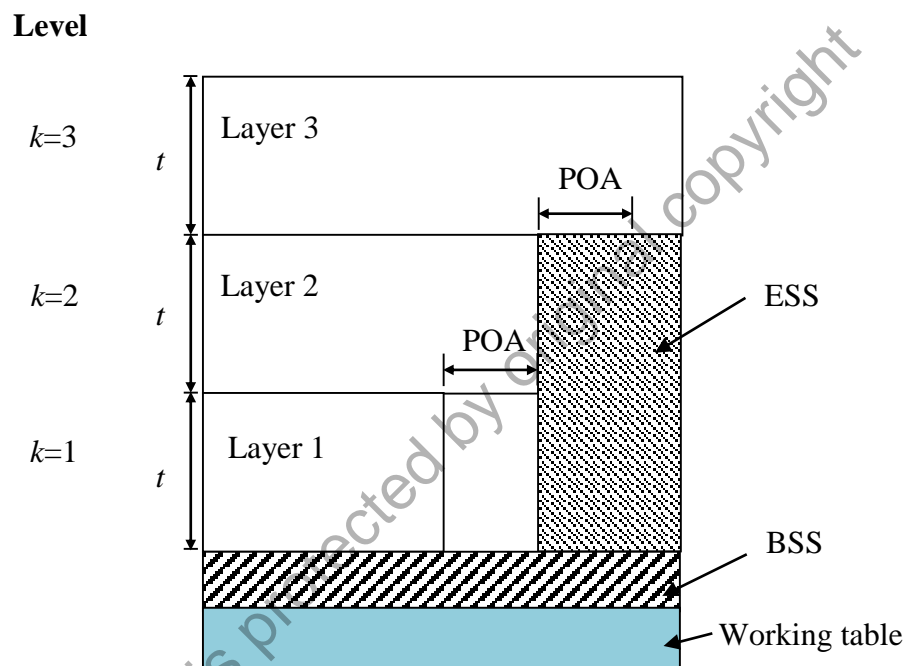


Figure 3.11: ESS and BSS developed in FDM process.

#### 3.4.3.1 External-Supported Features (ESF)

Phase 2 explains the methodology used for ESF identification (Case Studies 3 and 4 as described in Sections 3.3.3 and 3.3.4, respectively). The steps involved the determination of the area, the volume and the amount of ESSs. The features identification is described later in three stages.



At Stage 1 (Fig. 3.12), the system commenced with the extraction of the LM features using the Equation (3.9) by considering the offsetting generation of  $CSRA_k$ . Then, the Equations (3.8) and (3.9) can be re-written as follow:

$$CSRA_{Offset\_Lower\_layer} = CSRA'_k \quad (3.10)$$

$$RA' = CSRA_{k+1} - CSRA'_k \quad (3.11)$$

where,  $CSRA'_k$  is the *Cross-Sectional Slice Region Area* of offset lower layer and  $RA'$  is the Resultant Area of upper and offset lower layers. If  $RA' > 0$ , then the ESF was identified.

The system was continued to calculate the area of support and the volume of support structure with the use of the Equations (3.12) and (3.13) in Stage 2. At stage 3, the number of groups was identified. These calculated volume and the number of groups were used to select the OPDO. The Stages 2 and 3 are concurrently executed. The system determined the amount of support structure with two specific situations are described below.

The creation of area for support at layer  $k$ -th is explained as:

$$Area\ of\ Support_k = (RA_k \cup RA_{k+1}) - Area\ of\ Part\ Model_k \quad (3.12)$$

The collection of support area creates ESS which is used to sustain the detected ESF. The volume of ESS is defined as:

$$S_{ESS\ Volume} = \bigcup_{i=(1,k)} Support\ Area_i \times t \quad (3.13)$$

where,  $t$  is the thickness of layer.

The relationship between the volume(s) of support structures was checked with two situations in order to decide the amount of support structures. These conditions are:

***Situation 1***

$$\text{If Area of Support}_k \cap \text{Area of Support}_{k+1} = \emptyset, \quad (3.14)$$

then *Area of Support<sub>k</sub>* and *Area of Support<sub>k+1</sub>* are in the different structure.

***Situation 2***

$$\text{If Area of Support}_k \cap \text{Area of Support}_{k+1} \neq \emptyset, \quad (3.15)$$

then *Area of Support<sub>k</sub>* and *Area of Support<sub>k+1</sub>* are in the same structure.

A detailed algorithm process flow for feature identification in Stages 1 to 3 is represented in Fig. 3.12.

**3.4.3.2 Base-Support Structure (BSF)**

BSS refers to a support structure that is required to support the overhang volume of part model and volume of ESS at layer  $k=1$ . In FDM, the first layer of part model and ESS ( $k=1$ ) was not located straightly on the working table. The gap between  $k=1$  and the working table was filled with support volume of BSS (Fig.3.11) for obtaining the adjacency and hence, easy to manufacture. The total support volume of BSS is described as the following:

$$\text{Base-Support}_{\text{Volume}} = m \times t \times (RA_1 \cup RA_2 \cup \text{Area of Part Model}_1) \quad (3.16)$$

where,  $m$  is the amount of Base-Support layer and  $t$  is the thickness of the layer. In this work, the uniform slicing with layer thickness,  $t = 0.01$  mm and the quantity of layer for BSS,  $m = 5$  were utilized for every orientation of part deposition involved.

For both ESS and BSS, the total volume of support in the whole fabrication process of the part model is then explained as:

$$S_{Total\ Support\ Volume} = \sum_{i=1}^n S_{ESS\ Volume} + Base-Support_{Volume} \quad (3.17)$$

©This item is protected by original copyright

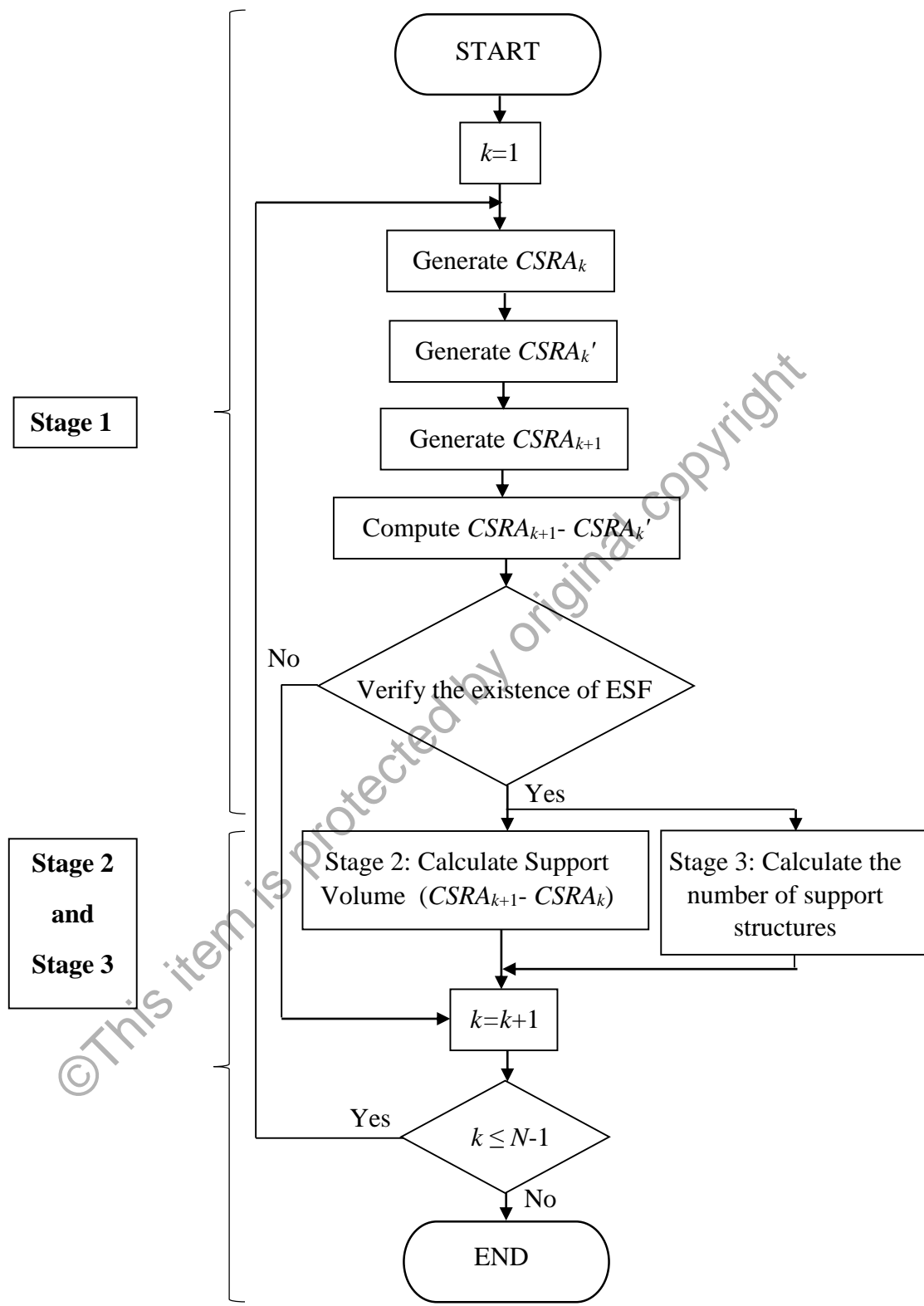


Figure 3.12: Algorithm flowchart for ESF extraction.

#### **3.4.4 Phase 3: Optimum Part Deposition Orientation (OPDO) Determination using MLP Network**

In Phase 3, the ANN was used as a tool for determining the OPDO. The neural network used in this work is the Multilayer Perceptron (MLP) network. Basically, the MLP network consists of number of layers which are an input layer, an output layer and one or more hidden layers. Each layer in MLP network has a number of basic processing elements called neurons or perceptrons. The layers in MLP network are connected in a feed-forward topology by weighted connections through which each neuron receives inputs, and after generating an output, broadcasts it to neurons in the next layer.

The Levenberg-Marquardt backpropagation algorithm is used to train the MLP network. The training algorithm has good convergence rate and suitable for training small and medium sized problem (Yu *et al.*, 2011).

First, all parameters for the Levenberg-Marquardt backpropagation algorithm are set to default values in the MATLAB neural network toolbox. Next, the hyperbolic tangent and linear which considered as the activation function will be selected for hidden and output layers, respectively. Then, the MLP network will be run for 5 times for each number of hidden nodes ranging from 1 to 50 nodes to avoid the network stuck in local minima and good generalization ability. This network is run with different sets of weight and bias initializations. Finally, the highest testing accuracy will be recorded.

The Optimum Part Deposition Orientation (OPDO) is determined by least total support structure volume which has least amount of support structure. Two stages of MLP networks (MLP 1 network and MLP 2 network) are developed in order to decide the OPDO. In this work, the correlation between input and output of MLP network will be designed to provide high classification accuracy and optimum network structure.

The network in Stage 1 involve the use of total volume of support structure as the inputs for MLP 1 network. The network in Stage 2 (MLP 2 network) consists of combination of outputs (from Stage 1, i.e. MLP 1 network) with the new features of amount of support structure.

Three structures of MLP 1 network and one structure of MLP 2 network are proposed in Stages 1 and 2, respectively are summarized in Table 3.2. These structures are analysed to find the best MLP 1 network structure that will be used with MLP 2 network.

Table 3.2: Structures of MLP 1 and 2 networks.

Stage	MLP Structure
1	Structure 1: MLP 1 (6 Input nodes, 6 Output nodes)
	Structure 2: MLP 1 (7 Input nodes, 6 Output nodes)
	Structure 3: MLP 1-6 : Parallel (7 Input nodes, 6 Output nodes)
2	Structure 4: MLP 2 (12 Input nodes, 6 Output nodes)
	Structure 5: MLP 1-6 : Parallel (7 Input nodes, 6 Output nodes) combined with MLP 2 (12 Input nodes, 6 Output nodes)

#### 3.4.4.1 Structure 1

In Stage 1, the MLP network is used to identify the minimum support volume. This network has six inputs,  $V_{pq}$  and six outputs,  $O_{rq}$  (Structure 1).  $V$  and  $O$  are the volumes of input and output of support structures, respectively.  $p$  is the model used in this optimization,  $q$  is the pre-defined orientation of part deposition direction and  $r$  is the stage of network. For example, the input volumes of support structure for Model 1 in six pre-determined directions are given by  $V_{11}$  to  $V_{16}$  and the outputs in Stage 1 of MLP network are given by  $O_{11}$  to  $O_{16}$ . The output in Stage 1 indicates “1” for the minimum volume of

support structure and “0” for the other given values. The inputs and outputs of MLP 1 network (Structure 1) are shown in Fig. 3.13.

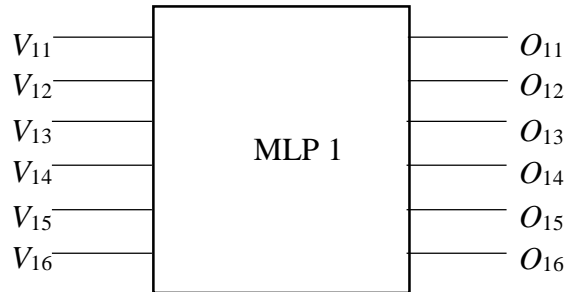


Figure 3.13: Six inputs nodes and six outputs nodes of MLP 1 network (Structure 1).

### 3.4.4.2 Structure 2

In order to increase the performance of MLP 1 network, a new feature, known as  $\text{Min}(V_{11}-V_{16})$  will be added. The  $\text{Min}(V_{11}-V_{16})$  will be selected as a minimum value among the previous six inputs,  $V_{11}$  to  $V_{16}$ . As a result, the new network consists of 7 inputs ( $V_{11}$  to  $V_{16}$  and  $\text{Min}(V_{11}-V_{16})$ ) with the same number of outputs (as previous network) are shown in Fig. 3.14.

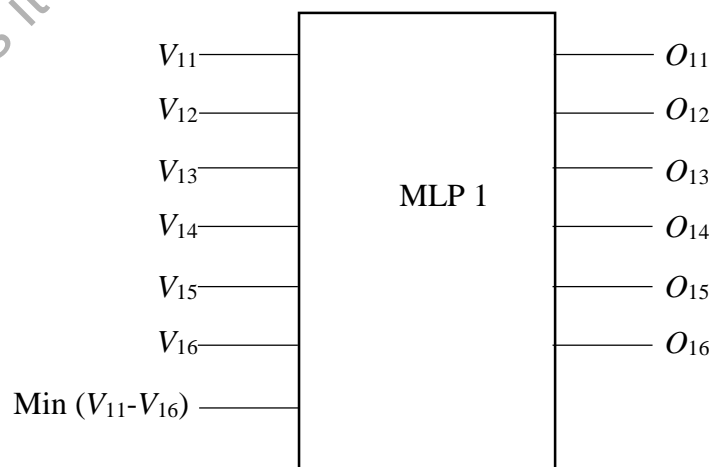


Figure 3.14: Seven inputs nodes and six outputs nodes of MLP 1 network (Structure 2).

### 3.4.4.3 Structure 3

To further improve the performance of the network and reduce the complexity of classification problems, a new design of a parallel MLP 1 structure will be proposed as depicted in Fig. 3.15 (Structure 3). In Structures 1 and 2, a single MLP network is used to classify 6 minimum volumes of support structure. The network requires to thoroughly learn all the output classes from a given set of input features. This problem can be reduced by assigning each output to an independent MLP 1 network. The same feature (as in Fig. 4.6) is used as an input (seventh input) to six MLP parallel networks (MLP 1-1 to MLP 1-6) in order to produce six different types of outputs ( $O_{11}$  to  $O_{16}$ ), respectively. For this MLP 1 parallel network, the number of hidden nodes are set to be the same values in order to ease the experimental analysis and to make it comparable with other structures.

The outputs of MLP 1-1 to MLP 1-6 indicate “1” for the minimum volume of support structure and “0” for the other given values. The inputs and outputs of MLP 1-1 to MLP 1-6 networks are shown in Fig. 3.15.

The three structures are analysed to determine the best performing network with the highest accuracy is selected and combined with the MLP 2 network (Structure 5) in Stage 2.



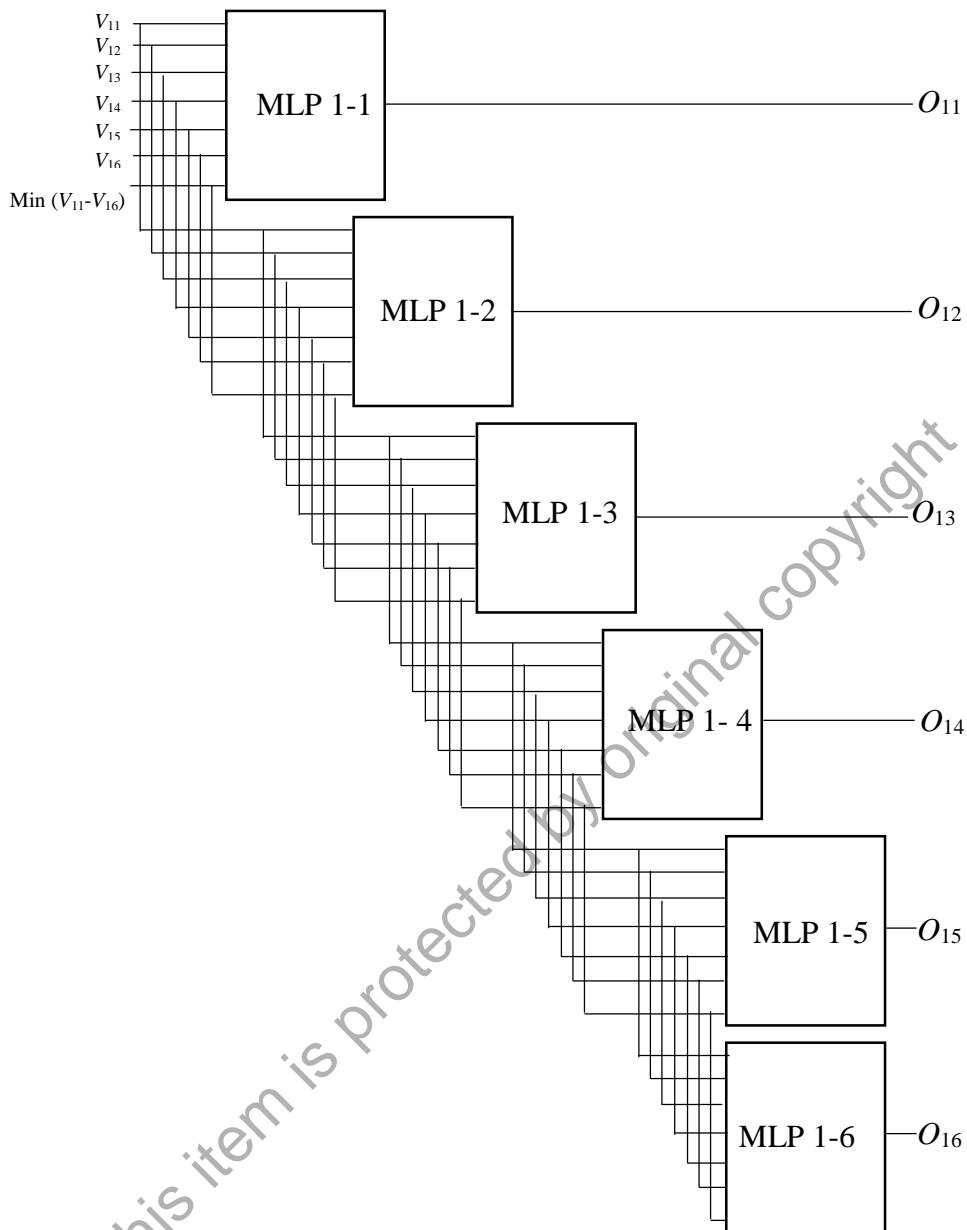


Figure 3.15: Parallel MLP structure (Structure 3).

#### 3.4.4.4 Structure 4

In Stage 2, there are 12 inputs and 6 outputs for MLP 2 network (Structure 4) as shown in Fig. 3.16. The 6 outputs ( $O_{11}$  to  $O_{16}$ ) from Stage 1 (desired outputs/design outputs) and another new six inputs (number of support structure in 6 pre-defined

orientations) will be taken as inputs for MLP 2 network. These number of support structures in six pre-determined directions are given by  $S_{pq}$ . The outputs of MLP 2 network are given by  $O_{rq}$ . The  $m$  is the model used in this optimization,  $q$  is the pre-defined orientation of part deposition direction and  $r$  is the stage of network. The output of MLP 2 indicates “1” for the optimum part deposition orientation and “0” for the other given values.

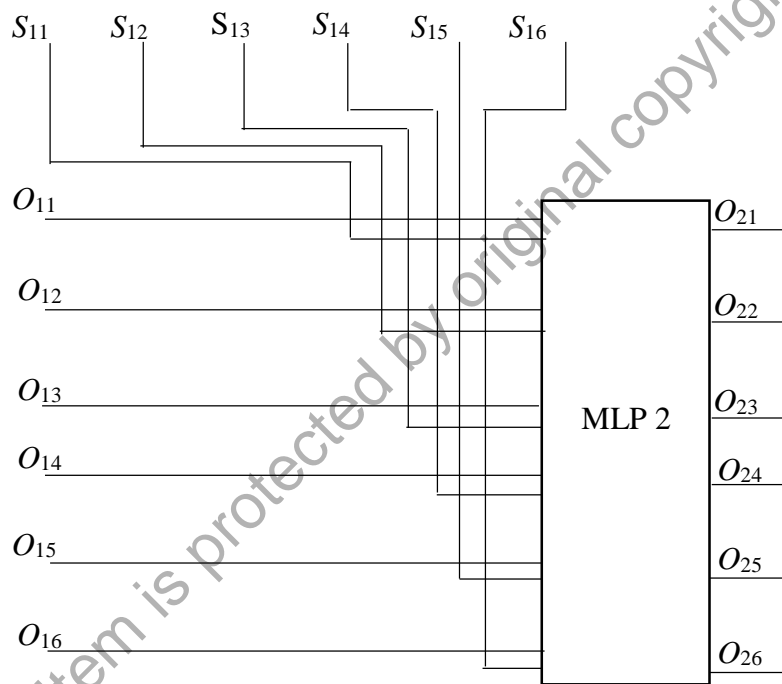


Figure 3.16: 12 input nodes and 6 output nodes of MLP 2 (Structure 4).

#### 3.4.4.5 Structure 5

Combination of MLP 1 network (Structure 3) and MLP 2 network (Structure 4) forms Structure 5 as shown in Fig. 3.17. The 6 outputs ( $O_{11}$  to  $O_{16}$ ) from Stage 1 (actual outputs/real outputs) and another new 6 inputs (number of support structure in 6 pre-defined orientations) for Structure 4 will be taken as inputs for Structure 5.

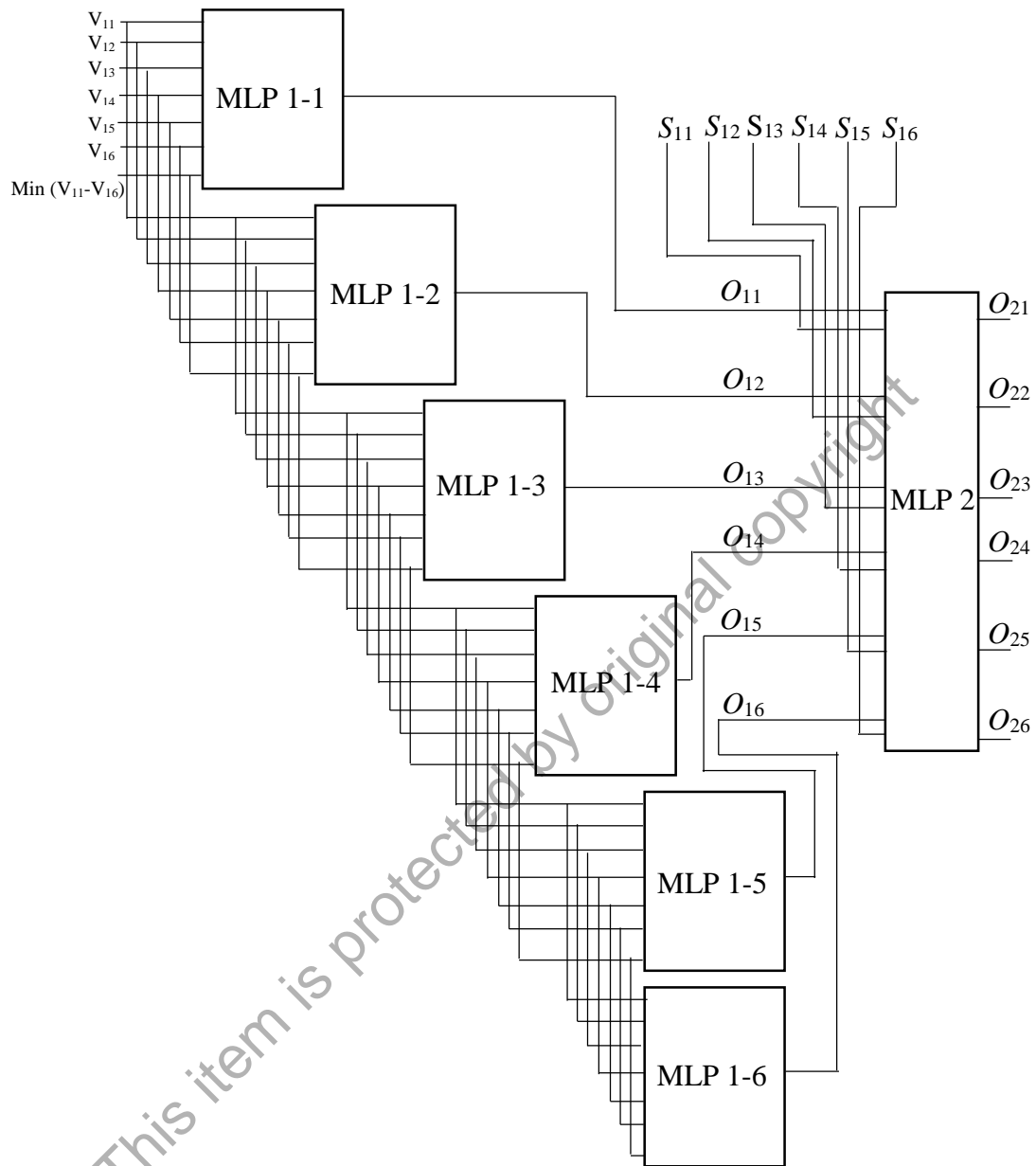


Figure 3.17: Combination of MLP 1 and MLP 2 networks (Structure 5).

If there is only one MLP 2 network outputs (in order from  $O_{21} - O_{26}$ ) which has number “1”, then assign it as the OPDO. This rule is simplified in Table 3.3.

Table 3.3: One MLP 2 network outputs has number “1”.

MLP 2 Network Outputs	Value	OPDO
$O_{21}$	0	
$O_{22}$	0	
$O_{23}$	0	
$O_{24}$	1	√
$O_{25}$	0	
$O_{26}$	0	
$sumOutput = \sum_{i=1}^6 O_{2i} = 1$		

In some cases, there will be more than one MLP 2 network outputs ( $O_{21} - O_{26}$ ) which has the same value of “1”. To overcome this problem, the study proposes the following rules;

- i. Find sum of MLP 2 network (Structure 5) outputs according to:

$$sumOutput = \sum_{i=1}^6 O_{2i} \quad (3.18)$$

- ii. If  $sumOutput > 1$ , choose the first MLP 2 network output (in order from  $O_{21}$  to  $O_{26}$ ) which has number “1” and then assign it as the OPDO. The rule is simplified in Table 3.4.

Table 3.4: More than one MLP 2 network outputs have number “1”.

MLP 2 Network Outputs	Value	OPDO
$O_{21}$	1	√ (the first MLP 2 Network Outputs has number “1”)
$O_{22}$	0	
$O_{23}$	1	
$O_{24}$	1	
$O_{25}$	0	
$O_{26}$	0	
$sumOutput = \sum_{i=1}^6 O_{2i} = 3$		

©This item is protected by original copyright

### 3.5 Part 3 – Surface Improvement

#### 3.5.1 Methodology

The methodology of this work involves two main steps; 1) the detection of ESF and 2) the developing of ESS considering the offset of SSF. In general, the process flow of the system for surface improvement is illustrated in Fig. 3.18.

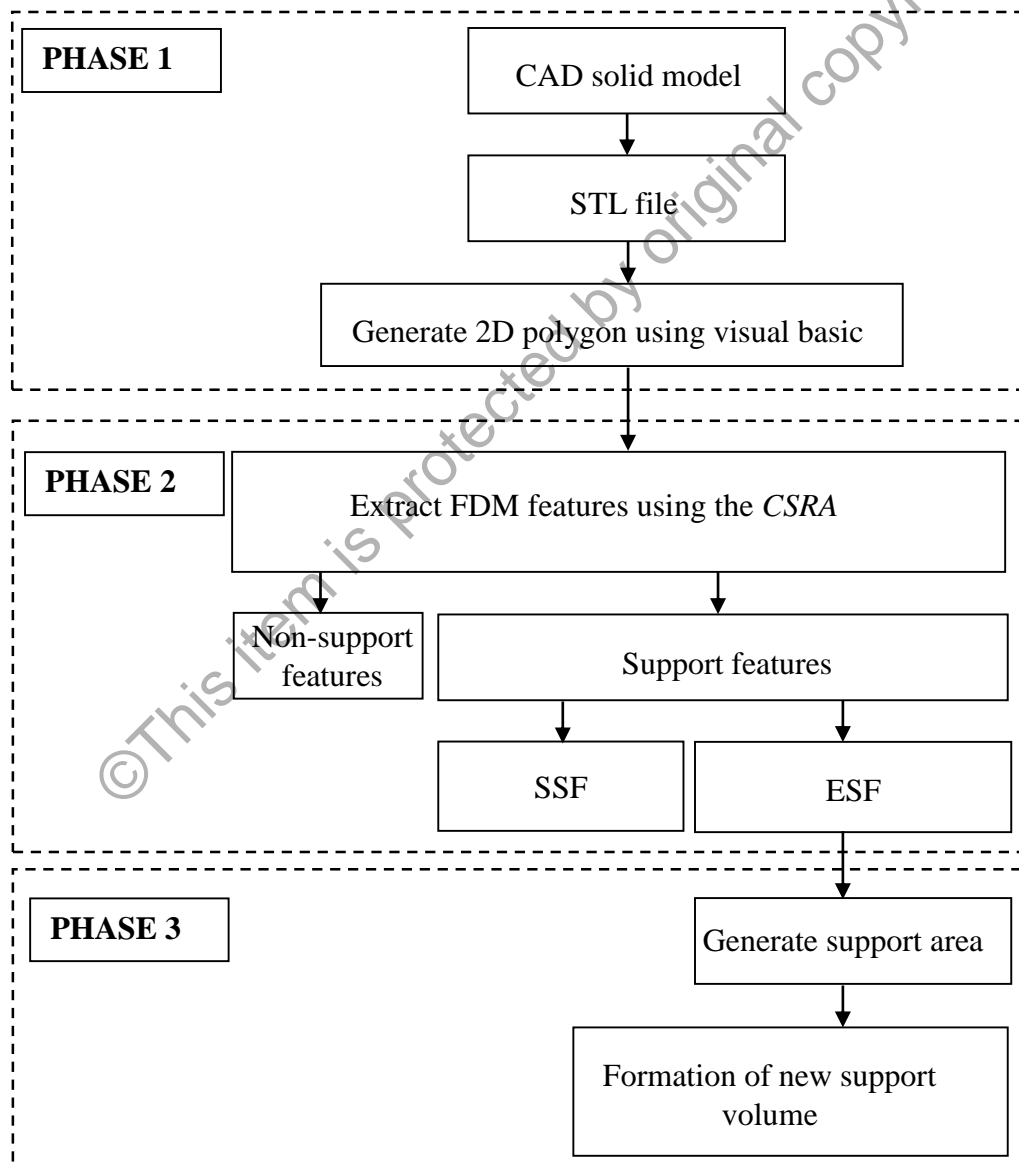


Figure 3.18: Flowchart for Feature-based Support Generation Data Extraction and formation of new support volume.

### 3.5.1.1 Step 1: Detection of ESF

The *Cross-Sectional slice Region Area (CSRA)* method (described in Section 3.4.3.1) was used to detect the ESF ( $RA' = CSRA_{k+1} - CSRA'_k > 0$ ) in each layer of part model.

### 3.5.1.2 Step 2: Development of ESS

Formation of new support volume at layer  $k$ -th is defined as:

$$\text{Formation of New Support Volume}_k = \Delta - \text{Volume of } CSRA'_k \quad (3.19)$$

where,  $\Delta = \text{Volume of } CSRA_k \cup \text{Volume of } CSRA_{k+1} \cup \text{Support Volume}_{k+1}$ ,  $CSRA'$  is offset  $CSRA$  and  $k \in \{1, 2, \dots, (N-1)\}$ , and  $N$  is the total number of layers for part model (i.e. the upper most layer of part model). The support volume at layer  $k=N$  is equal to zero.

The steps of detection of ESF and the development of ESS were used when comparing between two layers (upper  $(k+1)$  and lower  $(k)$  layers). A new part model was selected in explaining the development of ESS from the Upper\_most layer to the Lower\_most layer is shown in Fig. 3.19. The part model to be developed consists of all characteristics as in Case Studies 1 to 4 described in Chapter 3. The method used to develop support volume is described based on their case study.

**i) External-Supported Features using Support Material (A, B and C)**

Resultant Area,  $RA'$  between layers at level of layer  $k=4$  (A) and  $k=3$  (offset B and offset C) shows the existing of ESF, hence the support volume is required at layer  $k=3$  to support this feature. The support volume required at level of layer  $k=3$  was then developed using Boolean operation of Equation (3.13). The union operation between CSRAs at level of layer  $k=3$  (B and C),  $k=4$  (A) and support volume at level of layer  $k=4$  was performed. The support volume at level of layer  $k=3$  was then obtained by subtraction of volume of union operation and volume of CSRAs (offset B and offset C) at level of layer  $k=3$  (Fig. 5.4(b)(iii)).

**ii) Non-Supported Features (B and D) and Non-adjacency External-Supported Features using Support Material (C and D)**

The  $RA'$  between layers at level of layer  $k=3$  (B and C) and  $k=2$  (offset D) shows the non-supported features (B and D) and the non-adjacency ESF using support material (C and D). Hence the support volumes are required at level of layer  $k=2$  to support overhang of previous support volume and layer C at level of layer  $k=3$ . The support volume required at level of layer  $k=2$  was then developed using Boolean operation of Equation (3.13). The union operation between CSRAs at level of layer  $k=3$  (B and C),  $k=2$  (D) and support volume at level of layer  $k=3$  was performed. The support volume at layer  $k=2$  was then obtained by subtracting volume of union operation and volume of offset D at level of layer  $k=2$  (Fig. 3.19(c)(iii)).



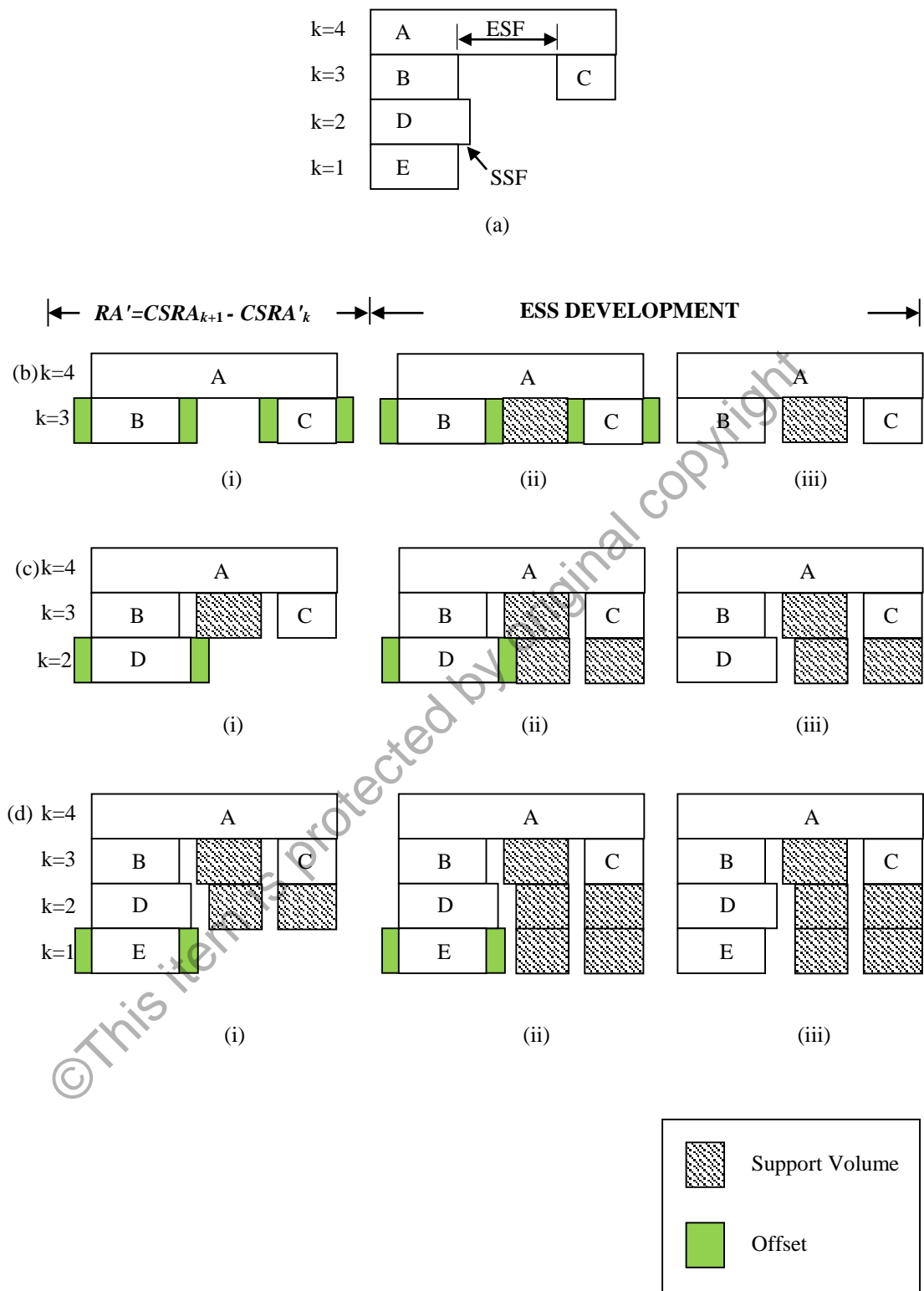


Figure 3.19: Model used to evaluate various of features using Feature-based Support Generation.

### iii) Self-Supported Features require no Support Material (D and E)

The  $RA'$  between layers at level of layer  $k=2$  (D) and  $k=1$  (offset E) shows the self-supported features that require no support material. Hence the support volume is required at level of layer  $k=1$  to support overhang of previous support volume at level of layer  $k=2$ . The support volume required at level of layer  $k=1$  was then developed using Boolean operation of Equation (3.13). The union operation between CSRAs at level of layer  $k=2$  (D),  $k=1$  (E) and support volume at level of layer  $k=2$  was done. The support volume at level of layer  $k=1$  was then obtained by subtraction of volume of union operation and volume of offset E at level of layer  $k=1$  (Fig. 3.19(d)(iii)).

The part model after surface improvement shown in Fig. 3.19(d)(iii) is discussed in details. Two ESSs, ESS 1 and ESS 2 (hatched) are required to support the ESF detected on the part model (Fig. 3.20). The ESS 1 has three parts, top, middle and bottom. The ESS 2 has two parts, top and bottom. It can be seen that there is no surface contact area between part model, ESS 1 and ESS 2. For ESS 1 and ESS 2, the top part is required to support the overhang ESF, while the middle or bottom parts are then used to support the overhang of previous support volume (the top part).

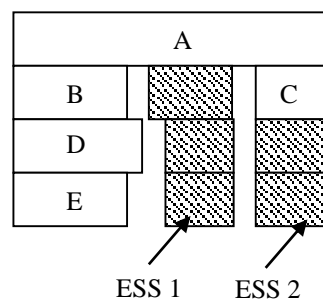


Figure 3.20: Development of ESS for part model.

### **3.6 Summary**

POA is used to distinguish between the support and non-support features. Four Case Studies are introduced. The approach in Case Studies 3 and 4 (External Support Feature using support material) are selected in calculating the total volume of support structure and the amount of support structure. The details are described in next chapter.

©This item is protected by original copyright

## CHAPTER 4

### RESULTS AND DISCUSSION

#### 4.1 Introduction

This chapter reports the results of determining the OPDO using the ANN and the improvement of surface finish of the contact area between part and support structure. The results of this work are displayed and discussed in this chapter. A detail extraction process of ESF in order to compute the ESS volume and amount of group used as inputs for ANN is explained.

#### 4.2 Optimum Part Deposition Orientation

##### 4.2.1 Extraction of ESF in Determining Volume and Number of Support Group

Sample of part model in pre-defined direction of  $x$ ,  $y$  and  $z$  axes was constructed and the uniform slicing technique was applied to explain the algorithm of the system. This system has two parts: ESF identification process and support generation data extraction. The part model used in this work is shown in Fig. 3.10.

Two out of the six directions analysed that correspond to the  $\pm x$ ,  $\pm y$  and  $\pm z$  axes were taken as samples and illustrated in Figs. 4.1 (Direction 1) and 4.2 (Direction 2).

Directions 1 and 2 were selected for a better understanding to clarify the theory of volume formation and number of support structure for the Part Model 1 (to explain Equations (3.14) and (3.15)).

Directions 3 and 4 can also be used to explain this theory. The similar technique to calculate the volume and number of support structure was implemented (as explained in Directions 1 and 2).

Directions 5 and 6 were unable to explain the theory volume formation and number of support structure due to the absent of external support structure.

The volume of support structure to support detected ESF and the process for determining the amount of support structures based on Situations 1 and 2 (as described in Section 3.4.3.1) are also shown in these figures.

The area for new lower layer as a result of offsetting generation was replicated for each pair of layers, in a sequence starting from the Upper\_most layer to the Lower\_most layer and will be discussed in the following section.

#### **4.2.1.1 Analysis of Orientation of Part Deposition in Direction 1**

For the ESF identification, the subtraction process between upper ( $CSRA_{Upper\_layer}$ ) and offset lower ( $CSRA'_{Lower\_layer}$ ) layers was used and presented in top and front views (Fig. 4.1). The offset lower layer is represented by a dashed line. This process involves the calculation of  $RA'$  from the Upper\_most layer (Layer 4) to the Lower\_most layer (Layer 1). The ESF is identified when  $RA' > 0$ . The ESF between Layer 4 and offsetting of Layer 3 is not identified as shown in Figs. 4.1(b)(i) and (ii). This situation can also be identified between Layer 3 and offsetting generating of Layer 2 (Fig. 4.1(b)(ii)).

The ESF are discovered for  $RA'$  between Layer 2 and offsetting generation of

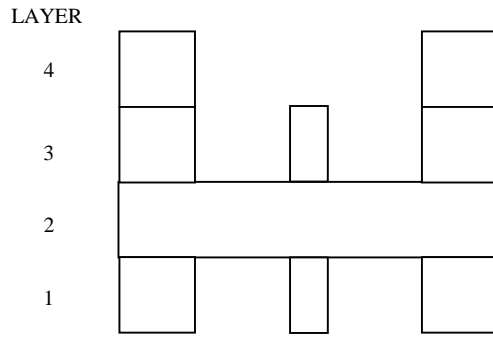
Layer 1. By using Equation (3.9), the support volume at Layer 1 is produced instantly under ESF of Layer 2. This process obtains the adjacency of Layer 2 in its building direction, and is thus easy to manufacture. Next, the support generation data extraction is done. Two parameters, the volume of support structure represented by hatched region and the amount of support group for identified ESF (Fig. 4.1(b)(iii)) are calculated.

The support volumes at the current layer were checked for the intersection with the developed support volumes of previous layer before calculating the overall amount of support group.

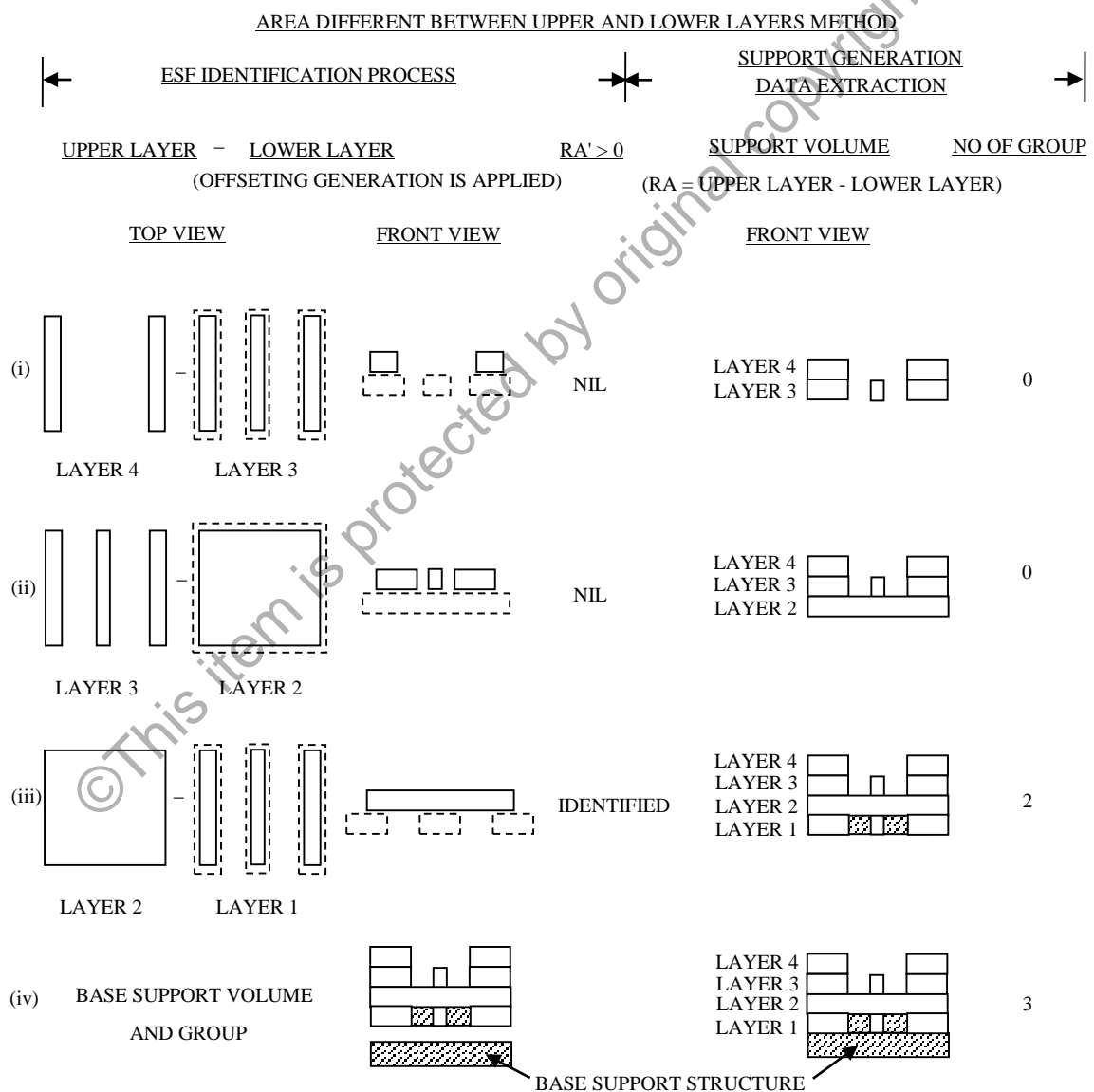
The number of ESS (Layer 1) has two groups of support volume. The intersection of these groups is not investigated. As a consequence, the structures of support volume are discovered to be two different structures. In this case, the amount of support group is 2.

In this study, the BSS is required for part model to support the overhang area of part and external support volume at level  $k=1$  is 1 unit, represented by hatched region in Fig. 4.1(b)(iv). Determining the amount of base support structure depends on part model area or ESS area which progressed at Layer 1. By using Equation (3.16), the volume for BSS was generated (Fig. 4.1(b)(iv)) to support any areas progressed at this level. The intersection between the volume of BSS generated and support volume instantly above it is not considered as a member of volume of ESS (since  $k \in \{1, 2, \dots, (N-1)\}$ ).

Finally, the total support structures in Direction 1 for the entire manufacturing process of this part model are 3 units. Next, the volumes for the support structures are calculated.



(a) Slice Part Model 1 in Direction 1.



(b) ESF identification process and support generation data extraction in Direction 1.

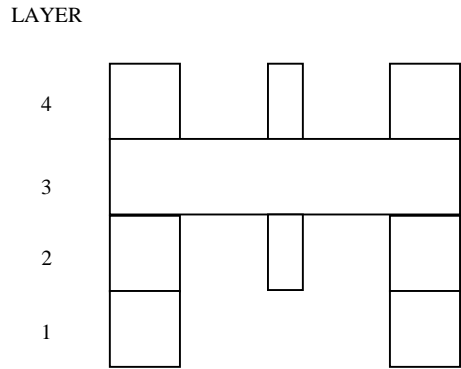
Figure 4.1: Illustrative example of Part Model 1 in Direction 1.

#### **4.2.1.2 Analysis of Orientation of Part Deposition in Direction 2**

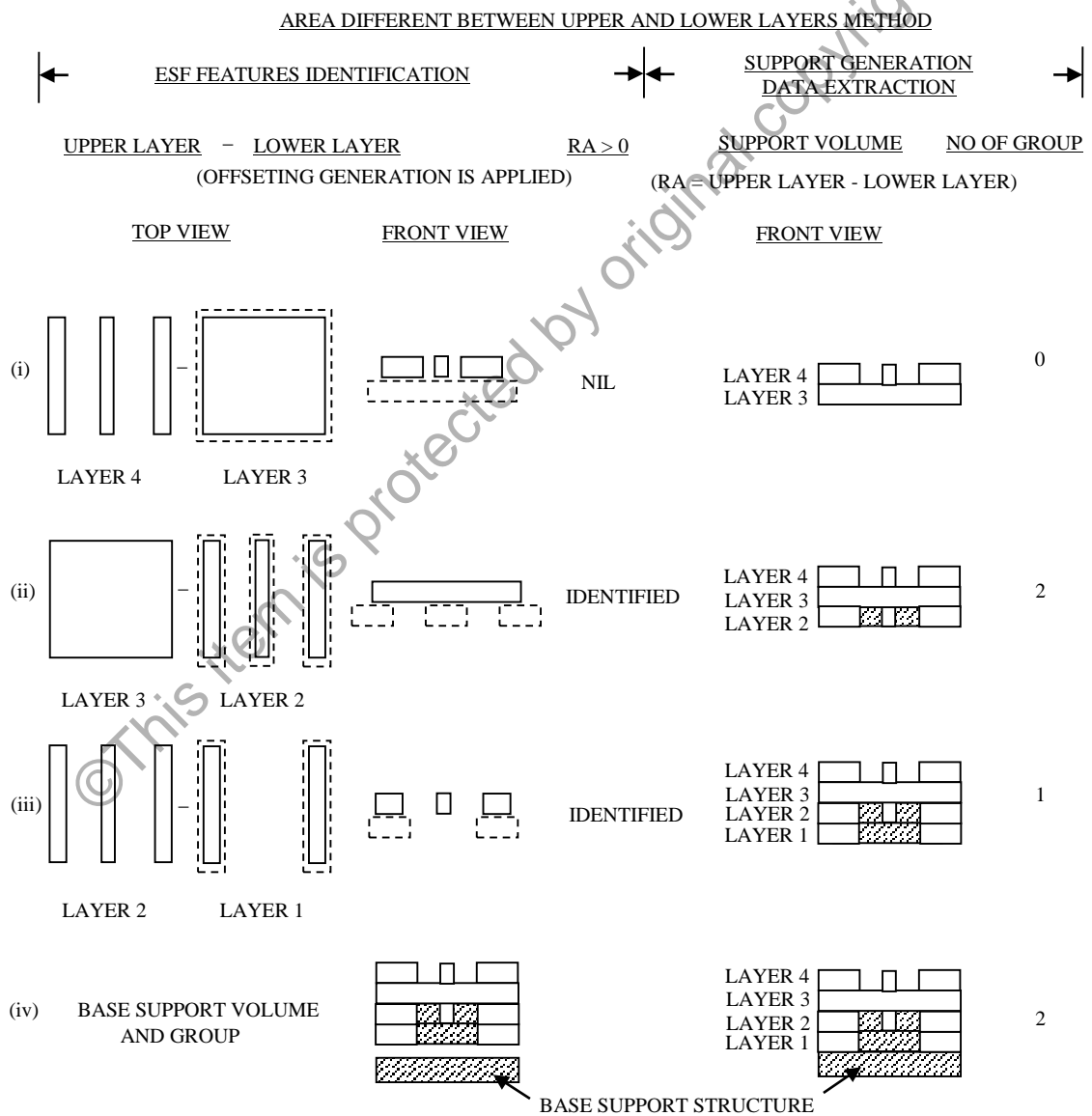
The same part model as used in Section 4.2.1.1 was taken for the analysis of the orientation of part deposition in Direction 2. The formation of support structure and amount of group are illustrated in Fig. 4.2. The ESF between Layer 4 and offsetting of Layer 3 is not identified (Fig. 4.2(b)(i)), then the support volume is not required at this level of layer. However, two groups of support volume are required to support the detected ESS at Layer 2. This condition occurs between Layer 3 and offsetting generation of Layer 2 (Fig. 4.2(b)(ii)).

©This item is protected by original copyright





(a) Slice part model 1 in Direction 2.



(b) ESF identification process and support generation data extraction in Direction 2.

Figure 4.2: Illustrative example of Part Model 1 in Direction 2.

Next, the new support volume is required at Layer 1 (Fig. 4.2 (b)(iii)). The ESF is found for *RA* between Layer 2 and the generation of offsetting of Layer 1. The detail process of support generation at this stage is illustrated in Fig. 4.3. Firstly, the support volume at Layer 1 is produced instantly under ESF of Layer 2 (Fig. 4.3(b)). At the same time, the two overhang support volumes generated at Layer 2 (i.e. at the left and right hand side) also require new support volumes to increase the adjacency in their building direction as shown in Fig. 4.3(a). Therefore, both ESF and the overhang support volumes can be manufactured (Fig. 4.3(c)).

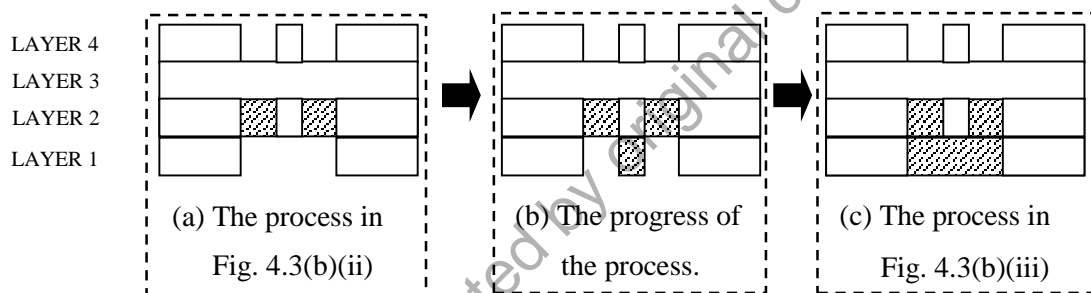


Figure 4.3: Process of support generation.

This work found that the Layer 2 has two non-intersection structures of support volume (Fig. 4.3(c)). The system recognizes these structures of support volume as two distinct structures. However, the intersection between the support volumes at layers 1 and 2 was referred as a similar member. Thus, these volumes develop a unit of support volume structure.

There are two groups of ESS at Layer 2 (Fig. 4.3(a)). The overall amount of external support group at Layer 1 (Fig. 4.3(c)) is 1 due to intersection between the support volumes created at Layers 1 and 2.

For orientation of part deposition in Direction 2, the total support structures in the entire manufacturing process are 2 units (one unit of ESS and BSS each) (Fig. 4.2(b)(iv)).

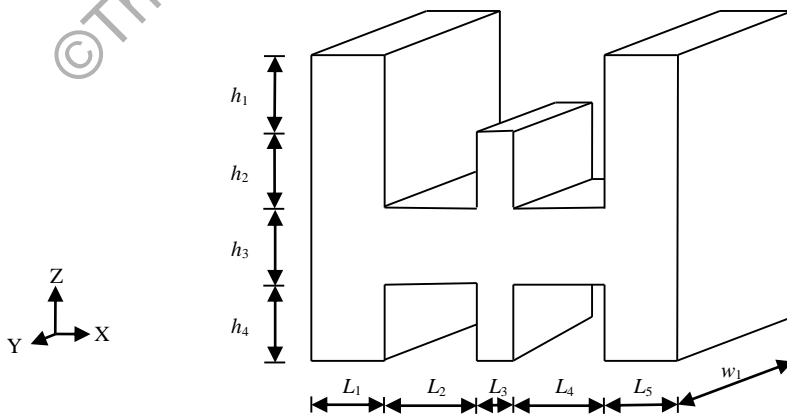
The technique of base support volume generation in Direction 2 is similar to the considerations that have been made in Direction 1, (since  $k \in \{1, 2, \dots, (N-1)\}$ ), as described in Section 4.2.1.1.

By considering the amount of support structure and BSS, hence, the total support structures in Direction 2 for entire manufacturing process of this part model are 2 units. Then, the volumes for these support structures were calculated.

In general, the Feature-based Support Generation for Part Model 1 considering the support volume and amount of support structure (Situations 1 and 2 as in Section 3.4.3.1) can be clearly explained in Directions 1 and 2.

#### 4.2.2 Results for Orientation of Part Deposition in All Pre-defined Directions

In this work, the persistent slice height,  $t$  of 0.01 mm and the base support layer,  $m$  of 5 was selected for the whole part orientations involved. For the new model, Part Model 1, was manufactured with geometries as shown in Fig. 4.4. The same model was used for all directions (1 to 6) in determining the optimum deposition part orientation using MLP network.



$$L_1 = L_2 = L_4 = L_5 = 10 \text{ mm}, L_3 = 5 \text{ mm}, w_1 = 20 \text{ mm}, h_1 = h_2 = h_3 = h_4 = 10 \text{ mm}.$$

Figure 4.4: Dimensions of Part Model 1.

The outcome of overall support volume and amount of support structure (Part Model 1) for orientation of part deposition in pre-defined Directions 1 to 6 are shown in Table 4.1. From the table, the least support volumes ( $57.5 \text{ mm}^3$ ) were observed in Directions 5 and 6. Meanwhile, both directions also show the same amount of support structure which is 1 unit. Hence, the best orientation of the part is in Directions 5 or 6. In this case, the least support volume are detected due to similar Feature-based Support Generation for both directions.

Table 4.1: Support volume and amount of support structure in pre-defined directions.

Pre-defined Direction	Total Support Volume ( $\text{mm}^3$ )	Amount of Support Structures
1	4045	3
2	9045	2
3	13040	4
4	13040	4
5	57.5	1
6	57.5	1

### 4.3 Artificial Neural Network

The results of the computational analysis for total support volume and amount of support structure are presented in this section. The determination of the OPDO for different selected models using MLP network is also described.

### 4.3.1 Training and Testing Data

The training process was conducted by varying the number of hidden nodes from 1 to 50 by trial and error in order to identify the optimum value of accuracy. For each hidden node, the classification accuracy was recorded. The accuracy of MLP output testing and training is given by Equation (4.1),

$$Accuracy = \left( \frac{\text{Number of correctly classify data}}{\text{Total number of data}} \right) \times 100 \quad (4.1)$$

For the classification performance in current work, the minimum acceptable accuracy is set as 85%. The accuracies of training and testing processes for all structures (Structures 1 to 5) are shown in Figs. 4.5 to 4.10. The selection of optimum output for training and testing is based on the highest accuracy during training and testing with the minimum number of hidden neurons.

From Fig. 4.5, the accuracy of optimum classification is obtained when the number of hidden node is 23. The selection of 50 hidden nodes is sufficient for the analysis. The method of selection of hidden nodes is by trial and error. The same method was used by previous researchers (Dreiseitl *et al.*, 2002; Feng *et al.*, 2009). The training for MLP 1 network using larger number of hidden nodes (>23) does not improve the classification accuracy. The accuracies of MLP 1 network (Structure 1) for training and testing processes are 67.00% and 62.50%, respectively.

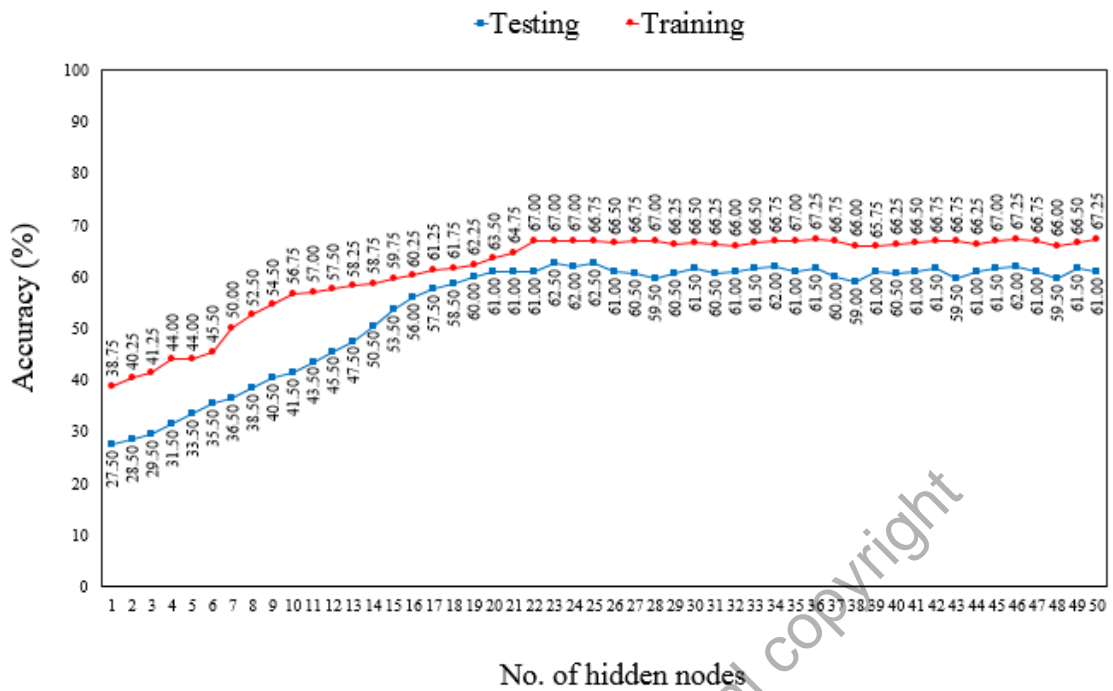


Figure 4.5: Accuracy of MLP 1 network for training and testing processes of Structure 1.

The accuracy of MLP 1 network as a function of the number of hidden nodes between training and testing processes is displayed in Fig. 4.6. Both training and testing processes of MLP 1 output are have higher accuracy compared to Structure 1 when the MLP 1 network have 7 inputs including  $\text{Min}(V_{11} \text{ to } V_{16})$ . From the plots, the accuracies for training and testing processes of Structure 2 are 77.25% and 75.00%, respectively. This occurs when the number of hidden node is 28. The classification accuracies for both training and testing processes do not improve when the number of hidden node is greater than 28.

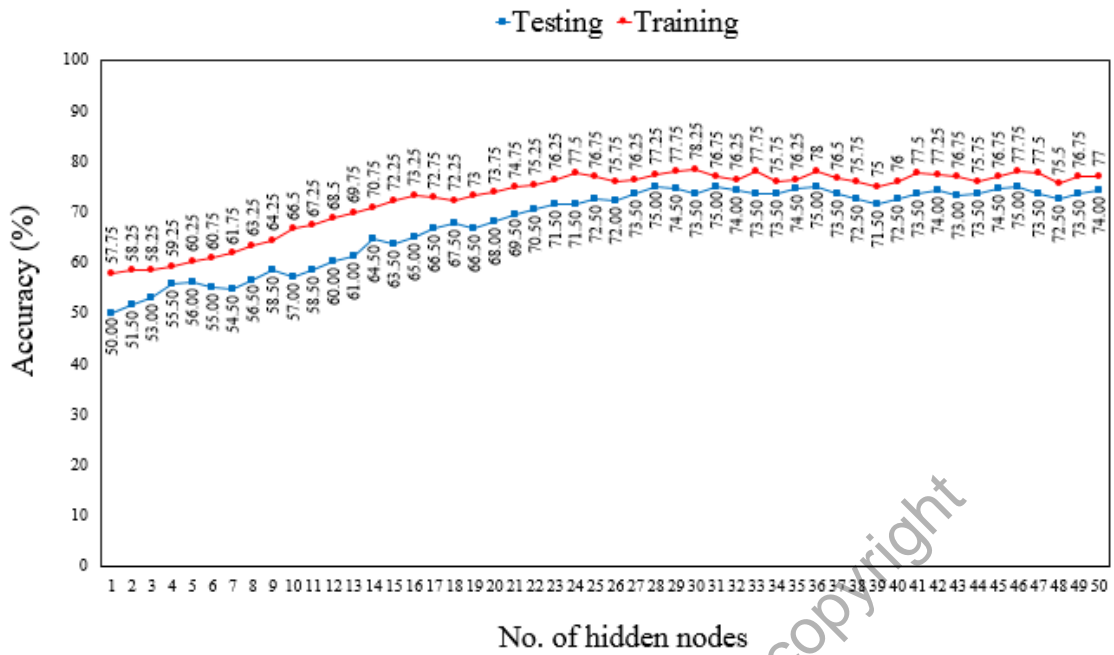


Figure 4.6: Accuracy of MLP 1 network for training and testing processes of Structure 2.

The accuracy of testing for Structure 2 is verified by the same inputs of  $V_{11}$  to  $V_{16}$  and the replacement of  $\text{Min}(V_{11}$  to  $V_{16})$  by  $\text{Max}(V_{11}$  to  $V_{16})$ . The result shows that the Structure 2 has a lower testing accuracy when the  $\text{Max}(V_{11}$  to  $V_{16})$  is used as the seventh input for MLP 1 network. The comparison between the accuracy of testing for Structures 1 and 2 ( $\text{Min}(V_{11}$  to  $V_{16})$  and  $\text{Max}(V_{11}$  to  $V_{16})$ ) are plotted in Fig. 4.7.

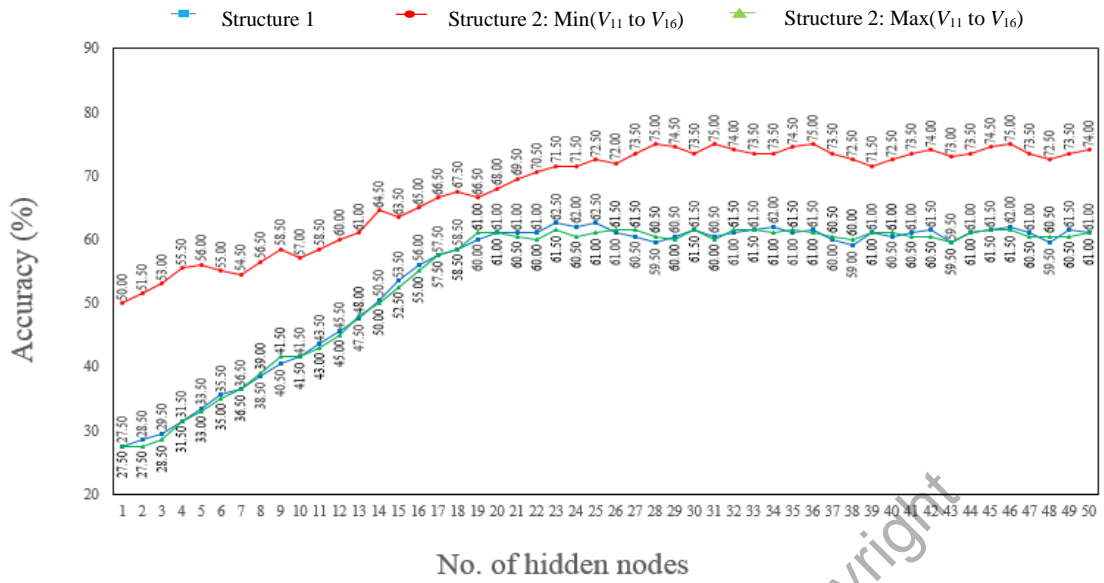


Figure 4.7: Comparison of testing accuracy between Structures 1 and 2 (for minimum and maximum input values).

The accuracies of training and testing processes for Structure 3 against the number of hidden nodes are presented in Fig. 4.8.

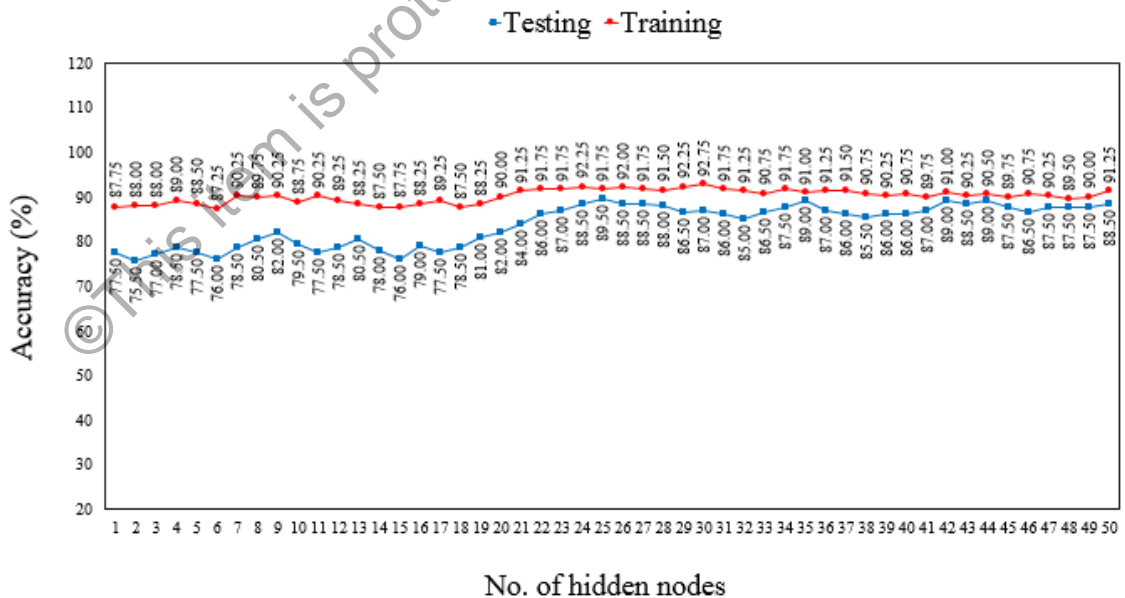


Figure 4.8: Accuracy of MLP 1 network for training and testing processes of Structure 3.



It can be seen that the accuracies for training and testing are 91.75% and 89.50%, respectively. Both accuracies achieved when the number of hidden node is 25. The classification accuracy does not improve when the number of hidden node is greater than 25

The accuracies of training and testing processes for Structure 4 (MLP 2 network which consists of 12 inputs and 6 outputs nodes network) is displayed in Fig. 4.9. The accuracies for training and testing processes are 99.25% and 97.50%, respectively when the hidden number of node is 15. These accuracies do not show any improvement beyond this node.

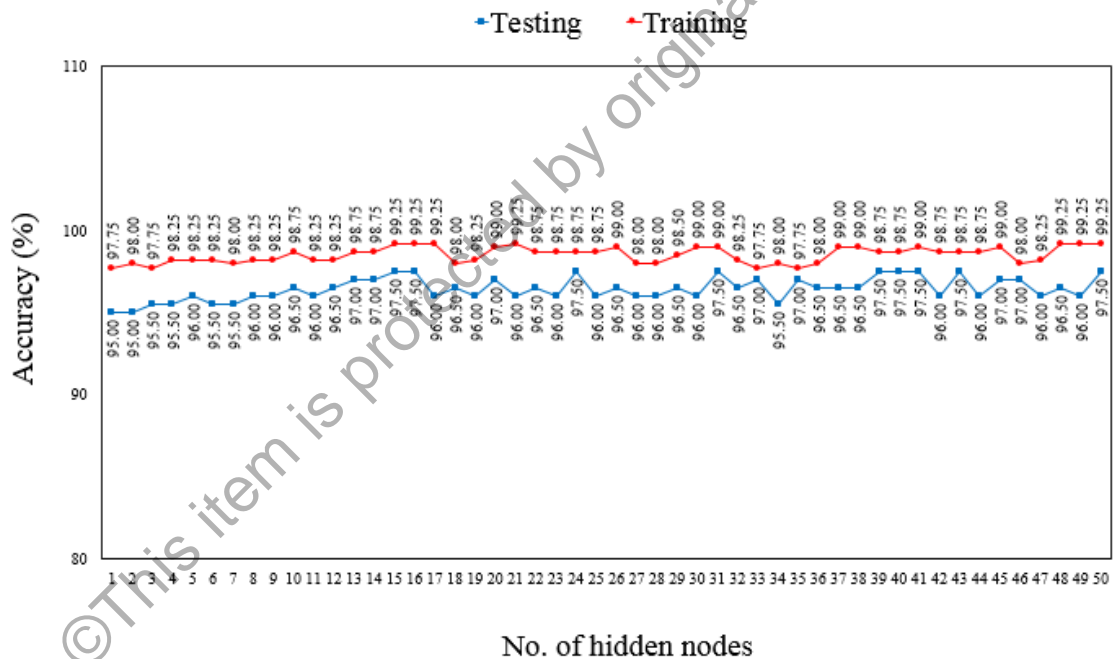


Figure 4.9: Accuracy of MLP 2 network training and testing processes of Structure 4.

The accuracies of training and testing for Structure 5 (combination between MLP 1 network designed for Structure 3 and MLP 2 network (12 Inputs and 6 Outputs)) are displayed in Fig. 4.10. The accuracies for training and testing processes are 88.25%

and 86.50%, respectively when the hidden number of node is 17. The greater number of hidden node (>17) does not change the classification accuracy.

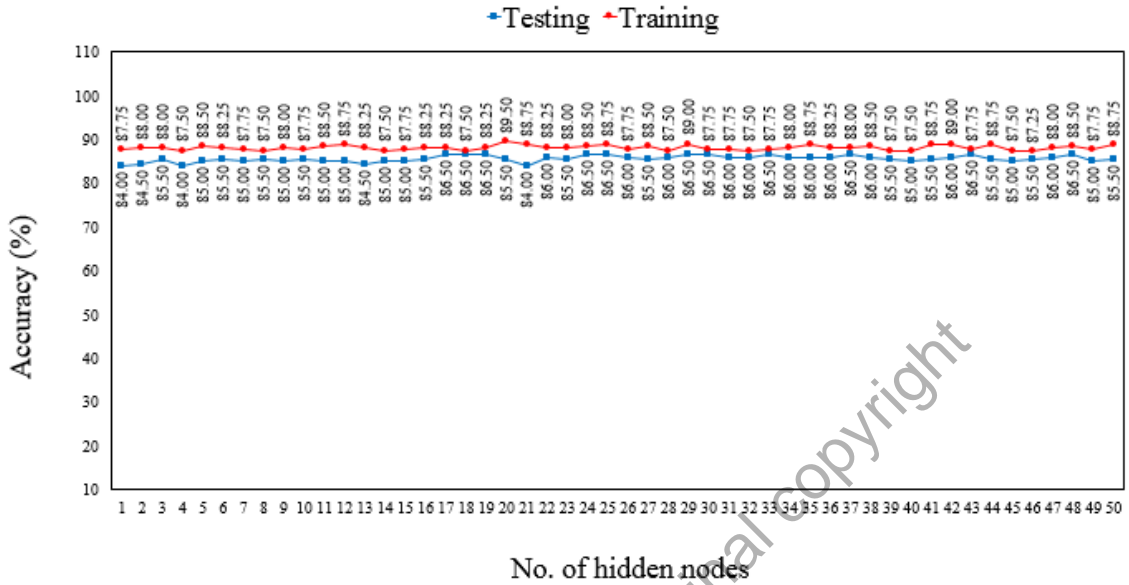


Figure 4.10: Accuracy of combination of MLP 1 and MLP 2 networks for training and testing processes (Structure 5).

Data of training and testing processes for all structures of MLP 1 and 2 are attached in Appendices A to E.

### 4.3.2 Summary

The accuracy of the network is determined through five MLP structures (Structures 1 to 5). The accuracies of MLP structures at specific hidden nodes are given in Table 4.2.

It can be seen that the performance (testing accuracy) of Structure 2 is improved from 62.50% to 75.00% when a new feature of  $\text{Min}(V_1 \text{ to } V_6)$  is proposed. This work also proposed new parallel MLP networks (Structure 3) in which each network is used to classify different outputs. The Structure 3 has the highest testing accuracy of 89.50% compared with other structures. The MLP 2 network (Structure 4) contains 12 inputs and

6 output nodes. The accuracy for this structure is 97.50%. Structure 5 has two types of inputs of total volume of support structure (output from MLP 1 of Structure 3) and number of support structure. The outputs of Structure 5 are trained to have a minimum total volume of support structure which also to have a minimum number of support structure. Structures 3 and 4 are selected and combined in order to produce Structure 5 which has the testing accuracy of 86.50%. From now onward, the Structure 5 will be chosen in this study.

Table 4.2: Training and testing accuracies for MLP structures.

<b>MLP Structure</b>	<b>Number of Hidden Node</b>	<b>Training Accuracy (%)</b>	<b>Testing Accuracy (%)</b>	<b>Selected Structure</b>
Structure 1	23	67.00	62.50	-
Structure 2	28	77.25	75.00	-
Structure 3	25	91.75	89.50	MLP 1
Structure 4	15	99.25	97.50	MLP 2
Structure 5	17	88.25	86.50	√
Note: Structure 5 is a combination of MLP 1 and MLP 2				

#### 4.4 Computation Analysis using Multilayer Perceptron Network

The results of computational analysis using MLP network in selecting the OPDO for all part models (Models 1 to 3) are discussed. For every part orientation, the overall volume and the amount of support structure were decided to be an input.

##### 4.4.1 Model 1: New Model

For Model 1, the OPDO in six pre-defined direction is determined by using MLP networks (Structure 5). The input and output for these networks is presented in Table 4.3. This table displays the total support volume as inputs for MLP 1 network. The least total support volume ( $57.5 \text{ mm}^3$ ) is identified as a seventh input for MLP 1 network. The combination of six outputs of MLP 1 and amount of support structure ( $S_{21}$ – $S_{26}$ ) become as inputs for MLP 2. Based on the result, the least total support volume and least amount of support structure are given by the MLP 2 network when the output indicates “1” ( $O_{25}$  and  $O_{26}$ ). Based on the rule defined in Equation (3.18),  $O_{25}$  in direction 5 is chosen as an OPDO.

Table 4.3: Input and output of MLP network (Structure 5) for Part Model 1.

Direction	Total Support Volume (mm <sup>3</sup> )	Amount of Support Structures		MLP 2 Output		Rule
		$S_{21}$		$O_{21}$		
1	4045	$S_{21}$	3	$O_{21}$	0	0
2	9045	$S_{22}$	2	$O_{22}$	0	0
3	13040	$S_{23}$	4	$O_{23}$	0	0
4	13040	$S_{24}$	4	$O_{24}$	0	0
5	57.5	$S_{25}$	1	$O_{25}$	1	1
6	57.5	$S_{26}$	1	$O_{26}$	1	0

The actual part models produced in Directions 5 and 6 using FDM machine are displayed in Figs. 4.11 and 4.12, respectively.

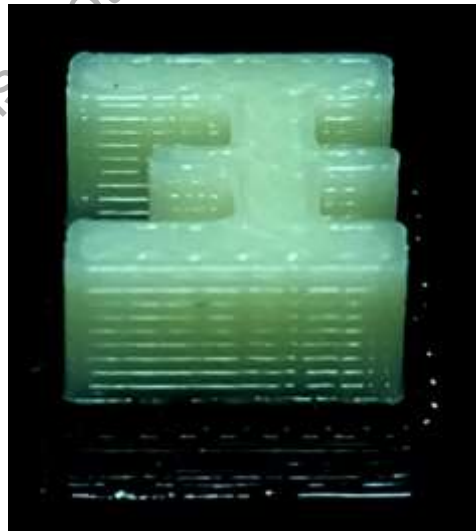


Figure 4.11: Part Model 1 orientated in Direction 5.

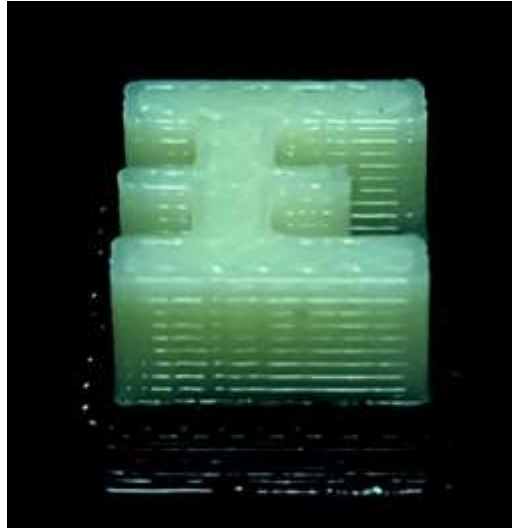


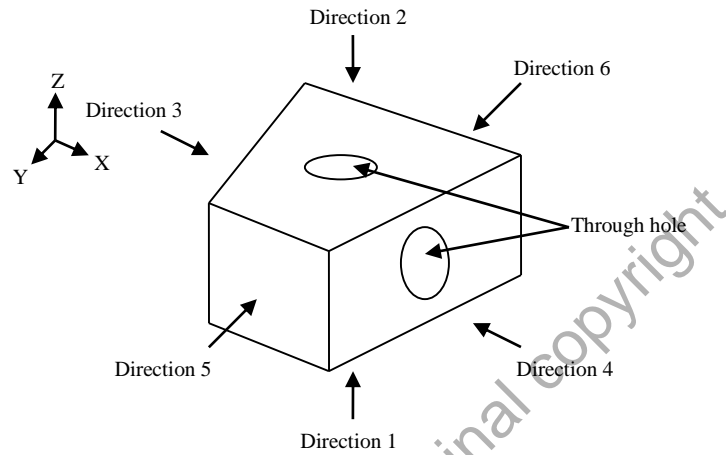
Figure 4.12: Part Model 1 orientated in Direction 6.

#### 4.4.2 Models 2 and 3: Existing Models

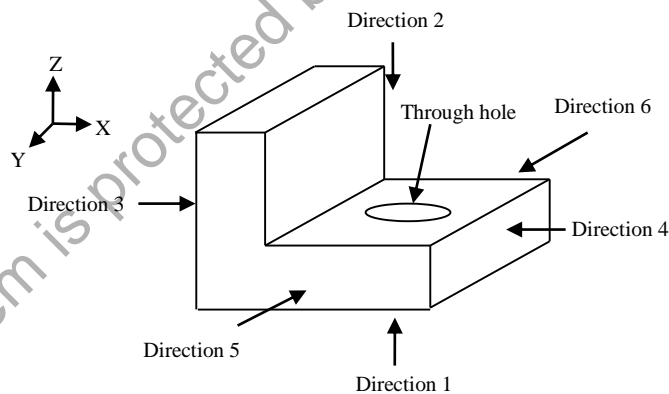
The method for Feature-based Support Generation used in selecting the OPDO was validated by constructing two part models as shown in Fig. 4.13. Previous work by Cheng *et al.* (1995) and Thrimurthulu *et al.* (2004) used the same Part Model 2 (Fig. 4.13(a)) to validate their different technique in selecting the OPDO in SLA and FDM, respectively. Another attempt in FDM was done by Masood *et al.* (2000) by using Part Model 3 (Fig. 4.13(b)).

In validating the OPDO, Cheng *et al.* (1995) used a multiple objective-function as a formulation to derive the optimal orientation for Stereolithography process. This algorithm is enable for simple surfaces (flat and cylindrical) and complex surfaces. Meanwhile Thrimurthulu *et al.* (2004) determined the OPDO by minimizing the support structure and using the adaptive slicing for similar model used by Cheng and his workers (1995). This approach can be used for complex surface (completely freeform). Masood *et al.* (2000) validated the OPDO for his model by developing a mathematical technique

based on minimum volumetric error values using the primitive volume approach (simple parts made from the primitives such as cylinders, cubes, spheres and pyramids. This approach also promise the computation of volumetric error for more complex part.



(a) Part Model 2 (Cheng *et al.*, 1995).



(b) Part Model 3 (Masood *et al.*, 2000).

Figure 4.13: Part models for validation using Feature-based Support Generation.

Input and output of MLP network analysis for validation of the OPDO using part model 2 are displayed in Table 4.4. For Model 2, the least total support volume (44018.47 mm<sup>3</sup>) and least amount of support structure (3) are given by the MLP 2 network when the output indicates “1” ( $O_{21}$  and  $O_{22}$ ). Using a similar rule defined in Equation (3.18),  $O_{21}$  in

direction 1 is selected as an OPDO. This finding is consistent with the build direction reported by Cheng *et al.* (1995) and Thrimurthulu *et al.* (2004).

Table 4.4: Input and output of MLP network (Structure 5) for Part Model 2.

Direction	Total Support Volume (mm <sup>3</sup> )	Amount of Support Structures		MLP 2 Output		Rule
		$S_{2i}$		$O_{2i}$		
1	44018.47	$S_{21}$	3	$O_{21}$	1	1
2	44018.47	$S_{22}$	3	$O_{22}$	0	0
3	58191.38	$S_{23}$	4	$O_{23}$	0	0
4	137691.38	$S_{24}$	4	$O_{24}$	0	0
5	152373.41	$S_{25}$	2	$O_{25}$	0	0
6	106998.41	$S_{26}$	2	$O_{26}$	0	0

The results of overall support volume and amount of support structure for Part Model 3 are shown in Table 4.5. For Model 3, the least total support volume (48.55 mm<sup>3</sup>) and least amount of support structure (1) are given by the MLP 2 network when the output indicates “1” and, this only occurs in one direction ( $O_{21}$ ). The rule defined in Equation (3.18),  $O_{21}$  in direction 1 is taken as an OPDO. This finding supports the work done by Masood *et al.* (2000), in which the selection of build direction is the same with this work.



Table 4.5: Input and output of MLP network (Structure 5) for Part Model 3.

Direction	Total Support Volume (mm <sup>3</sup> )	Amount of Support Structures		MLP 2 Output		Rule
		$S_{2i}$		$O_{2i}$		
1	48.55	$S_{21}$	1	$O_{21}$	1	1
2	14950.10	$S_{22}$	2	$O_{22}$	0	0
3	2359.07	$S_{23}$	2	$O_{23}$	0	0
4	21109.07	$S_{24}$	2	$O_{24}$	0	0
5	2361.57	$S_{25}$	2	$O_{25}$	0	0
6	2361.57	$S_{26}$	2	$O_{26}$	0	0

#### 4.5 General Discussion

The concept of Feature-based Support Generation is used to automate the selection of the OPDO. This work promises some extension of work done by Yang *et al.* (2003). Their work discussed on Feature-based Process Planning without mentions the OPDO while manufacturing the selected part model (Fig. 4.14) using the Orthogonal Deposition Manufacturing System (two-direction LM system, i.e. two nozzles). Based on the selected model, the support volume required in their work is considered higher than that of the support volume for the OPDO determined in this work. By comparing the support volume, the current method can offer lower build times and materials' cost. In conclusion, the selection of the OPDO is important in LM process planning either in FDM or orthogonal deposition manufacturing system.

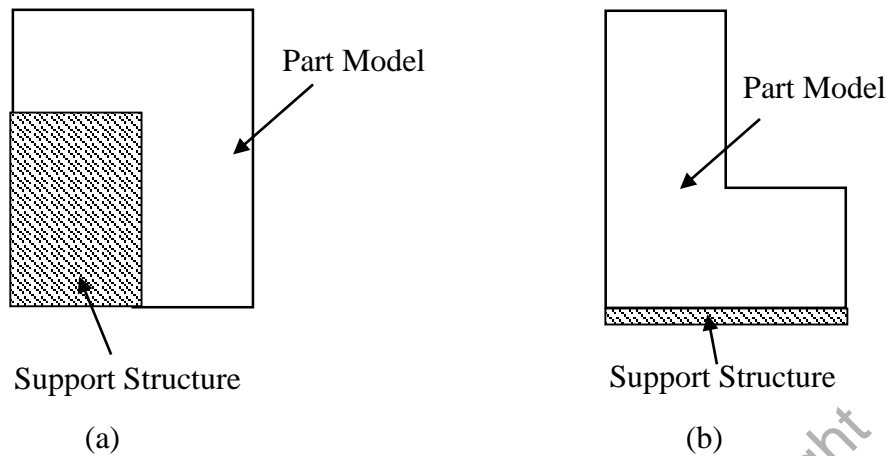


Figure 4.14: Comparison on the concept of feature-based extraction used in support generation; (a) without consideration of the OPDO (Yang *et al.*, 2003) and (b) with consideration of the OPDO.

The finding of the current work proves that the OPDO can be determined using the Feature-based Support Generation. In this generation, the volume and amount of support structure were used as criteria for orientation due to the involvement of external and base support structures. The direction for optimum part deposition in this work is found to be the same as direction suggested by Cheng *et al.* (1995) and Thrimurthulu *et al.* (2004) when the different criteria was used. This can be explained that the selection of the OPDO is subjected to many factors (Kulkarni *et al.*, 2000; Thrimurthulu *et al.*, 2004). This finding is consistent with the statement reported by Kulkarni *et al.* (2000) in which the total volume of support structure related to build time and cost of materials, can be used in determining the orientation for some LM technologies such as SLA and FDM. This work are also supported by Dutta *et al.* (2001) and Marsan *et al.* (1998) that emphasized the support generation as a key in these technologies.

There is an increase in both build time and cost of materials when increasing in volume and amount of support structure. The build time is influenced by both acceleration and deceleration of nozzle tips during material deposition of part or support material (Thrimurthulu *et al.*, 2004). The elapsed time occurs when the part material nozzle shifted to the support material nozzle and vice versa. Hence, by selecting the part orientation with least volume of support structure in the process of fabrication of part model allow to improve the build time. The smallest amount of support structure will be chosen for the case in which a few least volume of support structures are identified.

#### **4.5.1 Advantages and Limitations**

Some advantages of this work include; the process is not repeating since the best orientation is first identified; the choice of the orientation of part deposition has been automated using ANN, thus reduce human errors; the Feature-based Support Generation is a unique characteristic in FDM which can be performed theoretically and practically. Previously, the workers need to produce all products in all pre-defined directions. The product with a good quality will be selected as a final product regardless the orientation direction of the built. This work proposes the technique in which the operators require to choose the best direction that proposed by the MLP network (least overall support volume and the least amount of support structure).

The technique of Feature-based Support Generation has a limitation to be used in SLA and FDM. The main reason is that of the ESS and BSS are considered as apart of manufacturing process when producing the final product. Other limitations include the number of orientation to build the part, which is analysed only in six distinct directions that correspond to  $\pm x$ ,  $\pm y$  and  $\pm z$  axes (Table 3.1) with one build direction (single nozzle).

These directions are based on standard construction axis/plane in CAD system and working axis/plane in Insight software.

#### **4.6 Summary**

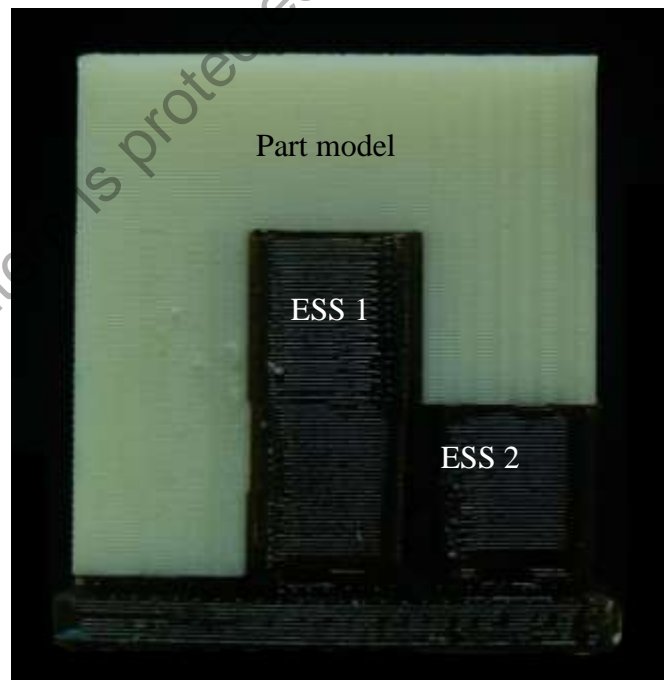
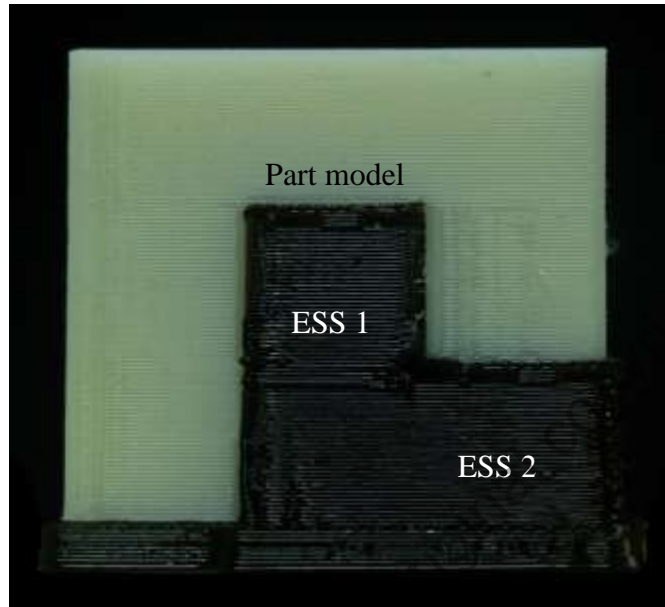
The activities in CAD and CAM can be integrated using the concept of Feature-based Support Generation. By using this approach, the LM cycle can be minimized due to the OPDO which has been decided before transferring data to the FDM machine. This concept offers less human error because the selection of orientation of part deposition (dependent on support volume and amount of support structure) has been automated using MLP networks.

#### **4.7 Results and Discussion – Surface Improvement**

The entire geometry of part models produced by FDM 3000 machine before and after surface improvement are displayed in Figs. 4.15(a) and (b), respectively. The part model and support structures of ESS 1 and ESS 2 can be clearly seen due to different colour of materials used in the process. The contact between part model and ESS is observed (Fig. 4.15(a)) before improvement using Feature-based Support Generation is made. In contrast, the gap is seen between part model and ESS after improvement as shown in Fig. 4.15(b). The CAD and STL files for this part model are attached in Appendices F and G, respectively.

The surface contact areas of ESS are observed from the top to the bottom section before surface improvement are shown Figs. 4.16(a) to (c). The surface improvement

(gap) results in producing the part model with uniform non-surface contact area containing the ESS 1 for both sides (Figs. 4.16(d) to (f)).



(b)

Figure 4.15: Actual part models produced by FDM machine; (a) Before improvement and (b) After improvement using Feature-based Support Generation.

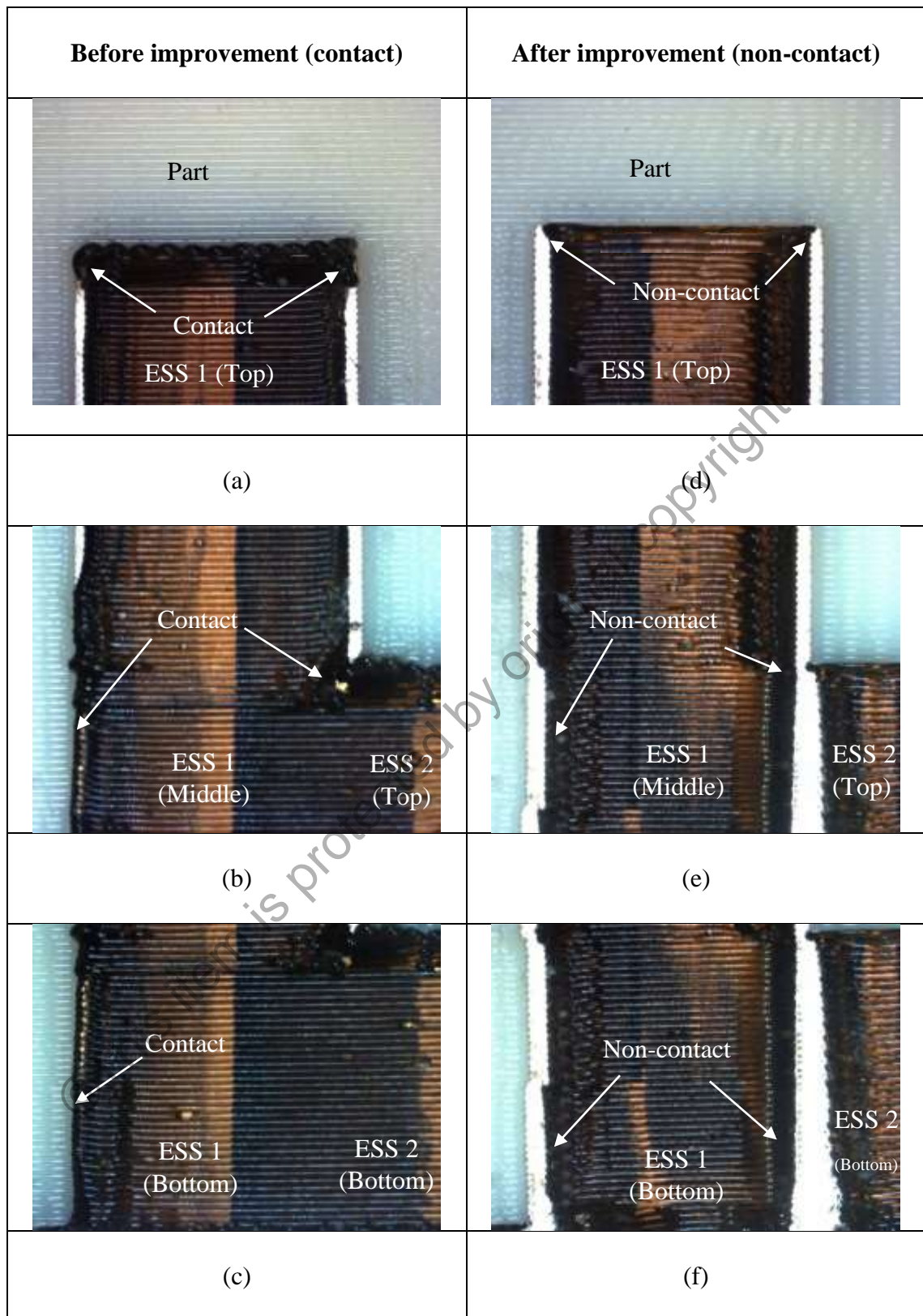
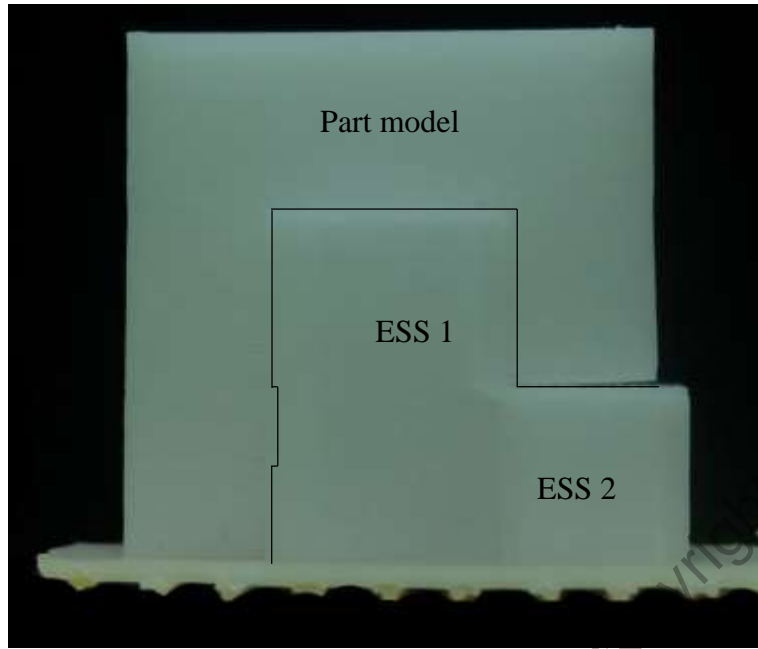


Figure 4.16: Actual part models produced by FDM machine; (a) to (c) Contact surface area and (d) to (f) Non-contact surface area.

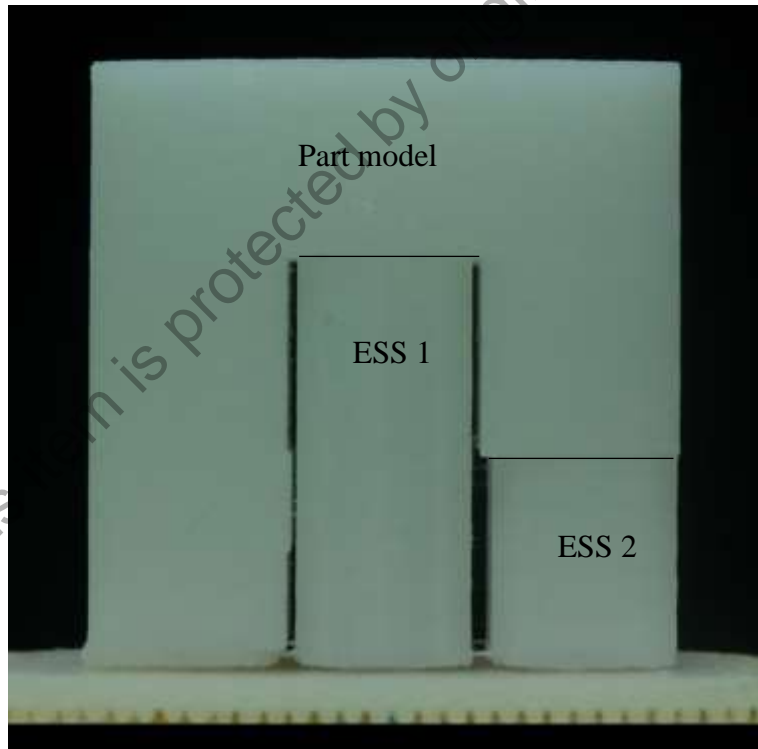
Next, the same part model as in Fig. 4.15 was successfully produced using the Zortrax 3D Printer machine. The whole size of the part model before and after surface improvement are depicted in Figs. 4.17(a) and (b). The part model and support structures are made of similar materials due to single nozzle of the machine and hard to differentiate between them. From Fig. 4.17(a), it can be seen that the amount of material required to develop the supports (ESS 1 and ESS 2) is higher than the material used in FDM machine.

Spacing between part model and support structure before and after surface improvement produced by Zortrax 3D Printer are shown in Figs. 4.18(a) and (b). The non-contact surface at unnecessary area between part model and ESS are clearly observed in Fig. 4.18(b). The surface improvement results in producing the part model with uniform non-surface contact using Zortrax 3D Printer machine and consistent with the results produced by FDM machine (Figs. 4.18(a) to (f)).

In the present work, the surface roughness on the part model at the contact surface area before and after improvement was measured using a Mitutoyo SURFTEST Model SV-400. The average surface roughness for the part model with uniform non-surface contact area using FDM and Zortrax 3D Printer machines are 5.43 and 5.7  $\mu\text{m}$ , respectively. The surface quality are improved approximately 38% (FDM) and 39% (Zortrax 3D Printer).



(a)



(b)

Figure 4.17: Actual part model produced by Zortrax 3D Printer machine; (a) Before improvement and (b) After improvement using Feature-based Support Generation.



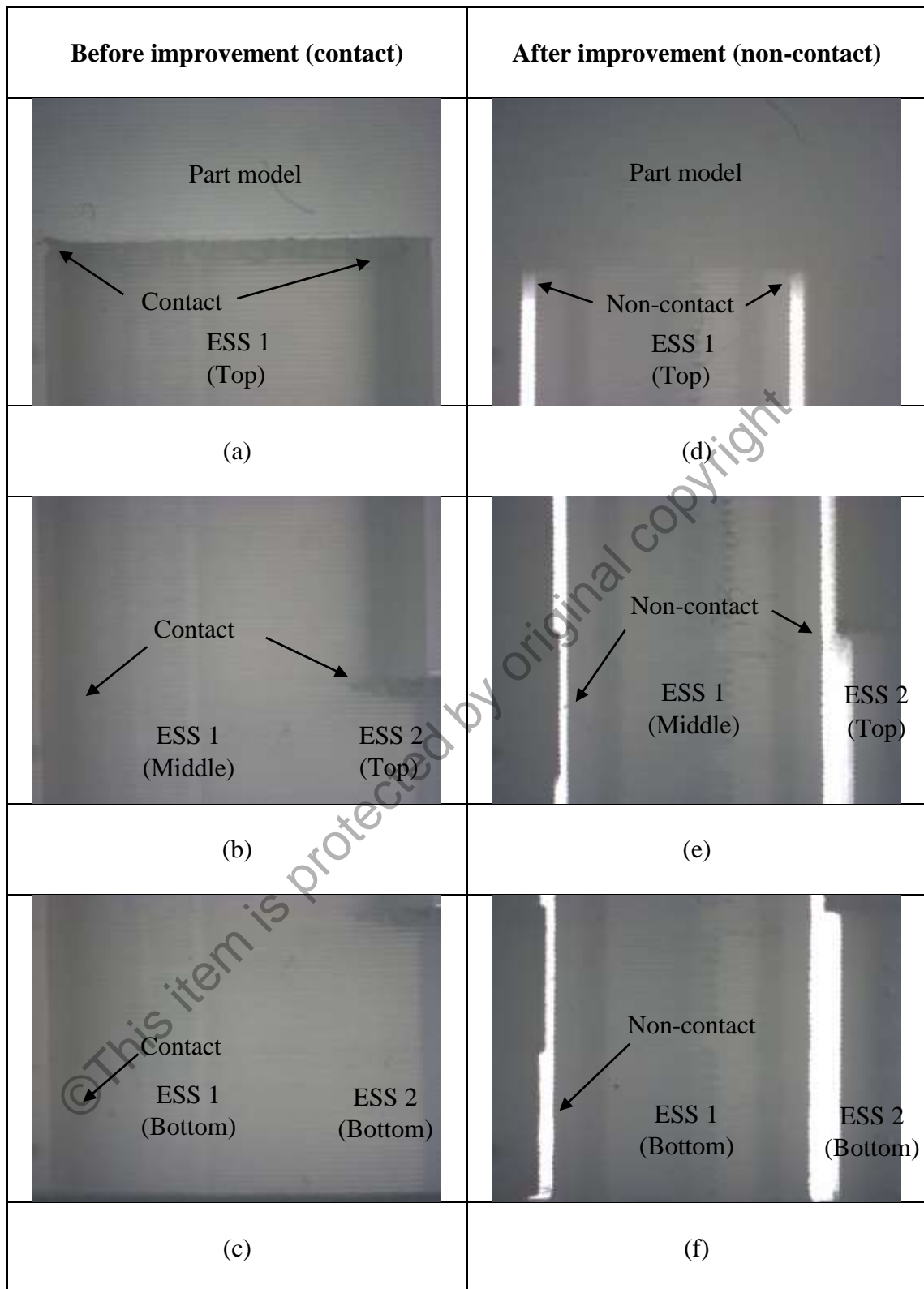


Figure 4.18: Actual part model produced by Zortrax 3D Printer machine;  
(a) to (c) Contact surface area and (d) to (f) Non-contact surface area.

### 4.7.1 Introduction

The objective of this section is to develop the non-contact surface between part model and ESS using Feature-based Support Generation by considering all four case studies which are previously described in Sections 3.3.1 to 3.3.4. This work leads to a higher quality product by eliminating the marks left at unnecessary area on the part surfaces.

The ESF has two overhang areas; 1) the area in the range of POA (i.e. SSF) and 2) the area that exceed POA. The construction of ESF is shown in Fig. 4.19.

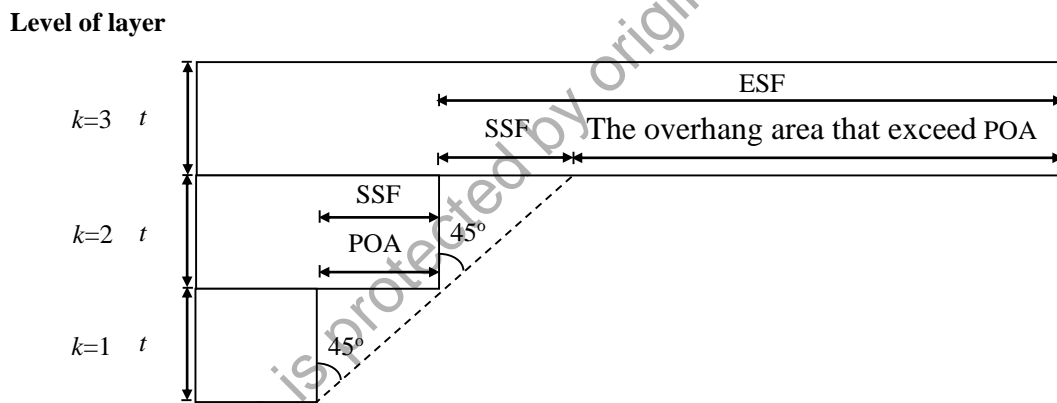
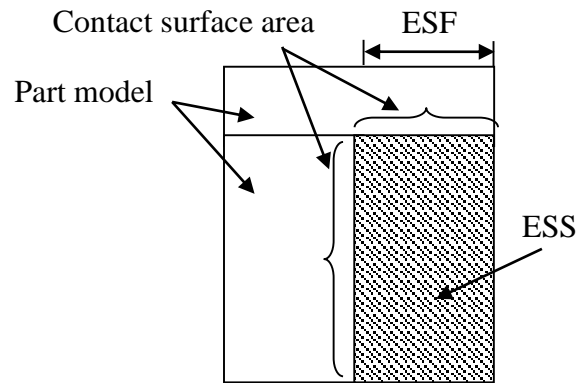


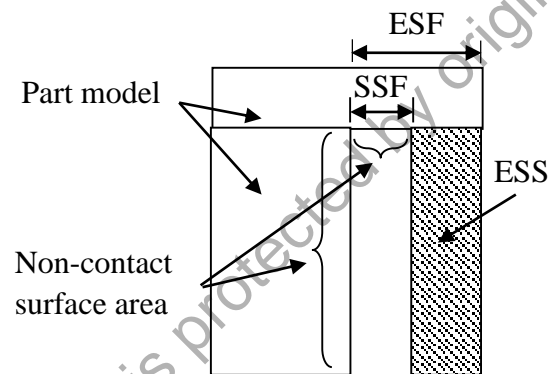
Figure 4.19: Construction of ESF.

In developing the part model, the support volume is not required to support the SSF ( $k=2$  in Fig.5.1). At Layer 3 ( $k=3$ ) in the same figure, the SSF is considered to be apart of ESF. Then, it can be avoided during fabricating the support volume to support ESF. The support volume of ESS developed in the system is used to support the ESF in horizontal direction. This support volume seems to have a contact with unnecessary part surface in vertical direction (Fig. 4.20(a)). The improvement by using the Feature-based

Support Generation reveal that there is no contact area at unnecessary part surface (vertical direction) and the support volume to support SSF (horizontal direction) as shown in Fig. 4.20(b). Finally, the surface quality of final part model can be improved.



(a) Contact surface between part model and ESS.



(b) Non-contact surface between part model and ESS.

Figure 4.20: Construction of ESS of part model. The part model and ESS interface; (a) contact surface (before improvement) and (b) Non-contact surface (after improvement) using Feature-based Support Generation.

#### 4.7.2 Discussion

This section provides the information of Feature-based Support Generation concept used for part model which requires a good surface finish. This concept is applied to give 'non-contact area' between the part model and ESS at unwanted regions. However the support structure is still required to support the detected ESF. This result increases the

efficiency of fabrication and quality of part model by minimizing the marks left on the surface.

In additional, the post-processes that required for cutting, trimming, and polishing of parts can be eliminated. This results in reducing the production time and possible errors that might be occurred in post-processing stages.

The non-contact between these two areas can produce a higher dimensional accuracy and excellent surface finish part known as a near-net shape product. This type of product require less post-processing to turn into final shape before it can be used.

In term of mechanical properties, the smooth surface finish gives a higher strength compared to product with non-uniform surface finish. Crack due to stress concentration on non-uniform surface can be avoided.

### **4.7.3 Summary**

The finding in this chapter shows that the surface quality of the part model can be enhanced by allowing gaps between the part model and ESS at unwanted contact area. The surface improvement using the features-based support generation technique can be applied in the other machines (e.g. Zortrax 3D Printer) when ESS becomes as apart of their manufacturing activity. The similar results are produced when different machines are used. This experiment shows that the Feature-Based Support Generation technique has a capability to produce a part with a good surface finish. The consistent result has been proven by using FDM and Zortrax 3D Printer. It can be concluded the Feature-Based Support Generation technique can be applied when the surface finish become as a key parameter in the work.

## CHAPTER 5

### CONCLUSION AND RECOMMENDATION FOR FUTURE WORK

#### 5.1 Conclusion

This research work involves the use of Feature-based Support Generation for determining the OPDO in the main work and next, improving surface finish of part model in fabrication. These two sections of work have been successfully carried out. The integration between CAD and CAM implies that the process planning in FDM can be automated with less human errors. The Optimum Part Deposition Orientation (OPDO) determination involving MLP Networks (considering build cost and time) can provide the best orientation of part during manufacturing processes.

The support generation is important in FDM. In this work, the features connected to this support are extracted according to unique features of additive technique (layer-by-layer). In this study, the work can be concluded as the following:

- i. Volume and amount of support structure are the most crucial parameters in deciding the OPDO. The Feature-based Support Generation data extraction technique has been successfully used to seek the information of volume and amount of support structure and. This can be achieved through the integration between CAD and CAM system. Part Model 1 (shown in Figure 4.4) can be manufactured with the lowest volume of support structure in Direction 5.

- ii. Feature-based Support Generation concept is used to improve the surface contact area between part model and support structure by reducing unnecessary support volume.

## **5.2 Recommendation for Future Work**

This research has been completed within the scope of work. Some suggestions for future work that related to the field are listed below:

- i. To develop less density support structure by optimizing the material fabrication process.
- ii. To minimize the total area of contact with support structure.
- iii. To extend the use of feature-based concept in other LM technology e.g. SLA.

## **5.3 Contribution to the Knowledge**

Feature-based technique has thus been rarely used in the LM technology (Zhang *et al.*, 2016). The steps of process planning in LM involve automatic operations except part deposition selection. In this research, the Feature-based Support Generation enables the automation of part deposition selection.

Support generation in manufacturing part is essential in FDM. It contributes to unnecessary build time and cost of material. Both parameters affect the efficiency of the entire manufacturing processes. In fact, this support is considered as a waste at the end of the process. This work found that the Feature-based Support Generation can be used to determine the OPDO based on support structure volume and group number of support structure.

This work has successfully introduced the concept of Feature-based Support Generation for additive process in FDM manufacturing. This concept is different compared to the feature introduced in conventional manufacturing (Kerbrat *et al.*, 2010). The introduced feature is unnecessary to be recognized as in conventional manufacturing (machining). This finding is able to resolve the problem related to features in additive manufacturing process of FDM.

In this work, the minimum support volume of ESS is a vital criteria in selecting the OPDO. This is due to the relationship between build time and the total cost of the material used in the build. The decrease in the support volume results in the decrease of the build time and the cost of the material.

The problem of surface contact between part model and ESS has also been improved using feature-based technique. This technique provides gap between these two entities thus increased the quality of surface finish without diminishing other structures and properties.

Structure 5 is a combination of MLP 1 (support volume) and MLP 2 (number of support structure) designed by ANN helps to select the OPDO with the testing accuracy over 85%.

The automated process planning produced throughout this research benefit the LM users in wide applications such as manufacturing, automotive, aerospace and biomedical.

## REFERENCES

- Ahn, D.-K., Kwon, S.-M., & Lee, S.-H. (2008). Expression for Surface Roughness Distribution of FDM Processed Parts. *Smart Manufacturing Application, 2008. ICSMA 2008. International Conference on IEEE*, 490-493.
- Ahn, D., Kim, H., & Lee, S. (2009). Surface Roughness Prediction using Measured Data and Interpolation in Layered Manufacturing. *Journal of Materials Processing Technology*, 209(2), 664-671.
- Ahn, D., Kweon, J.-H., Choi, J., & Lee, S. (2012). Quantification of Surface Roughness of Parts Processed by Laminated Object Manufacturing. *Journal of Materials Processing Technology*, 212, 339-346.
- Ahn, D., Kweon, J.-H., Kwon, S., Song, J., & Lee, S. (2009). Representation of Surface Roughness in Fused Deposition Modeling. *Journal of Materials Processing Technology*, 209, 5593-5600.
- Ahn, D. K., Kim, H. C., & Lee, S. H. (2005). Determination of Fabrication Direction to Minimize Post-machining in FDM by Prediction of Non-linear Roughness Characteristics. *Journal of Mechanical Science and Technology*, 19(1), 144-155.
- Ahn, D. K., Kim, H. C., & Lee, S. H. (2007). Fabrication Direction Optimization to Minimize Post-Machining in Layered Manufacturing. *International Journal of Machine Tools & Manufacture*, 47, 593-606.
- Ahn, S. H., Montero, M., Odell, D., Roundy, S., & Wright, P. K. (2002). Anisotropic Material Properties of Fused Deposition Modeling ABS. *Rapid Prototyping Journal*, 8(4), 248-257.
- Alexander, P., Allen, S., & Dutta, D. (1998). Part Orientation and Build Cost Determination in Layered Manufacturing. *Computer Aided Design*, 30(5), 343-356.
- Aylor, S., Rabelo, L., & Alptekin, S. (1992). Artificial Neural Networks for Robotics Coordinate Transformation. *Computers & Industrial Engineering*, 22(4), 481-493.
- Bandyopadhyay, A., Das, K., Marusich, J., & Onagoruwa, S. (2006). Application of Fused Deposition in Controlled Microstructure Metal-Ceramic Composites. *Rapid Prototyping Journal*, 12(3), 121-128.
- Barschdorff, D., & Monostori, L. (1991). Neural Networks: Their Applications and Perspectives in Intelligent Machining. *Computers in Industry*, 17, 101-119.
- Bellehumeur, C., Li, L., Sun, Q., & Gu, P. (2004). Modeling of Bond Formation Between Polymer Filaments in the Fused Deposition Modeling Process. *Journal of Manufacturing Processes*, 6(2), 170-178.



- Bellini, A., & Güçeri, S. (2003). Mechanical Characterization of Parts Fabricated using Fused Deposition Modeling. *Rapid Prototyping Journal*, 9(4), 252-264.
- Bellini, A., Shor, L., & Guceri, S. I. (2005). New developments in fused deposition modeling of ceramics. *Rapid Prototyping Journal*, 11(4), 214-220.
- Boschetto, A., & Bottini, L. (2015). Triangular Mesh Offset Aiming to Enhance Fused Deposition Modeling Accuracy. *The International Journal of Advanced Manufacturing Technology*, 80(1), 99-111.
- Boschetto, A., Giordano, V., & Veniali, F. (2012). Modelling Micro Geometrical Profiles in Fused Deposition Process. *The International Journal of Advanced Manufacturing Technology*, 61(9-12), 945-956.
- Boschetto, A., Giordano, V., & Veniali, F. (2013). 3D Roughness Profile Model in Fused Deposition Modelling. *Rapid Prototyping Journal*, 19(4), 240-252.
- Byun, H. S., & Lee, K. H. (2006a). Determination of Optimal Build Direction in Rapid Prototyping with Variable Slicing. *International Journal of Advanced Manufacturing Technology*, 28, 307-313.
- Byun, H. S., & Lee, K. H. (2006b). Determination of the Optimal Build Direction for Different Rapid Prototyping Processes using Multi-Criterion Decision Making. *Robotics and Computer-Integrated Manufacturing*, 22(1), 69-80.
- Campbell, R. I., Martorelli, M., & Lee, H. S. (2002). Surface Roughness Visualisation for Rapid Prototyping Models. *Computer-Aided Design*, 34(10), 717-725.
- Chalasanani, K., Jones, L., & Roscoe, L. (1995). Support Generation for Fused Deposition Modeling. *Proceedings of Solid Freeform Fabrication Symposium, Austin, Texas*.
- Chang, D.-Y., & Huang, B.-H. (2011). Studies on Profile Error and Extruding Aperture for the RP Parts using The Fused Deposition Modeling Process. *The International Journal of Advanced Manufacturing Technology*, 53(9-12), 1027-1037.
- Cheng, W., Fuh, J. Y. H., Nee, A. Y. C., Wong, Y. S., Loh, H. T., & Miyazawa, T. (1995). Multi-Objective Optimization of Part-Building Orientation in Stereolithography. *Rapid Prototyping Journal*, 1(4), 12-23.
- Dai, L., & Hong, X. (2014). The Development of 3D Print Technology. *Applied Mechanics and Materials*, 644-650, 4856-4859.
- Daniel, B., Georgeta, I., Mihai, A., Lucian, B., & Alina, S. (2014). 3D CAD, CAM and Rapid Prototyping Applied for Cam Fabrication. *Applied Mechanics and Materials*, 658, 553-556.
- Deitel, H.M., Deitel, P.J. & Nieto, T.R. (2002). Visual Basic 6, Prentice Hall, International Edition.

- Dreiseitl, S., & Ohno-Machado, L. (2002). Logistic Regression and artificial Neural Network Classification Models: A Methodology Review. *Journal of Biomedical Informatics*, 35, 352-359.
- Drummer, D., Cifuentes-Cueíllar, S., & Rietzel, D. (2012). Suitability of PLA/TCP for Fused Deposition Modeling. *Rapid Prototyping Journal*, 18(6), 500-507.
- Durgun, I., & Ertan, R. (2014). Experimental Investigation of FDM Process for Improvement of Mechanical Properties and Production Cost. *Rapid Prototyping Journal*, 20(3), 228-235.
- Dutta, D., Prinz, F., Rosen, D., & Weiss, L. (2001). Layered Manufacturing: Current Status and Future Trends. *Transactions of the ASME Journal of Computing and Information Science in Engineering*, 1, 60-71.
- Fatimatuzahraa, A. W., Farahaina, B., & Yusoff, W. A. Y. (2011). The Effect of Employing Different Raster Orientations on the Mechanical Properties and Microstructure of Fused Deposition Modeling Parts. *2011 IEEE Symposium on Business, Engineering and Industrial Applications (ISBEIA)*, 22-27.
- Feng, G., Huang, G. B., Lin, Q., & Gay, R. (2009). Error Minimized Extreme Learning Machine with Growth of Hidden Nodes and Incremental Learning. *IEEE Transactions on Neural Networks*, 20(8), 1352-1357.
- Frank, D., & Fadel, G. (1995). Expert System Based Selection of the Preferred Direction of Build for Rapid Prototyping. *Journal of Intelligent Manufacturing*, 6, 339-345.
- Galantucci, L. M., Lavecchia, F., & Percoco, G. (2009). Experimental Study Aiming to Enhance the Surface Finish of Fused Deposition Modeled Parts. *CIRP Annals - Manufacturing Technology*, 58(1), 189-192.
- Garg, H. K., & Singh, R. (2015). Development of New Composite Materials for Rapid Tooling using Fused Deposition Modelling. *Materials Science Forum*, 808, 103-108.
- Ghorpade, A., Karunakaran, K. P., & Tiwari, M. K. (2007). Selection of Optimal Part Orientation in Fused Deposition Modelling using Swarm Intelligence. *Proceedings of the Institution of Mechanical Engineers, Part B: Journal of Engineering Manufacture*, 221(7), 1209-1219.
- Guo, K.-B., Zhang, L.-C., Wang, C.-J., & Huang, S.-H. (2007). Boolean Operations of STL Models Based on Loop Detection. *The International Journal of Advanced Manufacturing Technology*, 33, 627-633.
- Haykin, S., & Network, N. (2004). A Comprehensive Foundation. *Neural Networks*, 2, 41.
- Hope, R. L., Roth, R. N., & Jacobs, P. A. (1997). Adaptive Slicing with Sloping Layer Surfaces. *Rapid Prototyping Journal*, 3(3), 89-98.

<https://www.mathworks.com/products/neural-network.html>

<http://www.stratasys.com/>.

<https://zortrax.com/>.

Huang, B., & Singamneni, S. (2014). Raster Angle Mechanics in Fused Deposition Modelling. *Journal of Composite Materials*, 49(3), 363-383.

Huang, S. H., & Bang, H.-C. (1993). Neural Networks in Manufacturing: A Survey. *IEEE/CHMT International Electronics Manufacturing Technology Symposium*.

Huang, S. H., Liu, P., Mokasdar, A., & Hou, L. (2013). Additive Manufacturing and Its Societal Impact: A Literature Review. *International Journal Advance Manufacturing Technology*, 67, 1191-1203.

Huang, S. H., & Zhang, H.-C. (1994). Artificial Neural Networks in Manufacturing: Concepts, Applications, and Perspectives. *IEEE Transactions on Components, Packaging, and Manufacturing Technology-Part A*, 17(2), 212-228.

Huang, T., Solvang, W. D., & Yu, H. (2016). An Introduction of Small-Scale Intelligent Manufacturing System. In *Small-scale Intelligent Manufacturing Systems (SIMS), International Symposium on IEEE*, 31-39.

Huang, X., Ye, C., Wu, S., Guo, K., & Mo, J. (2009). Sloping Wall Structure Support Generation for Fused Deposition Modeling. *The International Journal of Advanced Manufacturing Technology*, 42, 1074-1081.

Huang, Z., Ma, Y., Wei, J., Pan, A., & Liu, J. (2015). Research of Fused Deposition Modeling Process Oriented Component Design. *Advanced Materials Research*, 1095, 828-832.

Hui, Z., Yuan, Z. H., Long, Z. Y., & Wen, W. Q. (2011). Research of Wood Plastic Composites Application Based on Fused Deposition Modeling Technology. *2011 International Conference on Electronic & Mechanical Engineering and Information Technology*, 3, 1560-1562.

Hur, J., & Lee, K. (1998). The Development of a CAD Environment to Determine the Preferred Build-up Direction for Layered Manufacturing. *The International Journal of Advanced Manufacturing Technology*, 14, 247-254.

İpek, M., Selvi, İ. H., Findik, F., Torkul, O., & Cedimoğlu, I. H. (2013). An expert System Based Material Selection Approach to Manufacturing. *Materials & Design*, 47, 331-340.

Ivan, G., Emil, S., Ľuboš, K., & Volodymyr, K. (2015). Surface Finish Techniques for FDM Parts. *Materials Science Forum*, 818, 45-48.

- Ivanova, O., Williams, C., & Campbell, T. (2013). Additive Manufacturing (AM) and Nanotechnology: Promises and Challenges. *Rapid Prototyping Journal*, 19(5), 353-364.
- Jami, H., Masood, S. H., & Song, W. Q. (2013). Dynamic Response of FDM Made ABS Parts in Different Part Orientations. *Advanced Materials Research*, 748, 291-294.
- Jin, Y.-a., He, Y., & Fu, J.-z. (2015). Support Generation for Additive Manufacturing Based on Sliced Data. *The International Journal of Advanced Manufacturing Technology*, 80(9), 2041-2052.
- Jin, Y.-a., Li, H., He, Y., & Fu, J.-z. (2015). Quantitative Analysis of Surface Profile in Fused Deposition Modelling. *Additive Manufacturing*, 8, 142-148.
- Kankal, M., Akpınar, A., Kömürcü, M. İ., & Özşahin, T. Ş. (2011). Modeling and Forecasting of Turkey's Energy Consumption using Socio-Economic and Demographic Variables. *Applied Energy*, 88(5), 1927-1939.
- Kannan, S., Senthilkumaran, D., & Elangovan., K. (2013). Development of Composite Materials by Rapid Prototyping Technology using FDM Method. *International Conference on Current Trends in Engineering and Technology, ICCTET'13*, 281-283.
- Kasabov, N. K. (1996). *Foundations of Neural Network, Fuzzy Systems and Knowledge Engineering*. Cambridge, Massachusetts: Massachusetts Institute of Technology.
- Kerbrat, O., Mognol, P., & Hascoet, J.-Y. (2010). Manufacturing Complexity Evaluation at the Design Stage for Both Machining and Layered Manufacturing. *CIRP Journal of Manufacturing Science and Technology*, 2, 208-215.
- Kim, C., Espalin, D., Cuaron, A., Perez, M. A., MacDonald, E., & Wicker, R. B. (2015). A Study to Detect a Material Deposition Status in Fused Deposition Modeling Technology. *2015 IEEE International Conference on Advanced Intelligent Mechatronics (AIM)*, 779-783.
- Kim, G. D., & Oh, Y. T. (2008). A Benchmark Study on Rapid Prototyping Processes and Machines: Quantitative Comparisons of Mechanical Properties, Accuracy, Roughness, Speed, and Material Cost. *Proceedings of the Institution of Mechanical Engineers, Part B: Journal of Engineering Manufacture*, 222(2), 201-215.
- Kulkarni, P., Marsan, A., & Dutta, D. (2000). A Review of Process Planning Techniques in Layered Manufacturing. *Rapid Prototyping Journal*, 6, 18-35.
- Kumar, G. P., & Regalla, S. P. (2012). Optimization of Support Material and Build Time in Fused Deposition Modeling (FDM). *Applied Mechanics and Materials*, 110-116, 2245-2251.

- Lan, P.-T., Chou, S. Y., Chen, L. L., & Gemmill, D. (1997). Determining Fabrication Orientation for Rapid Prototyping with Stereolithography Apparatus. *Computer Aided Design*, 29( 1), 53-62.
- Latiff, Z. A., Rahman, M. R. A., & Saad, F. (2014). Dimensional Accuracy Evaluation of Rapid Prototyping Fused Deposition Modeling Process of FDM200mc Machine on Basic Engineering Profiles. *Applied Mechanics and Materials*, 465-466, 96-100.
- Leacock, A. G., Cowan, G., Cosby, M., Volk, G., McCracken, D., & Brown, D. (2015). Structural and Frictional Performance of Fused Deposition Modelled Acrylonitrile Butadiene Styrene (P430) with a View to Use as Rapid Tooling Material in Sheet Metal Forming. *Key Engineering Materials*, 639, 325-332.
- Leary, M., Babaei, M., Brandt, M., & Subic, A. (2013). Feasible Build Orientations for Self-Supporting Fused Deposition Manufacture: A Novel Approach to Space-Filling Tesselated Geometries. *Advanced Materials Research*, 633, 148-168.
- Leary, M., Merli, L., Torti, F., Mazur, M., & Brandt, M. (2014). Optimal Topology for Additive Manufacture: A Method for Enabling Additive Manufacture of Support-Free Optimal Structures. *Materials and Design*, 63, 678-690.
- Lee, B. H., Abdullah, J., & Khan, Z. A. (2005). Optimization of Rapid Prototyping Parameters for Production of Flexible ABS Object. *Journal of Materials Processing Technology*, 169(1), 54-61.
- Li, C., Fu, G., & Guo, K. (2011). Study on Forecast of Forming Temperature of ABS Resin During Fused Deposition Manufacturing by Fuzzy Comprehensive Evaluation. *Key Engineering Materials*, 464, 264-267.
- Li, P., & Huang, S. (2014). Application of Rapid Prototyping Technology in Automobile Manufacturing Industry. *Applied Mechanics and Materials*, 533, 106-110.
- Lirabi, I., & Amirabadi, H. (2015). Multi-objective Modeling and Optimization of Hybrid Layered Manufacturing under Maximum Allowable Heat Constraint. *Journal of Modares Mechanical Engineering*, 15(9), 153-160.
- Ludmila, N.-M., & Jozef, N.-M. (2013a). Application of Rapid Prototyping Technology in Intelligent Optimization Design Area. *Applied Mechanics and Materials*, 404, 754-757.
- Ludmila, N.-M., & Jozef, N.-M. (2013b). Experimental Testing of Materials Used in Fused Deposition Modeling Rapid Prototyping Technology. *Advanced Materials Research*, 740, 597-602.
- Ludmila, N.-M., & Jozef, N.-M. (2013c). Selected Testing for Rapid Prototyping Technology Operation. *Applied Mechanics and Materials*, 308, 25-31.

- Luo, N., & Wang, Q. (2015). Fast Slicing Orientation Determining and Optimizing Algorithm for Least Volumetric Error in Rapid Prototyping. *The International Journal of Advanced Manufacturing Technology*, 1-17.
- Ma, W., & He, P. (1999). An Adaptive Slicing and Selective Hatching Strategy for Layered Manufacturing. *Journal of Materials Processing Technology*, 89-90, 191-197.
- Majhi, J., Janardan, R., Michieland, S., & Gupta, P. (1999). On Some Geometric Optimization Problems in Layered Manufacturing. *Computational Geometry, Theory and Application*, 12, 219-239.
- Mani, K., Kulkarni, P., & Dutta, D. (1999). Region-based Adaptive Slicing. *Computer-Aided Design*, 31(5), 317-333.
- Márkus, A., & Hatvany, J. (1987). Matching AI Tools to Engineering Requirements. *CIRP Annals - Manufacturing Technology*, 36(1), 311-315.
- Marsan, A., Kumar, V., Dutta, D., & Pratt, M. (1998). An Assessment of Data Requirements and Data Transfer Formats for Layered Manufacturing. *Technical Report NISTIR 6216. Gaithersburg, MD: NIST*.
- Martinez, W. L., & Martinez, A. R. (2007). *Computational Statistics Handbook with MATLAB (22)*. CRC press.
- Masood, S. H., Mau, K., & Song, W. Q. (2010). Tensile Properties of Processed FDM Polycarbonate Material. *Materials Science Forum*, 654-656, 2556-2559.
- Massod, S. H., Rattanawong, W., & Iovenitti, P. (2000). Part Build Orientations Based on Volumetric Error in Fused Deposition Modelling. *The International Journal of Advanced Manufacturing Technology*, 16, 162-168.
- Massod, S. H., Rattanawong, W., & Iovenitti, P. (2003). A Generic Algorithm for Part Orientation System for Complex Parts in Rapid Prototyping. *Journal of Material Processing Technology*, 139(1-3), 110-116.
- McClurkin, J. E., & Rosen, D. W. (1998). Computer-Aided Build Style Decision Support for Stereolithography. *Rapid Prototyping Journal*, 4 (1), 4-13.
- McCullough, E. J., & Yadavalli, V. K. (2013). Surface Modification of Fused Deposition Modeling ABS to Enable Rapid Prototyping of Biomedical Microdevices. *Journal of Materials Processing Technology*, 213(6), 947-954.
- McMahon, C., & Brown, J. (1993). *CADCAM: From Principle to Practice*: Addison-Wesley, Wokingham, England, UK.
- Mirzadeh, H., & Najafizadeh, A. (2008). Correlation Between Processing Parameters and Strain-Induced Martensitic Transformation in Cold Worked AISI 301 Stainless Steel. *Materials characterization*, 59(11), 1650-1654.

- Montero, M., Roundy, S., Odell, D., Ahn, S.-H., & Wright, P. K. (2001). Material Characterization of Fused Deposition Modeling (FDM) ABS by Designed Experiments. *In Proceedings of rapid prototyping and manufacturing conference, Society of Manufacturing Engineers*, 1-21.
- Moroni, G., Syam, W. P., & Petrò, S. (2015). Functionality-based Part Orientation for Additive Manufacturing. *Procedia CIRP*, 36, 217-222.
- Nezhad, A. S., Vatani, M., Barazandeh, F., & Rahimi, A. R. (2009). Determining the Optimal Build Directions in Layered Manufacturing. *WSEAS Transactions on Applied and Theoretical Mechanics*, 4(4), 185-194.
- Ngai, E. W. T., Peng, S., Alexander, P., & Moon, K. K. (2014). Decision Support and Intelligent Systems in the Textile and Apparel Supply Chain: *An academic review of research articles. Expert Systems with Applications*, 41(1), 81-91.
- Nguyen, L., & Patel, R. V. (1991). Neural Network Architectures for the Forward Kinematics Problem in Robotics. *Joint IEEE Int. Neural Network Conf., San Diego, CA*, 3, 393-399.
- Novakova-Marcincinova, L., Fecova, V., Novak-Marcincin, J., Janak, M., & Barna, J. (2012). Effective Utilization of Rapid Prototyping Technology. *Materials Science Forum*, 713, 61-66.
- Onuh, S. O., & Hon, K. K. B. (1998). Optimising Build Parameters for Improved Surface Finish in Stereolithography. *International Journal Machining Tools Manufacturing*, 38(4), 329-392.
- Panda, B. N., Bahubalendruni, M. V. A. R., & Biswal, B. B. (2015). A General Regression Neural Network Approach for the Evaluation of Compressive Strength of FDM Prototypes. *Neural Computing and Applications*, 26(5), 1129-1136.
- Pandey, P. M. (2003). *Enhancement of Surface Finish in Fused Deposition Modeling*. (Ph.D. Thesis), I.I.T., Kanpur, India.
- Pandey, P. M. (2012). On the Rapid Prototyping Technologies and Applications in Product Design and Manufacturing. *Materials Science Forum*, 710, 101-109.
- Pandey, P. M., Reddy, N. V., & Dhande, S. G. (2003a). Improvement of Surface Finish by Staircase Machining in Fused Deposition Modeling. *Journal of Materials Processing Technology*, 132(1-3), 323-331.
- Pandey, P. M., Reddy, N. V., & Dhande, S. G. (2003b). Real Time Adaptive Slicing for Fused Deposition Modelling. *International Journal of Machine Tools and Manufacture*, 43(1), 61-71.
- Pandey, P. M., Reddy, N. V., & Dhande, S. G. (2007). Part Deposition Orientation Studies in Layered Manufacturing. *Journal of Materials Processing Technology*, 185, 125-131.

- Peng, A., & Wang, Z. (2010). Researches into Influence of Process Parameters on FDM Parts Precision. *Applied Mechanics and Materials*, 34-35, 338-343.
- Peng, A., Xiao, X., & Yue, R. (2014). Process Parameter Optimization for Fused Deposition Modeling using Response Surface Methodology Combined with Fuzzy Inference System. *The International Journal of Advanced Manufacturing Technology*, 73(1-4), 87-100.
- Phatak, A. M., & Pande, S. S. (2012). Optimum Part Orientation in Rapid Prototyping using Genetic Algorithm. *Journal of Manufacturing Systems*, 31(4), 395-402.
- Qian, X., & Dutta, D. (2001). Feature Based Fabrication in Layered Manufacturing. *Journal of Mechanical Design*, 123, 337-345.
- Rahmati, S., & Vahabli, E. (2015). Evaluation of Analytical Modeling for Improvement of Surface Roughness of FDM Test Part using Measurement Results. *The International Journal of Advanced Manufacturing Technology*, 79, 823-829.
- Ramanath, H. S., Chua, C. K., Leong, K. F., & Shah, K. D. (2008). Melt Flow Behaviour of Poly-E-Caprolactone in Fused Deposition Modelling. *Journal of Materials Science: Materials in Medicine*, 19(7), 2541-2550.
- Raut, S., Jatti, V. S., Khedkar, N. K., & T.P.Singh. (2014). Investigation of the Effect of Built Orientation on Mechanical Properties and Total Cost of FDM Parts. *Procedia Materials Science*, 6, 1625-1630.
- Rayegani, F., & Onwubolu, G. C. (2014). Fused Deposition Modelling (FDM) Process Parameter Prediction and Optimization using Group Method for Data Handling (GMDH) and Differential Evolution (DE). *The International Journal of Advanced Manufacturing Technology*, 73, 509-519.
- Salomons, O. W., Houten, F. J. A. M. v., & Kals, H. J. J. (1993). Review of Research in Feature-Based Design. *Journal of Manufacturing Systems*, 12(2), 113-132.
- Sahu, R. K., Mahapatra, S. S., & Sood, A. K. (2013). A Study on Dimensional Accuracy of Fused Deposition Modeling (FDM) Processed Parts using Fuzzy Logic. *Journal for Manufacturing Science & Production*, 13(3), 183-197.
- Shuaib, A. A., Olalere, F. E., & Daud, K. A. b. M. (2015). Rapid Prototyping Technology: The Next Keystone for Small and Medium Ceramic Industry. *Applied Mechanics and Materials*, 789-790, 1207-1211.
- Song, S., Wang, A., Huang, Q., & Tsung, F. (2014). Shape Deviation Modeling for Fused Deposition Modeling Processes. *2014 IEEE International Conference on Automation Science and Engineering (CASE)*, 758-763.
- Sood, A. K., Ohdar, R. K., & Mahapatra, S. S. (2009). Improving Dimensional Accuracy of Fused Deposition Modelling Processed Part using Grey Taguchi Method. *Materials and Design*, 30, 4243-4252.



- Sood, A. K., Ohdar, R. K., & Mahapatra, S. S. (2010). Parametric Appraisal of Mechanical Property of Fused Deposition Modelling Processed Parts. *Materials & Design*, 31(1), 287-295.
- Sunil, V. B., & Pande, S. S. (2009). Automatic Recognition of Machining Features using Artificial Neural Networks. *The International Journal of Advanced Manufacturing Technology*, 41(9), 932-947.
- Thrimurthulu, K., Pandey, P. M., & Reddy, N. V. (2004). Optimum Part Deposition Orientation in Fused Deposition Modeling. *International Journal of Machine Tools & Manufacture*, 44, 585-594.
- Tyberg, J., & Bøhn, J. H. (1999). FDM Systems and Local Adaptive Slicing. *Materials and Design*, 20, 77-82.
- Vijayaraghavan, V., Garg, A., Lam, J. S. L., Panda, B., & Mahapatra, S. S. (2015). Process Characterisation of 3D-Printed FDM Components using Improved Evolutionary Computational Approach. *The International Journal of Advanced Manufacturing Technology*, 78, 781-793.
- Villalpando, L., Eiliat, H., & Urbanic, R. J. (2014). An Optimization Approach for Components Built by Fused Deposition Modeling with Parametric Internal Structures. *Procedia CIRP*, 17, 800-805.
- West, A. P., Sambu, S. P., & Rosen, D. W. (2001). A Process Planning Method to Improve Build Performance in Stereolithography. *Computer Aided Design*, 33, 65-79.
- Witten, I. H., Frank, E., Hall, M. A., & Pal, C. J. (2016). *Data Mining: Practical Machine Learning Tools and Techniques*. Morgan Kaufmann.
- Xiaomao, H., Chunsheng, Y., Jianhua, M., & Haitao, L. (2009). Slice Data Based Support Generation Algorithm for Fused Deposition Modeling. *TSINGHUA SCIENCE AND TECHNOLOGY*, 14(1), 223-228.
- Xu, F., Wong, Y. S., Loh, H. T., Fuh, J. Y. H., & Miyazawa, T. (1997). Optimal Orientation with Variable Slicing in Stereolithography. *Rapid Prototyping Journal*, 3 (3), 76-88.
- Xueling, Y., Di, W., & Dongman, Y. (2012). Development and Application of Four Typical Rapid Prototyping Technologies. *160*, 165-169.
- Yang, S., Du, Z., & Kang, H. (2014). Application of Rapid Prototyping Technology on Development of Medical Equipment. *Advanced Materials Research*, 1030-1032, 2326-2329.
- Yang, Y., Loh, H. T., Fuh, J. Y. H., & Wang, Y. G. (2002). Equidistant Path Generation for Improving Scanning Efficiency in Layered Manufacturing. *Rapid Prototyping Journal*, 8(1), 30-37.

- Yang, Y., Loh, H. T., Fuh, J. Y. H., & Wong, Y. S. (2003). Feature Extraction and Volume Decomposition for Orthogonal Layered Manufacturing. *Computer-Aided Design*, 35, 1119-1128.
- Yu, H., & Wilamowski, B. M. (2011). Levenberg–Marquardt Training. *Industrial Electronics Handbook 5*(12), 1.
- Zhang, N., & Behera, P. K. (2012). Solar Radiation Prediction Based on Recurrent Neural Networks Trained by Levenberg-Marquardt Backpropagation Learning Algorithm. In *Innovative Smart Grid Technologies (ISGT), 2012 IEEE PES*, 1-7.
- Zhang, H.-C., & Alting, L. (1994). *Computerized Manufacturing Process Planning Systems*. London, UK.: Chapman & Hall, Ltd.
- Zhang, Y., Bernard, A., Harik, R., & Karunakaran, K. P. (2015). Build Orientation Optimization for Multi-Part Production in Additive Manufacturing. *Journal of Intelligent Manufacturing*, 1-15.
- Zhang, Y., Bernard, A., Gupta, R. K., Gupta, & Harik, R. (2016). Feature Based Building Orientation Optimization for Additive Manufacturing. *Rapid Prototyping Journal*, 22(2), 358-376.
- Zhang, Z., Li, D., Deng, J., Huang, M., Wan, X., Wu, Q., & Zhou, Y. (2014). Fixtures Design Based On RP Technology. *Applied Mechanics and Materials*, 615, 31-35.
- Zhenwen, Z., & Xicong, Y. (2015). The progress and application of rapid prototyping technology. *Applied Mechanics and Materials*, 697, 340-343.
- Zulkifli, A. H. (1999). *A feature-recognition system using neural networks*. (PhD Thesis), University of Dundee, UK.

## APPENDIX A

Data for training and testing processes to determine optimum hidden node (Structure 1).

No. of Hidden Nodes	No. of Training Data correctly classified	No. of Testing Data correctly classified	Training Accuracy (%)	Testing Accuracy (%)
1	155	55	38.75	27.50
2	161	57	40.25	28.50
3	165	59	41.25	29.50
4	176	63	44.00	31.50
5	176	67	44.00	33.50
6	182	71	45.50	35.50
7	200	73	50.00	36.50
8	210	77	52.50	38.50
9	218	81	54.50	40.50
10	227	83	56.75	41.50
11	228	87	57.00	43.50
12	230	91	57.50	45.50
13	233	95	58.25	47.50
14	235	101	58.75	50.50
15	239	107	59.75	53.50
16	241	112	60.25	56.00
17	245	115	61.25	57.50
18	247	117	61.75	58.50
19	249	120	62.25	60.00
20	254	122	63.50	61.00
21	259	122	64.75	61.00
22	268	122	67.00	61.00
23	268	125	67.00	62.50
24	268	124	67.00	62.00
25	267	125	66.75	62.50
26	266	122	66.50	61.00
27	267	121	66.75	60.50
28	268	119	67.00	59.50
29	265	121	66.25	60.50
30	266	123	66.50	61.50

Continued

<b>No. of Hidden Nodes</b>	<b>No. of Training Data correctly classified</b>	<b>No. of Testing Data correctly classified</b>	<b>Training Accuracy (%)</b>	<b>Testing Accuracy (%)</b>
31	265	121	66.25	60.50
32	264	122	66.00	61.00
33	266	123	66.50	61.50
34	267	124	66.75	62.00
35	268	122	67.00	61.00
36	269	123	67.25	61.50
37	267	120	66.75	60.00
38	264	118	66.00	59.00
39	263	122	65.75	61.00
40	265	121	66.25	60.50
41	266	122	66.50	61.00
42	267	123	66.75	61.50
43	267	119	66.75	59.50
44	265	122	66.25	61.00
45	268	123	67.00	61.50
46	269	124	67.25	62.00
47	267	122	66.75	61.00
48	264	119	66.00	59.50
49	266	123	66.50	61.50
50	269	122	67.25	61.00

©This item is protected by original copyright

## APPENDIX B

Data for training and testing processes to determine optimum hidden node (Structure 2).

No. of Hidden Nodes	No. of Training Data correctly classified	No. of Testing Data correctly classified	Training Accuracy (%)	Testing Accuracy (%)
1	231	100	57.75	50.00
2	233	103	58.25	51.50
3	233	106	58.25	53.00
4	237	111	59.25	55.50
5	241	112	60.25	56.00
6	243	110	60.75	55.00
7	247	109	61.75	54.50
8	253	113	63.25	56.50
9	257	117	64.25	58.50
10	266	114	66.50	57.00
11	269	117	67.25	58.50
12	274	120	68.50	60.00
13	279	122	69.75	61.00
14	283	129	70.75	64.50
15	289	127	72.25	63.50
16	293	130	73.25	65.00
17	291	133	72.75	66.50
18	289	135	72.25	67.50
19	292	133	73.00	66.50
20	295	136	73.75	68.00
21	299	139	74.75	69.50
22	301	141	75.25	70.50
23	305	143	76.25	71.50
24	310	143	77.50	71.50
25	307	145	76.75	72.50
26	303	144	75.75	72.00
27	305	147	76.25	73.50
28	309	150	77.25	75.00
29	311	149	77.75	74.50
30	313	147	78.25	73.50

Continued

<b>No. of Hidden Nodes</b>	<b>No. of Training Data correctly classified</b>	<b>No. of Testing Data correctly classified</b>	<b>Training Accuracy (%)</b>	<b>Testing Accuracy (%)</b>
31	307	150	76.75	75.00
32	305	148	76.25	74.00
33	311	147	77.75	73.50
34	303	147	75.75	73.50
35	305	149	76.25	74.50
36	312	150	78.00	75.00
37	306	147	76.50	73.50
38	303	145	75.75	72.50
39	300	143	75.00	71.50
40	304	145	76.00	72.50
41	310	147	77.50	73.50
42	309	148	77.25	74.00
43	307	146	76.75	73.00
44	303	147	75.75	73.50
45	307	149	76.75	74.50
46	311	150	77.75	75.00
47	310	147	77.50	73.50
48	302	145	75.50	72.50
49	307	147	76.75	73.50
50	308	148	77.00	74.00

©This item is protected by original copyright

## APPENDIX C

Data for training and testing processes to determine optimum hidden node (Structure 3).

<b>No. of Hidden Nodes</b>	<b>No. of Training Data correctly classified</b>	<b>No. of Testing Data correctly classified</b>	<b>Training Accuracy (%)</b>	<b>Testing Accuracy (%)</b>
1	351	155	87.75	77.50
2	352	151	88.00	75.50
3	352	154	88.00	77.00
4	356	157	89.00	78.50
5	354	155	88.50	77.50
6	349	152	87.25	76.00
7	361	157	90.25	78.50
8	359	161	89.75	80.50
9	361	164	90.25	82.00
10	355	159	88.75	79.50
11	361	155	90.25	77.50
12	357	157	89.25	78.50
13	353	161	88.25	80.50
14	350	156	87.50	78.00
15	351	152	87.75	76.00
16	353	158	88.25	79.00
17	357	155	89.25	77.50
18	350	157	87.50	78.50
19	353	162	88.25	81.00
20	360	164	90.00	82.00
21	365	168	91.25	84.00
22	367	172	91.75	86.00
23	367	174	91.75	87.00
24	369	177	92.25	88.50
25	367	179	91.75	89.50
26	368	177	92.00	88.50
27	367	177	91.75	88.50
28	366	176	91.50	88.00
29	369	173	92.25	86.50
30	371	174	92.75	87.00

Continued

<b>No. of Hidden Nodes</b>	<b>No. of Training Data correctly classified</b>	<b>No. of Testing Data correctly classified</b>	<b>Training Accuracy (%)</b>	<b>Testing Accuracy (%)</b>
31	367	172	91.75	86.00
32	365	170	91.25	85.00
33	363	173	90.75	86.50
34	367	175	91.75	87.50
35	364	178	91.00	89.00
36	365	174	91.25	87.00
37	366	172	91.50	86.00
38	363	171	90.75	85.50
39	361	172	90.25	86.00
40	363	172	90.75	86.00
41	359	174	89.75	87.00
42	364	178	91.00	89.00
43	361	177	90.25	88.50
44	362	178	90.50	89.00
45	359	175	89.75	87.50
46	363	173	90.75	86.50
47	361	175	90.25	87.50
48	358	175	89.50	87.50
49	360	175	90.00	87.50
50	365	177	91.25	88.50



## APPENDIX - D

Data for training and testing processes to determine optimum hidden node (Structure 4).

No. of Hidden Nodes	No. of Training Data correctly classified	No. of Testing Data correctly classified	Training Accuracy (%)	Testing Accuracy (%)
1	391	190	97.75	95.00
2	392	190	98.00	95.00
3	391	191	97.75	95.50
4	393	191	98.25	95.50
5	393	192	98.25	96.00
6	393	191	98.25	95.50
7	392	191	98.00	95.50
8	393	192	98.25	96.00
9	393	192	98.25	96.00
10	395	193	98.75	96.50
11	393	192	98.25	96.00
12	393	193	98.25	96.50
13	395	194	98.75	97.00
14	395	194	98.75	97.00
15	397	195	99.25	97.50
16	397	195	99.25	97.50
17	397	192	99.25	96.00
18	392	193	98.00	96.50
19	393	192	98.25	96.00
20	396	194	99.00	97.00
21	397	192	99.25	96.00
22	395	193	98.75	96.50
23	395	192	98.75	96.00
24	395	195	98.75	97.50
25	395	192	98.75	96.00
26	396	193	99.00	96.50
27	392	192	98.00	96.00
28	392	192	98.00	96.00
29	394	193	98.50	96.50
30	396	192	99.00	96.00

Continued

<b>No. of Hidden Nodes</b>	<b>No. of Training Data correctly classified</b>	<b>No. of Testing Data correctly classified</b>	<b>Training Accuracy (%)</b>	<b>Testing Accuracy (%)</b>
31	396	195	99.00	97.50
32	393	193	98.25	96.50
33	391	194	97.75	97.00
34	392	191	98.00	95.50
35	391	194	97.75	97.00
36	392	193	98.00	96.50
37	396	193	99.00	96.50
38	396	193	99.00	96.50
39	395	195	98.75	97.50
40	395	195	98.75	97.50
41	396	195	99.00	97.50
42	395	192	98.75	96.00
43	395	195	98.75	97.50
44	395	192	98.75	96.00
45	396	194	99.00	97.00
46	392	194	98.00	97.00
47	393	192	98.25	96.00
48	397	193	99.25	96.50
49	397	192	99.25	96.00
50	397	195	99.25	97.50

## APPENDIX - E

Data for training and testing processes to determine optimum hidden node (Structure 5).

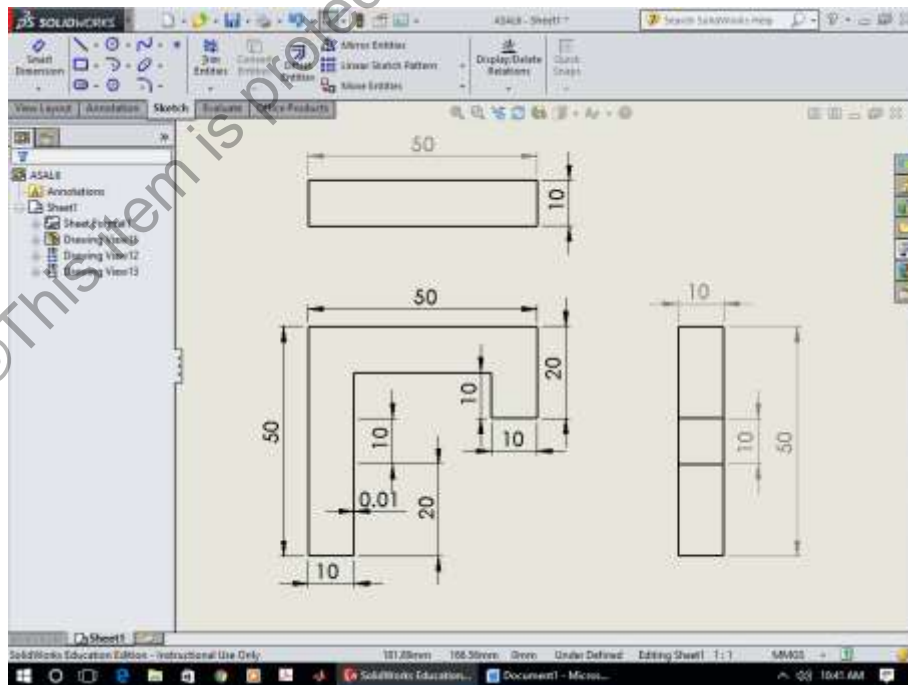
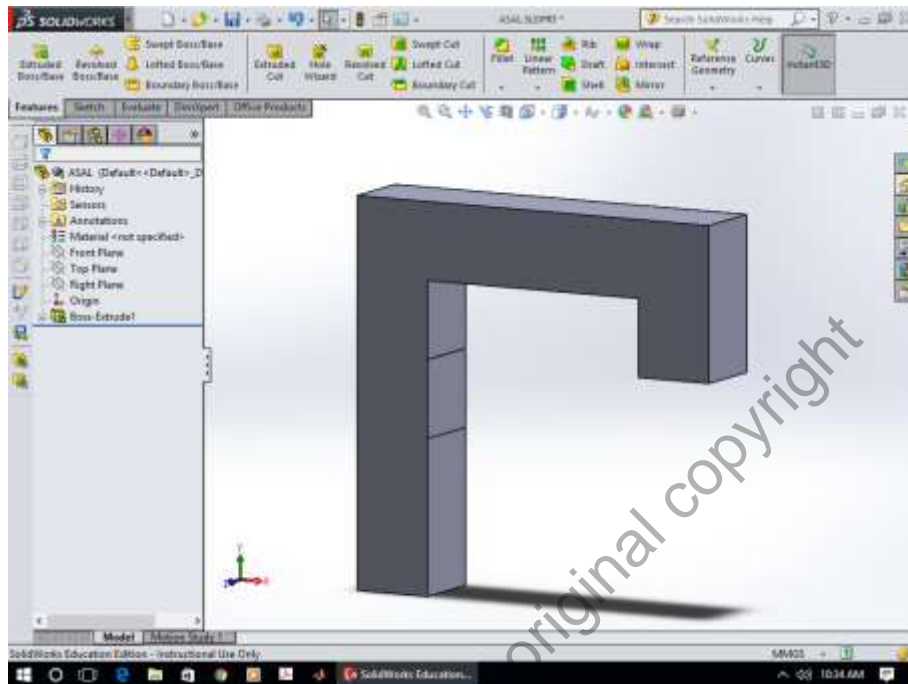
No. of Hidden Nodes	No. of Training Data correctly classified	No. of Testing Data correctly classified	Training Accuracy (%)	Testing Accuracy (%)
1	351	168	87.75	84.00
2	352	169	88.00	84.50
3	352	171	88.00	85.50
4	350	168	87.50	84.00
5	354	170	88.50	85.00
6	353	171	88.25	85.50
7	351	170	87.75	85.00
8	350	171	87.50	85.50
9	352	170	88.00	85.00
10	351	171	87.75	85.50
11	354	170	88.50	85.00
12	355	170	88.75	85.00
13	353	169	88.25	84.50
14	350	170	87.50	85.00
15	351	170	87.75	85.00
16	353	171	88.25	85.50
17	353	173	88.25	86.50
18	350	173	87.50	86.50
19	353	173	88.25	86.50
20	358	171	89.50	85.50
21	355	168	88.75	84.00
22	353	172	88.25	86.00
23	352	171	88.00	85.50
24	354	173	88.50	86.50
25	355	173	88.75	86.50
26	351	172	87.75	86.00
27	354	171	88.50	85.50
28	350	172	87.50	86.00
29	356	173	89.00	86.50
30	351	173	87.75	86.50

Continued

<b>No. of Hidden Nodes</b>	<b>No. of Training Data correctly classified</b>	<b>No. of Testing Data correctly classified</b>	<b>Training Accuracy (%)</b>	<b>Testing Accuracy (%)</b>
31	351	172	87.75	86.00
32	350	172	87.50	86.00
33	351	173	87.75	86.50
34	352	172	88.00	86.00
35	355	172	88.75	86.00
36	353	172	88.25	86.00
37	352	173	88.00	86.50
38	354	172	88.50	86.00
39	350	171	87.50	85.50
40	350	170	87.50	85.00
41	355	171	88.75	85.50
42	356	172	89.00	86.00
43	351	173	87.75	86.50
44	355	171	88.75	85.50
45	350	170	87.50	85.00
46	349	171	87.25	85.50
47	352	172	88.00	86.00
48	354	173	88.50	86.50
49	351	170	87.75	85.00
50	355	171	88.75	85.50

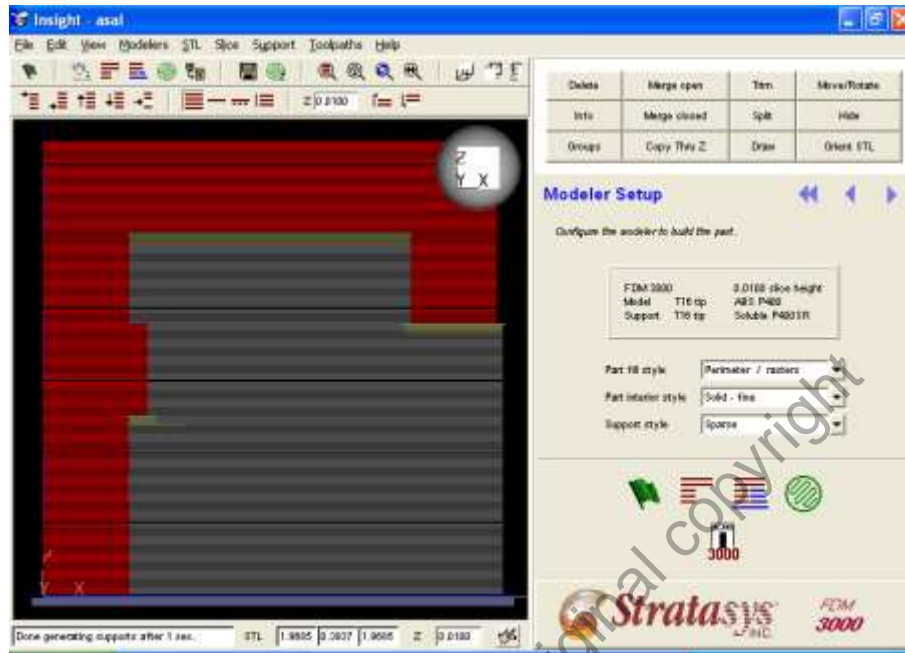
## APPENDIX F

Construction of part model used to evaluate various of features using Feature-based Support Generation using Solid Works software.

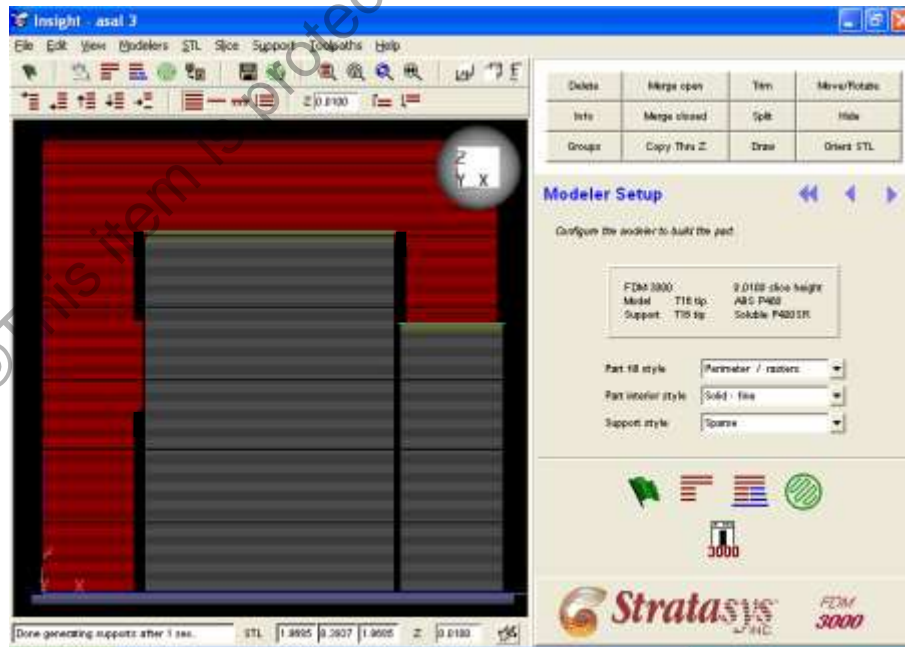


## APPENDIX G

Development and simulation of part model using Insight software.



(a) Before improvement using Feature-based Support Generation.



(b) After improvement using Feature-based Support Generation.

## APPENDIX H

### LIST OF PUBLICATIONS

#### Journals

- 1) Karim, K. F., Hazry, D., Zulkifli, A. H., Ahmed, S. F., Razlan, Z. M., Wan, K., & Bakar, S. A. (2015). Feature Extraction and Optimum Part Deposition Orientation for FDM. In *Applied Mechanics and Materials*, 793, 642-646. Trans Tech Publications.

#### Conferences

- 1) Karim, K. F., Hazry, D., Zulkifli, A. H., Ahmed, S. F., Joyo, M. K., Razlan, Z. M., Wan, K., & Bakar, S. A. (2014). Feature-based Support Generation for Optimum Part Deposition Orientation in FDM. *International conference on electronics design 2014 (ICED 2014)*, Penang, Malaysia, 19-21 August 2014.
- 2) Karim, K. F., Hazry, D., Zulkifli, A. H., Ahmed, S. F., Joyo, M. K., Razlan, Z. M., Wan, K., & Bakar, S. A. (2014). Feature Extraction and Optimum Part Deposition Orientation for FDM. *International Conference on Electrical Power Engineering and Applications (ICEPEA2014)*, Langkawi, Malaysia, 14-16 November 2014.
- 3) Karim, K. F., Hazry, D., Zulkifli, A. H. (2011). A Feature Recognition System using Artificial Neural Network (ANN) to Select the Optimum Part Deposition Orientation in Fused Deposition Modeling (FDM) Machine. *The first International Conference on Advanced Manufacturing (ICAM2011)*, Terengganu, Malaysia, 23-24 May 2011.